UNIVERSITEIT VAN PRETORIA
UNIVERSITY OF PRETORIA
YUNIBESITHI YA PRETORIA

Antiplasmodial properties of extracts from *Pappea capensis* Eckl. & Zeyh. (Sapindaceae)

by

Mcebisi Junior Mabuza

Submitted in fulfillment of the requirements for the degree

Master of Science

(Option: Medicinal Plant Science)

In the Faculty of Natural and Agricultural Sciences

University of Pretoria

Pretoria

February 2022

Supervisor: Dr M.J Bapela

DECLARATION

I, Mcebisi Junior Mabuza, declare that the thesis/dissertation, which I hereby submit for the degree Master of Science (Option: Medicinal Plant Science) at the University of Pretoria, is my work and has not previously been submitted by me for a degree in this or any other tertiary institution.

SIGNATURE: ……

DATE: …….....

PREFACE

Sections of this research have been presented in academic conferences, and parts are being prepared for peer-review journal publication.

Conferences:

Mabuza, M.J., Kaiser, M., Bapela, M.J., 2019. Antiplasmodial activity of *Pappea capensis* Eckl. & Zeyh. (Sapindaceae). Southern Africa Malaria Research Conference. Pretoria, Gauteng, South Africa. Poster presentation.

Mabuza, M.J., Kaiser, M., Bapela, M.J., 2021. Antiplasmodial properties of extracts from *Pappea capensis* Eckl. & Zeyh. (Sapindaceae). Southern Africa Malaria Research Conference. Pretoria, Gauteng, South Africa. Poster presentation.

Mabuza, M.J., Kaiser, M., Bapela, M.J., 2021. Antiplasmodial activity of *Pappea capensis* Eckl. & Zeyh (Sapindaceae). Departmental Postgraduate Seminars. Department of Plant and Soil Science, University of Pretoria. Pretoria, Gauteng, South Africa. Oral Presentation.

Mabuza, M.J., Kaiser, M., Bapela, M.J., 2022. Antiplasmodial properties of extracts from *Pappea capensis* Eckl. & Zeyh. (Sapindaceae) twigs. South African Association of Botanists (SAAB), Qwaqwa, North-West, South Africa. Oral presentation.

Journal articles in preparation:

Mabuza, M.J., Kaiser, M., Bapela, M.J., 2022. Antiplasmodial activity of crude extracts from *Pappea capensis* Eckl & Zeyh. (Sapindaceae) twigs.

Mabuza, M.J., Kaiser, M., Alberts, P.S.F., Bapela, M.J., 2022. ^{1}H NMR and GC–MS metabolomics is applied to dereplicate antimalarial constituents from *Pappea capensis* Eckl. & Zehy. (Sapindaceae) twigs.

ACKNOWLEDGMENTS

- Dr. Bapela is acknowledged for going to great lengths to assist me in this research as my supervisor. In her, I am blessed with the best academic mentor.
- My gratitude goes to Marcel Kaiser for running my antiplasmodial and cytotoxicity biological assays.
- Sincere gratitude goes to Sewes Alberts and Vuyokazi Matshaya for assisting me with metabolomics analysis and to Dr. Selepe for running my ^{1}H NMR samples.
- To my family, thank you for being there throughout my studies, *bo Ludvonga Lwa Mavuso waNgwane.* I dedicate this to you.
- My most sincere gratitude to Nompumelelo Magadlela for editing grammar and word processing. Your love and support have carried me through *Ngiyabonga Ndlovukazi!*
- To my brother, Immer Mbele, your love, and passion for the academy remain unmatched. Stay the course; the best is yet to come.
- I am deeply indebted to the Department of Plant and Soil Science staff and postgraduate students. I have been nurtured by the best academics who constantly motivate me to academic prowess.
- My lab mates: Precious Ramontja, Treasure Thipe, Nhlakanipho Nzama, Zimasa Mkatshane, Urvishi Baba, and Leshaye Domingo. You are all the best!
- My sincere gratitude to the National Research Foundation (NRF) and the University of Pretoria Institute for Sustainable Malaria Control (UPISMC) for funding this research.

ABSTRACT

Malaria continues to wreak havoc in the sub-Saharan African (SSA) region, where the burden is the highest. It has been further complicated by the widespread effects of the COVID-19 pandemic caused by the SARS-CoV-2 virus, which displays similar symptoms to malaria. The coronavirus pandemic contributes to increased malaria prevalence in many endemic countries. However, medicinal plants are constantly relied on for primary health care in many endemic countries. These plants have a long-standing history of using indigenous people to cure malaria and its related symptoms. Drugs have also been delivered by employing ethnopharmacology-based approaches to curb the spread of malaria. This research aims to validate the ethnobotanical utilization of *Pappea capensis* Eckl. & Zeyh. (Sapindaceae) in treating malaria. It is an important plant that forms part of the Vha-Venda people's *materia medica* to treat malaria and its related symptoms.

The plant was evaluated for antiplasmodial activity and cytotoxicity. Its ground twigs were extracted using dichloromethane (DCM): 50% methanol (MeOH) (1:1, v/v), and dried to yield DCM (I = 60 g) and aqueous (II = 287 g) extracts. Extract I was partitioned using DCM: MeOH (1:1, v/v), yielding a second DCM (III = 20 g) and MeOH (IV = 15 g) extracts. In order to simulate the traditional preparation mode, a water-based decoction (V = 10 g) was prepared by boiling 500 g of plant material for 30 minutes to an hour. In total, five extracts were prepared (I – V). Column chromatographic fractionation for extracts II, III, and IV was conducted using a series of solvents with increasing polarity. Extract II was fractionated using ethyl acetate (EtOAc): MeOH, MeOH: distilled water (dH_2O) at ratios of 1:10→10:1. Extract III was fractionated using hexane (H): DCM, DCM: EtOAc, EtOAc: MeOH, and MeOH: dH_2O

at ratios of 1:10→10:1 for each solvent system. Extract IV was fractionated using DCM: EtOAc, EtOAc: MeOH, and MeOH: dH_2O at solvent ratios 1:10⟶10:1. Fractions with similar chemical profiles based on thin-layer chromatography (TLC) analysis were pooled together, yielding 25 fractions (A – Y). The crude extracts (I – V) and fractions (A – Y) were assayed for *in vitro* antiplasmodial activity on *Plasmodium falciparum* (NF54). Cytotoxicity evaluations were performed on mammalian L-6 rat skeletal myoblast cells, and the selectivity indices (SI) were calculated. The crude extracts and fractions were subjected to 1H NMR and GC-MS for chemical profile analysis. Metabolomics using ^{1}H NMR and GC-MS was conducted on fractions A – Y to discriminate between selective and non-selective fractions.

Of all the assayed crude extracts, only three (I, III, and IV) demonstrated significant antiplasmodial activity at IC_{50} of 2.93, 2.59 and 3.56 µg /ml, respectively. I, III, and IV selectivity indices were 14, 21, and 13, respectively. Only N, D and E showed the best antiplasmodial activity at 0.6, 0.85 and 0.91 µg /ml from the assayed chromatographic fractions. Selectivity indices were recorded at 91, 37 and 30, respectively. Organic extracts and fractions displayed higher bioactivity when compared to the polar ones. When the ^{1}H NMR spectra of extracts I, III, and IV were stacked and analyzed, their chemical profiles were tentatively identified to represent the aliphatic-based class of constituents. The GC-MS data analysis for extracts (I, III, and IV) displayed the presence of lupin-3-one, lupeol acetate, α-amyrin, and β-amyrin phytoconstituents. These are all triterpenoids (aliphatic-based constituents) with established antiplasmodial activity, and the observed antiplasmodial activity of *P. capensis* can be attributed to them. The results obtained from the GC-MS and 1H NMR data analysis can be correlated with the observed antiplasmodial biological activity of *P. capensis* crude extracts. All 25 fractions derived from extracts II, III, and IV were

subjected to metabolomics using ^{1}H NMR and GC-MS. The unsupervised Principal Component Analysis (PCA) score plots derived from ^{1}H NMR and GC-MS analysis failed to discriminate between selective and non-selective fractions. Failure to discriminate warrants applying the supervised Orthogonal Projections to Latent Structures Discriminant Analysis (OPLS-DA) model to distinguish between selective and non-selective antiplasmodial fractions. The OPLS-DA model derived from ^{1}H NMR spectral data successfully determined selective and non-selective antiplasmodial fractions with a *P*-value of 0.007. When a contribution plot was generated, it showed a prevalence of aliphatic, allylic, and methyl ketone-based class of secondary compounds at 0.9 – 1.5 ppm, 1.6 – 1.9 ppm, and 2.0 – 2.2 ppm, respectively, in the selective region. In the non-selective region, there was a prevalence of sugar (3.1 – 3.8 ppm), alcohol (4 – 4.8 ppm), vinylic (6.3 – 7.2 ppm), and aromatic (8.5 – 8.9 ppm) based constituents. Aliphatic and aromatic constituents contributed significantly to the discrimination between the selective and non-selective fractions.

The samples clustered according to the observed antiplasmodial biological activity when the OPLS-DA algorithm was applied to the GC-MS-derived model. However, a clear clustering pattern was observed upon validating the model; it ran a very high risk of overfitting with a *P*-value of 0.74. From the contribution plot generated from the OPLS-DA, octasiloxane, β-amyrin, pentadecanon, 3-O-methyl-d-glucose, and tetradecane were identified to have contributed significantly to the observed variations. β-amyrin has established antiplasmodial bioactivity, and it is interesting to also have it as one of the constituents contributing to the discrimination of antiplasmodial fractions. These two spectroscopy techniques are powerful tools that complement each other in the dereplication of antiplasmodial phytoconstituents. Efforts can be maximized to isolate and characterize phytoconstituents with antiplasmodial bioactivity that have not

been studied before. In the search for novel compounds with different mechanisms of action, priority must be accorded to constituents that have not been studied before. Against this backdrop, the dereplication approach to compound isolation is significant. It prevents the redundant isolation of compounds from plants that have already been isolated and expands the current constituent database, which is an important compound identification resource.

The study has validated the ethnomedicinal use of *P. capensis* for malaria treatment and demonstrated the potential of discovering novel antiplasmodial constituents that could serve as potential drug hits. Further analysis of the active crude extracts is underway to isolate unknown compounds attributable to the observed antiplasmodial activity.

TABLE OF CONTENTS

LIST OF ABBREVIATIONS……xiii

LIST OF FIGURES……xv

LIST OF TABLES……xix

CHAPTER 1: INTRODUCTION……1

1.1. Problem statement……2

1.2. Hypotheses……5

1.3. Aim……5

1.4. Objectives……5

1.5. Structure of the dissertation……6

1.6. References……7

CHAPTER 2: LITERATURE REVIEW……11

2.1. Introduction……13

2.2. Environmental and socio-economic effects of malaria……13

2.3. The life cycle of *Plasmodium falciparum*……15

2.4. Malaria transmission in South Africa……17

2.5. Malaria vaccine development and its prospects……20

2.6. Malaria chemotherapy……21

2.7. Plants as sources for antimalarial drug leads……27

2.8. Taxonomy, distribution, and description of *Pappea capensis*……28

2.9. Ethnomedicinal uses of *Pappea capensis*……..29

2.10. Phytochemistry of *Pappea capensis*……..32

2.11. Pharmacological properties of *Pappea capensis*……...34

2.12. Antiplasmodial activity of *Pappea capensis*……..34

2.13. Plant metabolomics and analysis……...35

2.14. Application of metabolomics in phytomedicine……...36

2.15. Different types of metabolomics analysis in phytomedicine……..36

2.16. Chemical analytical techniques used in plant metabolomics……37

2.17. References……39

CHAPTER 3: ANTIPLASMODIAL ACTIVITY OF *PAPPEA CAPENSIS* ECKL. & ZEYH. (SAPINDACEAE) TWIGS……...56

3.1. Introduction……..57

3.2. Materials and methods……..58

3.2.1. General……58

3.2.2. Plant sample collection……...58

3.2.3. Extraction of plant samples……...58

3.2.4. Column chromatography of crude extracts of *Pappea capensis*……59

3.2.5. *In vitro* antiplasmodial assay……..60

3.2.6. Cytotoxicity assay of *Pappea capensis* crude extracts……..60

3.2.7. 1H NMR spectroscopy analysis of *Pappea capensis* crude extracts……61

3.2.8. GC-MS analysis of Pappea capensis crude extracts……62

3.3. Results and discussions……62

3.4. Conclusion……...76

3.5. References……...76

CHAPTER 4: THE APPLICATION OF ^{1}H NMR AND GC – MS METABOLOMICS TO DEREPLICATE ANTIMALARIAL CONSTITUENTS FROM *PAPPEA CAPENSIS* ECKL. & ZEHY. (SAPINDACEAE) TWIGS……...82

4.1. Introduction……....83

4.2. Materials and methods……..84

4.2.1. Plant sample collection……...85

4.2.2. Extraction of plant samples……85

4.2.3. Column chromatography of *Pappea capensis* extracts……....86

4.2.4. ^{1}H NMR spectroscopy of *Pappea capensis* fractions……86

4.2.5. GC-MS analysis of *Pappea capensis* fractions……..87

4.2.6. Statistical analysis using multivariate data analysis (MDA)……....88

4.3. Results and discussion……....88

4.4. Conclusion……..98

4.5. References……98

CHAPTER 5: GENERAL CONCLUSION……..……..101

5.1. General conclusion……..101

5.2. Challenges and prospects……..……...102

CHAPTER 6: APPENDIX……..…104

LIST OF ABBREVIATIONS

^{1}H NMR: Proton Nuclear Magnetic Resonance

2D NMR: Two-Dimensional Nuclear Magnetic Resonance

ACT: Artemisinin Combination Therapy

CC: Column Chromatography

CE – MS: Capillary Electrophoresis – Mass Spectrometry

GC – MS: Gas Chromatography-Mass Spectrometry

GDP: Gross Domestic Product

HEPES: 4-(2-hydroxyethyl)-1-piperazineethanesulfonic acid

LC-GC: Liquid Chromatography/Gas Chromatography

LC-FTIR: Liquid Chromatography – Fourier – Transform Infrared Spectroscopy

LC-MS: Liquid Chromatography-Mass Spectrometry

LC-NMR: Liquid Chromatography – Nuclear Magnetic Resonance

MMV: Medicines for Malaria Venture

MS: Mass Spectrometry

NIST: National Institute of Standards and Technology

OPLS-DA: Orthogonal Projections to Latent Structures – Discriminant Analysis

PCA: Principal Component Analysis

QC: Quality Control

SI: Selectivity Index

SSA: sub-Saharan Africa

TMS: Trimethylsilyl

WHO: World Health Organization

LIST OF FIGURES

Figure 2.1. Global malaria distribution map (WHO, 2019) …..……14

Figure 2.2. *Plasmodium falciparum* proliferation (Ashley et al., 2018) …..……16

Figure 2.3. Malaria distribution in South Africa (National Department of Health, 2018) …..……...18

Figure 2.4. Malaria reported cases in South Africa between 2010 and 2018 (Aide et al., 2019) …..……..19

Figure 2.5. Chemical structures of quinine and artemisinin……..23

Figure 2.6. Antiplasmodial drugs with limited bioavailability..……..23

Figure 2.7. Chemical structures of artemisinin derivatives……...24

Figure 2.8. Some companion drugs used with artemisinin in ACTs……26

Figure 2.9. Antiplasmodial compounds isolated from *Pappea capensis*……33

Figure 3.1. Stacked ^{1}H NMR spectra of *Pappea capensis* crude fractions showing the different chemical shift similarities highlighted……...69

Figure 3.2. The GC-MS spectra of *Pappea capensis* crude extracts. The major phytoconstituents have been highlighted……72

Figure 3.3. ^{1}H NMR spectra of the most active fractions of *Pappea capensis*……..74

Figure 3.4. Stacked GC-MS spectra of the most active fractions of *Pappea capensis* showing myristic acid and palmitic acid……...75

Figure 4.1. The summarized steps followed in metabolomics analysis of *Pappea capensis*……..85

Figure 4.2. Principal Component Analysis (PCA) score plots of *Pappea capensis* fractions generated from GC-MS (A) and (B) ^{1}H NMR spectral datasets: S – Selective and NS – Non-selective……90

Figure 4.3. (A) The OPLS-DA score plots for *Pappea capensis* fractions were generated from ^{1}H NMR. (B) Permutation score plots validating the OPLS-DA generated from ^{1}H NMR data. (C) The OPLS-DA plots for *Pappea capensis* fractions were generated from GC-MS data. (D) Permutation score plot validating the OPLS-DA generated from GC-MS data……..91

Figure 4.4. The contribution plot generated from ^{1}H NMR data of *Pappea capensis* fractions comparing selective (bars projecting up) and non-selective (bars projecting down) clusters……..……95

Figure 4.5. The contribution plot generated from GC-MS data of *Pappea capensis* fractions displaying the comparison between the selective (bars projecting up) and non-selective (bars projecting down) constituents……97

Figure 6.1. ^{1}H NMR spectrum of A……120

Figure 6.2. ^{1}H NMR spectrum of B……121

Figure 6.3. ^{1}H NMR spectrum of C……122

Figure 6.4. ^{1}H NMR spectrum of D……123

Figure 6.5. ^{1}H NMR spectrum of E……124

Figure 6.6. ^{1}H NMR spectrum of F……..……125

Figure 6.7. ^{1}H NMR spectrum of G……126

Figure 6.8. ^{1}H NMR spectrum of H……127

Figure 6.9. ^{1}H NMR spectrum of I……..128

Figure 6.10. ^{1}H NMR spectrum of J……...129

Figure 6.11. ^{1}H NMR spectrum of K. 130

Figure 6.12. ^{1}H NMR spectrum of L.....131

Figure 6.13. ^{1}H NMR spectrum of M.....132

Figure 6.14. ^{1}H NMR spectrum of N.....133

Figure 6.15. ^{1}H NMR spectrum of O. 134

Figure 6.16. ^{1}H NMR spectrum of P.....135

Figure 6.17. ^{1}H NMR spectrum of Q.....136

Figure 6.18. ^{1}H NMR spectrum of R.....137

Figure 6.19. ^{1}H NMR spectrum of S.....138

Figure 6.20. ^{1}H NMR spectrum of T.....139

Figure 6.21. ^{1}H NMR spectrum of U.....140

Figure 6.22. ^{1}H NMR spectrum of V.....141

Figure 6.23. ^{1}H NMR spectrum of W.....142

Figure 6.24. ^{1}H NMR spectrum of X.....143

Figure 6.25. ^{1}H NMR spectrum of Y.....144

Figure 6.26. GC-MS spectrum of A.....145

Figure 6.27. GC-MS spectrum of B.....146

Figure 6.28. GC-MS spectrum of C.....147

Figure 6.29. GC-MS spectrum of D.....148

Figure 6.30. GC-MS spectrum of E.....149

Figure 6.31. GC-MS spectrum of F……150

Figure 6.32. GC-MS spectrum of G……151

Figure 6.33. GC-MS spectrum of H……152

Figure 6.34. GC-MS spectrum of I……153

Figure 6.35. GC-MS spectrum of J……154

Figure 6.36. GC-MS spectrum of K……155

Figure 6.37. GC-MS spectrum of L……156

Figure 6.38. GC-MS spectrum of M……157

Figure 6.39. GC-MS spectrum of N……158

Figure 6.40. GC-MS spectrum of O……159

Figure 6.41. GC-MS spectrum of P……160

Figure 6.42. GC-MS spectrum of Q……161

Figure 6.43. GC-MS spectrum of R……162

Figure 6.44. GC-MS spectrum of S……163

Figure 6.45. GC-MS spectrum of T……164

Figure 6.46. GC-MS spectrum of U……165

Figure 6.47. GC-MS spectrum of V……166

Figure 6.48. GC-MS spectrum of W……167

Figure 6.49. GC-MS spectrum of X……168

Figure 6.50. GC-MS spectrum of Y……169

LIST OF TABLES

Table 2.1. Ethnomedicinal uses of *Pappea capensis*……31

Table 3.1. The antiplasmodial activity (IC_{50} values (µg/ml)) and cytotoxicity of *Pappea capensis* crude extracts and fractions with a selectivity index (SI) value were computed. Mean values were calculated for two independent experiments conducted in duplicate……..64

Table 3.2. The percentage proportion of constituent classes identified in the individual extracts of *Pappea capensis* using GC-MS……70

Table 6.1. Metabolite composition of Extract I……..…108

Table 6.2. Metabolite composition of extract II……....110

Table 6.3. Metabolite composition of Extract III……..…113

Table 6.4. Metabolite composition of Extract IV……..115

Table 6.5. Metabolite composition of Extract V……....118

CHAPTER 1: INTRODUCTION

1.1. Problem statement……...2

1.2. Hypotheses……...5

1.3. Aim…….....5

1.4. Objectives…….....5

1.5. Structure of the dissertation……6

1.6. References…….....7

1.1. Problem statement

Plasmodium falciparum accounts for the high fatality rates in most malaria-endemic countries. More than half of the world's population is in jeopardy of incurring malaria (WHO, 2020). Pregnant women and children are at higher risk due to their imperiled immune systems (Saito et al., 2020). Africa and East Asia have the highest burden compared to other parts of the world (Alegana et al., 2020). In the sub-Saharan African (SSA) region, the burden continues to be elusive, and difficult to ascertain its true impact (WHO, 2020). There are myriad factors that influence the prevalence of malaria in many endemic countries. Malaria interferes with societal wellbeing, hindering the thriving and prospering of communities. Most malaria-endemic countries are in tropical regions where a poor economic status (low gross domestic product) characterizes them (Tusting et al., 2016). Poverty, especially in Africa, exacerbates the malaria burden, and the fight against it is compromised by many societal realities (Worrall et al., 2005). Due to malaria-causing protozoans mysterious and elusive nature, government health departments and institutions find it difficult to implement their malaria elimination strategic plans. *Plasmodium* parasites are evasive because some aspects of malaria etiology are less considered than others.

Malaria eradication and elimination approaches have focused more on surveillance, vector, or parasite control. These have been the primary focus areas on which many African countries spend their national health budgets. The focus should be on the disease and on structural realities that compound the malaria burden (Santos-Vega et al., 2016). Structural poverty has contributed to the many failures incurred by most African health departments and ministries in implementing their malaria elimination strategic plans (Ingstad et al., 2012). Structural poverty is the

systematic impoverishment of a sect of the population caused by the economic structural model (Ricci, 2012). A large majority of the African countries are a product of similar capital-oriented economic structured models, and these have created the problem of structural poverty, which frustrates proposed malaria elimination strategies. Poor African countries find expensive antimalarial drugs and other prevention measures a luxury (Palafox et al., 2016). In some coastal regions, especially some parts of Mozambique, it has been reported that distributed malaria-treated nets catch more fish than they are supposed to catch mosquitoes (Jones & Unsworth, 2020). In the malaria prevention and elimination agenda, this redirected purpose of malaria prevention intended merchandise is counterproductive. Africa is slowly losing the malaria battle to poverty. The continued emphasis on discovering new effective and affordable drugs will be irrelevant in the long run if these socio-economic ills are not equally addressed. Until this social malady of poverty can be resolved, malaria will continue imperiling the African continent with no hope for relief.

Although malaria-related deaths have significantly declined around the globe, the burden has not been entirely extirpated, especially in SSA (WHO, 2020). For optimal results, vector control and drug interventions must be considered when devising the antimalaria arsenal (Sougoufara et al., 2020). Treated bed nets and indoor sprays are top-of-the-list vector controls (Shah et al., 2020). Malaria surveillance is indispensable, but many African countries are still falling behind (Lourenço et al., 2019). Antimalarial vaccine development is a complicated process. However, some vaccines are still in the developmental pipeline, and they promise to provide the much-desired relief (Rampling et al., 2020). More robust malaria drug regimens have been developed and have significantly reduced the malaria burden (Penny et al., 2020). Though efficient malaria drugs have been developed and are continuously improved

to treat malaria, the disease burden continues to intensify. *Plasmodium* has manifested resistance against many prescribed antimalarial drugs (Slater et al., 2021). Malaria combination treatments (current first-line response) have been reported to harbor some long-term negative effects, and the parasites slowly develop resistance to them. However, novel drug development and other vector control measures will ensure malaria eradication.

Producing more effective interventions has necessitated discovering new drugs with novel properties. Plants present promising prospects for bioprospecting: they consist of secondary metabolites with diverse chemical structures, biological activities, and mechanisms of action (Geilfus, 2019). Most prescribed antimalaria drugs come from plant sources (Wan et al., 2020). Quinine and artemisinin were both discovered from plant species, and they were among the earliest antimalarial drugs (Liu et al., 2014). Many medicines derived from plant species warrant further research towards discovering more drug interventions from the plant kingdom (Fabricant and Farnsworth, 2001). The extensive exploration of botanicals to find new phytochemicals with unique modes of action and chemical structures with drug-like properties are scant. Most studies on plant extracts' antiplasmodial properties do not extend to the phytoconstituent level. Specific pure compounds responsible for the observed pharmacological activity have not been isolated and characterized (Bapela et al., 2014; Clarkson et al., 2004; Koch et al., 2005; Mokoka et al., 2013; Pendota et al., 2017). Medicinal plants with antiplasmodial activity should be investigated to isolate bioactive phytochemicals. The process of antimalarial drug discovery will benefit from such endeavors.

Continuous antimalarial drug discovery will be instrumental in creating diverse and robust therapeutic weaponry against *Plasmodium* parasites. The availability of a vast array of antimalarials with different mechanisms of action will economically benefit many malaria-endemic countries under the yoke of poverty. Even though drug discovery from botanical species is long and laborious, it is an absolute necessity. If the African continent is to win the malaria battle, discovering new drugs with novel mechanisms of action is her best shot.

1.2. Hypotheses

- The antiplasmodial activity will increase with downstream fractionation of the crude extracts of *Pappea capensis*.
- Metabolomics using GC-MS and ^{1}H NMR will discriminate between selective and non-selective antiplasmodial fractions of *Pappea capensis*.
- Metabolomics using GC-MS and ^{1}H NMR will dereplicate known antiplasmodial constituents from the unknown in *Pappea capensis*.

1.3. Aim

- To apply GC-MS and ^{1}H NMR metabolomics in dereplicating known antiplasmodial constituents from unknown ones, thus prioritizing isolating novel antiplasmodial components.

1.4. Objectives

- To obtain the polar and non-polar crude extracts from *Pappea capensis* twigs using dichloromethane: 50% methanol
- To fractionate aqueous and organic extracts of *Pappea capensis*.

- To test *Pappea capensis* extracts and fractions for antiplasmodic and cytotoxicity activities.
- To conduct GC-MS and ^{1}H NMR metabolomics of *Pappea capensis* fractions.
- To dereplicate known antiplasmodial phytoconstituents from unknown.

1.5. Structure of the dissertation

All chapters are structured according to the South African Journal of Botany format.

Chapter 1: The challenges and difficulties confronted to restrain and extirpate malaria are detailed. This chapter also outlines the hypotheses, study objectives, and the structure of the dissertation.

Chapter 2: Reviews the intricate life cycle of *Plasmodium* and outlines the socio-economic realities that compound the malaria burden. Available chemotherapeutic agents used to treat malaria, vector control strategies, and vaccines in the pipeline to fight malaria are discussed. Parasite resistance to chemotherapeutics, bioprospecting from *P. capensis*, pharmacological relevance of its constituents, and the potential of metabolomics in drug discovery form the backbone of this chapter.

Chapter 3: Describes the extraction and fractionation of crude extracts. It also analyses the results obtained from the antiplasmodial and cytotoxicity screening of all the *Pappea capensis* crude extracts and fractions acquired from column chromatography fractionation.

Chapter 4: ^{1}H NMR and GC-MS metabolomics analysis of all *Pappea capensis* fractions underscore the scope of this chapter. It zeroes in on the potential

of GC-MS and ^{1}H NMR-based metabolomics approaches in dereplicating known isolated constituents with established antiplasmodial activity from unknown compounds.

Chapter 5: An analysis and a comprehensive general interpretation of the results based on the study's outcomes underscore the scope of the chapter. The epistemological gaps in malaria research and prospects of research will be highlighted in this chapter.

Chapter 6: This chapter contains supplemental data and relevant information about the study.

1.6. References

Alegana, V.A., Okiro, E.A., Snow, R.W., 2020. Routine data for malaria morbidity estimation in Africa: challenges and prospects. BMC Medicine 18, 1–13.

Bapela, M.J., Meyer, J.J.M., Kaiser, M., 2014. *In vitro* antiplasmodial screening of ethnopharmacologically selected South African plant species used to treat malaria. Journal of Ethnopharmacology 156, 370–373.

Clarkson, C., Maharaj, V.J., Crouch, N.R., Grace, O.M., Pillay, P., Matsabisa, M.G., Bhagwandin, N., Smith, P.J., Folb, P.I., 2004. In vitro antiplasmodial activity of medicinal plants native to or naturalized in South Africa. Journal of Ethnopharmacology 92, 177–191.

Fabricant, D.S., Farnsworth, N.R., 2001. The value of plants used in traditional medicine for drug discovery. Environmental Health Perspectives 109, 69–75.

Geilfus, C.-M., 2019. Plant secondary compounds, in: Controlled Environment Horticulture: Improving Quality of Vegetables and Medicinal Plants. Springer Nature, Geneva, pp. 19–33.

Ingstad, B., Munthali, A.C., Braathen, S.H., Grut, L., 2012. The evil circle of poverty: a qualitative study of malaria and disability. Malaria Journal 11, 1–6.

Jones, B.L., Unsworth, R.K.F., 2020. The perverse fisheries consequences of mosquito net malaria prophylaxis in East Africa. Ambio 49, 1257–1267.

Koch, A., Tamez, P., Pezzuto, J., Soejarto, D., 2005. Evaluation of plants used for antimalarial treatment by the Maasai of Kenya. Journal of Ethnopharmacology 101, 95–99.

Liu, Y.-X., Wu, W., Liang, Y.-J., Jie, Z.-L., Wang, H., Wang, W., Huang, Y.-X., 2014. New uses for old drugs: the tale of artemisinin derivatives in the elimination of schistosomiasis japonica in China. Molecules 19, 15058–15074.

Lourenço, C., Tatem, A.J., Atkinson, P.M., Cohen, J.M., Pindolia, D., Bhavnani, D., le Menach, A., 2019. Strengthening surveillance systems for malaria elimination: a global landscaping of system performance, 2015-2017. Malaria Journal 18, 315.

Mokoka, T.A., Xolani, Peter.K., Zimmermann, S., Hata, Y., Adams, M., Kaiser, M., Moodley, N., Maharaj, V., Koorbanally, N.A., Hamburger, M., Brun, R., Fouche, G., 2013. Antiprotozoal screening of 60 South African plants, and the identification of the antitrypanosomal germacranolides schkuhrin I and II. Planta Medica 79, 1380–1384.

Palafox, B., Patouillard, E., Tougher, S., Goodman, C., Hanson, K., Kleinschmidt, I., Torres Rueda, S., Kiefer, S., O'Connell, K., Zinsou, C., Phok, S.,

Akulayi, L., Arogundade, E., Buyungo, P., Mpasela, F., Poyer, S., Chavasse, D., 2016. Prices and mark-ups on antimalarials: evidence from nationally representative studies in six malaria-endemic countries. Health Policy and Planning 31, 148–160.

Pendota, S.C., Aderogba, M.A., Moyo, M., McGaw, L.J., Mulaudzi, R.B., van Staden, J., 2017. Antimicrobial, antioxidant, and cytotoxicity of isolated compounds from leaves of Pappea capensis. South African Journal of Botany 108, 272–277.

Penny, M.A., Camponovo, F., Chitnis, N., Smith, T.A., Tanner, M., 2020. Future use-cases of vaccines in malaria control and elimination. Parasite Epidemiology and Control 10, e00145.

Rampling, T., Ewer, K.J., Bowyer, G., Edwards, N.J., Wright, D., Sridhar, S., Payne, R., Powlson, J., Bliss, C., Venkatraman, N., Poulton, I.D., de Graaf, H., Gbesemete, D., Grobbelaar, A., Davies, H., Roberts, R., Angus, B., Ivinson, K., Weltzin, R., Rajkumar, B.Y., Wille-Reece, U., Lee, C., Ockenhouse, C., Sinden, R.E., Gerry, S.C., Lawrie, A.M., Vekemans, J., Morelle, D., Lievens, M., Ballou, R.W., Lewis, D.J.M., Cooke, G.S., Faust, S.N., Gilbert, S., Hill, A.V.S., 2020. Safety and efficacy of novel malaria vaccine regimens of RTS, S/AS01B alone, or with concomitant ChAd63-MVA-vectored vaccines expressing ME-TRAP. npj Vaccines 3, 1–15.

Ricci, F., 2012. Social implications of malaria and their relationships with poverty. Mediterranean Journal of Hematology and Infectious Diseases 4, e2012048.

Saito, M., Briand, V., Min, A.M., McGready, R., 2020. Deleterious effects of malaria in pregnancy on the developing fetus: a review on prevention and treatment with antimalarial drugs. The Lancet Child and Adolescent Health 4, 761–774.

Santos-Vega, M., Bouma, M.J., Kohli, V., Pascual, M., 2016. Population density, climate variables, and poverty synergistically structure spatial risk in urban malaria in India. PLOS Neglected Tropical Diseases 10, e0005155.

Shah, M.P., Steinhardt, L.C., Mwandama, D., Mzilahowa, T., Gimnig, J.E., Bauleni, A., Wong, J., Wiegand, R., Mathanga, D.P., Lindblade, K.A., 2020. The effectiveness of older insecticide-treated bed nets (ITNs) to prevent malaria infection in an area of moderate pyrethroid resistance: results from a cohort study in Malawi. Malaria Journal 19, 24.

Slater, L., Betson, M., Ashraf, S., Sargison, N., Chaudhry, U., 2021. Current methods for the detection of antimalarial drug resistance in *Plasmodium* parasites infecting humans. Acta Tropica 216, 105828.

Sougoufara, S., Ottih, E.C., Tripet, F., 2020. The need for new vector control approaches targeting outdoor biting *Anopheline* malaria vector communities. Parasites and Vectors 13, 1–15.

Tusting, L.S., Rek, J., Arinaitwe, E., Staedke, S.G., Kamya, M.R., Cano, J., Bottomley, C., Johnston, D., Dorsey, G., Lindsay, S.W., Lines, J., 2016. Why is malaria associated with poverty? Findings from a cohort study in rural Uganda. Infectious Diseases of Poverty 5, 1–11.

Wan, H., Tian, Y., Jiang, H., Zhang, X., Ju, X., 2020. An NMR-based drug screening strategy for discovering active substances from herbal medicines: using Radix polygoni multiflori as an example. Journal of Ethnopharmacology 254, 112712.

WHO, 2020. Malaria [WWW Document]. World Health Organization, Geneva. URL https://www.who.int/news-room/fact-sheets/detail/malaria (accessed 11.22.19).

Worrall, E., Basu, S., Hanson, K., 2005. Is malaria a disease of poverty? a review of the literature. Tropical Medicine and International Health 10, 1047–1059.

CHAPTER 2: LITERATURE REVIEW

2.1. Introduction……13

2.2. Environmental and socio-economic effects of malaria……..12

2.3. The life cycle of *Plasmodium falciparum*……14

2.4. Malaria in South Africa……17

2.5. Malaria vaccine development and its prospects……19

2.6. Malaria chemotherapy……...20

2.7. Plants as sources for antimalarial drug leads……26

2.8. Taxonomy, distribution, and description of *Pappea capensis*……27

2.9. Ethnomedicinal uses of *Pappea capensis*……..28

2.10. Phytochemistry of *Pappea capensis*……...31

2.11. Pharmacological properties of *Pappea capensis*……..33

2.12. Antiplasmodial activity of *Pappea capensis*……33

2.13. Plant metabolomics and analysis……34

2.14. Application of metabolomics in phytomedicine……..35

2.15. Different types of metabolomics analysis in phytomedicine……35

2.16. Chemical analytical techniques used in plant metabolomics……...36

2.17. References……..38

2.1. Introduction

This malaria disease caused by *Plasmodium* protozoans is responsible for high global fatality rates, especially in sub-Saharan Africa (SSA). An estimated 50% of the global population is in danger of infection (WHO, 2020). Reported global cases and deaths are 241 million and 627 000, respectively (WHO, 2021). The burden is generally the highest in Africa and Southeast Asia, where high malaria cases and deaths are reported annually (WHO, 2020). Pregnant women and infants are at an even greater risk of infection due to their imperiled immune systems (Obebe & Falohun, 2021). Socio-economically impoverished communities are also in grave danger of suffering the worst malaria burden due to social factors conglomerated with economical struggles that compound the malaria burden even more. Since 2000, malaria-related deaths have significantly declined by 25% globally and 33% in SSA (Varo et al., 2020). Local governments and stakeholders have attempted to curb malaria transmission for years now, but eradication is still not yet achieved (Medicines for Malaria Venture, 2019). Therefore, it is imperative that in the struggle to eradicate malaria, a clear path towards that should be crafted to include all aspects of malaria transmission.

2.2. Environmental and socio-economic effects of malaria

Environmental and climatic conditions also contribute sizably to the spread of malaria. Most countries located in the tropical regions (Figure 2.1) are malaria-endemic due to high temperatures and rainfall that provide a suitable atmosphere for *Plasmodium* parasites to thrive (Traoré et al., 2020). High temperatures and rainfall are directly proportional to the increased malaria burden observed in prevalent tropical regions (Shapiro et al., 2017). These water reservoirs initially constructed to address water scarcities become excellent breeding grounds for the *Anopheles* vector.

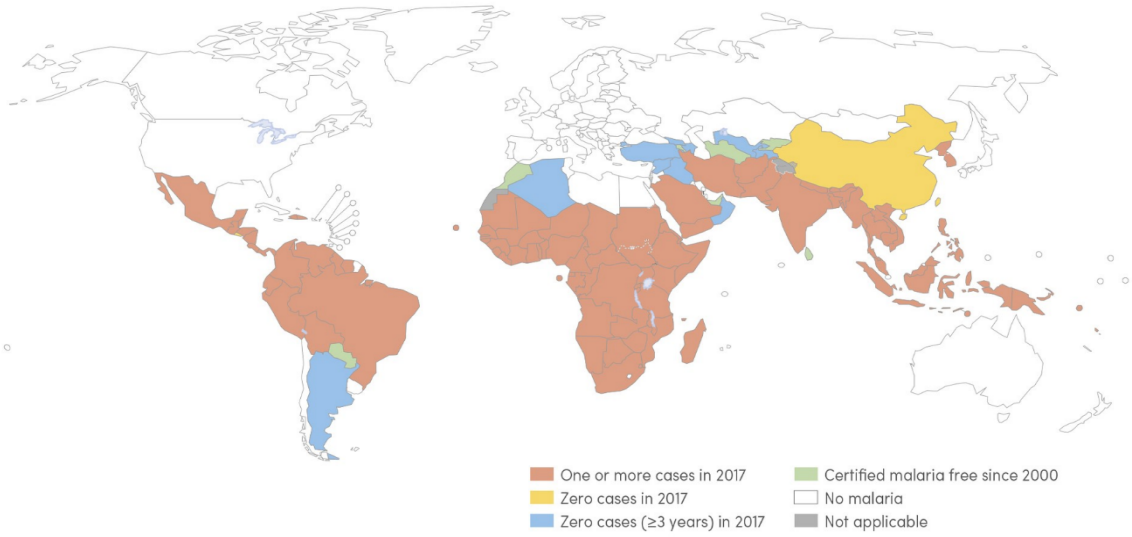

Figure 2.1. Global malaria distribution map (WHO, 2019).

Migration and urbanization contribute to the spread of malaria, especially in regions where high migration is prevalent (Mukhtar et al., 2020). A larger percentage of the world's population resides in the cities, and the rapid urban population growth leads to the eruption of social ills like poor sanitation, inappropriate housing, and poor nutrition needed to promote human well-being (Hassen & Dinka, 2020). These unfavorable conditions indirectly contribute to the increased malaria burden in urban cities. Economic impoverishment is another contributing factor exacerbating the malaria burden. A large proportion of the countries in the tropics where malaria is prevalent have a low Gross Domestic Product (GDP), which correlates with the notion that malaria breeds poverty (Wang et al., 2021). In many societies, malaria's prevalence hinders development, thus subsequently hindering population growth and fertility. These social ills bar societies from attaining full economic stability and rigor. The high costs of drugs and medical supplies fundamentally prevent many developing countries from eradicating malaria. A conglomeration of these environmental and

socio-economic ills contributes largely to the continued prevalence of malaria in many poverty-stricken African societies (MacArayan et al., 2020).

2.3. The life cycle of *Plasmodium falciparum*

About 200 different *Plasmodium* protozoans are known (Sato, 2021). Six proliferate in humans: *Plasmodium falciparum, P. vivax, P. ovale curtisi*, *P. ovale wallikeri*, *P. malariae,* and *P. knowlesi*. *Plasmodium falciparum* and *P. vivax* are the most dangerous humans (Stresman et al., 2020). It is maintained that the first four proliferate specifically in the human host, while *P. knowlesi* is the main causative agent of zoonotic malaria in Southeast Asia (Sato, 2021). *Plasmodium falciparum* accounts for an estimated 99.7% and 71% of malaria cases in Africa and Southeast Asia. In the Eastern Mediterranean and Western Pacific, 69% and 79.9% of cases, respectively, resulted from *P. falciparum*. *Plasmodium vivax* is mostly predominant in the North and South American continents, where it accounts for an estimated total of 74.1% of malaria cases (WHO, 2020). These unicellular malaria-causing protozoans have complicated life cycles, which involve the female *Anopheles* mosquito as the vector and the human as the host. *Plasmodium falciparum* has two stages in its life cycle (Figure 2.2): sexual and asexual stages (Amoah et al., 2020). Asexual stages occur in the human host, while the asexual ones occur in the mosquito vector. The female *Anopheles* is not just a mere carrier of the *Plasmodium* protozoans; it is also a definitive host where sexual reproduction occurs (Mota & Mello-Vieira, 2019).

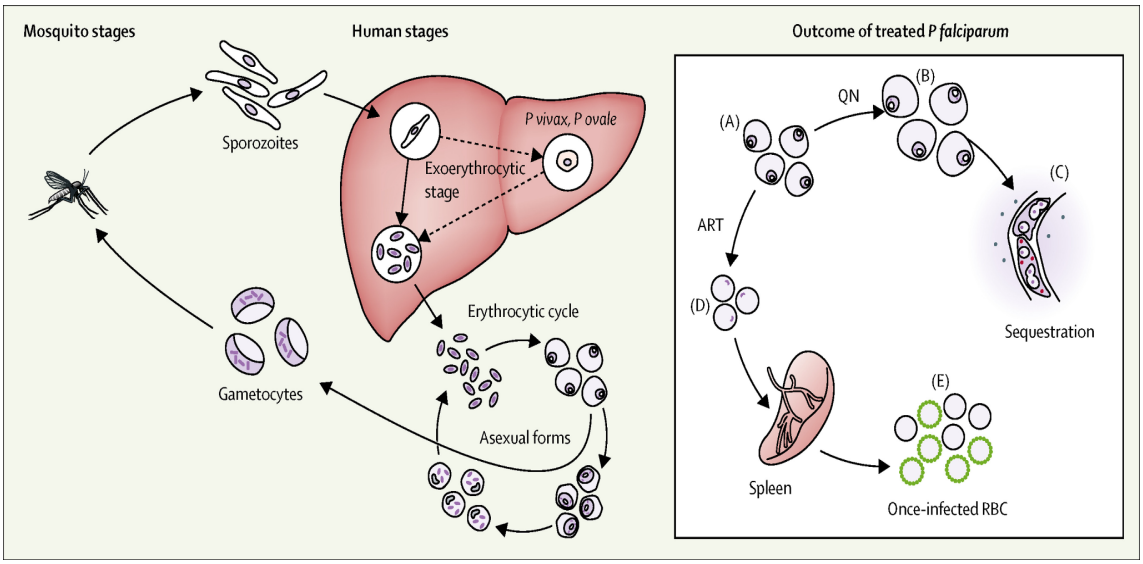

Figure 2.2. *Plasmodium falciparum* proliferation (Ashley et al., 2018).

Sporozoites are transferred from the mosquito to the human host during a blood meal, and this signals the beginning of the life cycle of *Plasmodium* (Amoah et al., 2020). The sporozoites invade the human host and first colonize the hepatocytes through sporozoite traversal (Tougan et al., 2020). After the hepatocyte infection, the sporozoites mature to form schizonts (*P. falciparum*) or liver hypnozoites (*P. ovale* and *P. vivax*) about two weeks before erythrocyte penetration (Ashley et al., 2018). When the schizonts or hypnozoites have matured in the erythrocytes, the cells rupture and release merozoites which mature to form protozoa gametes to signal the completion of asexual reproduction (Schneider & Reece, 2021). The zygotes forming from the fusion of ingested gametes mature into sporozoites, releasing oocysts to signal the completion of the cycle.

Malaria pathogenesis results from the asexual blood stages that produce symptoms like fever, cold, and chills, which occur each time the blood cells rupture to release schizonts (Malaria Vaccine Initiative, 2021). General malaise, headaches, and vomiting are more advanced symptoms occurring later during the sexual blood stages

of malaria if it remains untreated (Bartoloni & Zammarchi, 2012). It is thus expedient to better grasp the complexities of the *Plasmodium* life cycle to prevent malaria transmission. Malaria interventions intended to bring about relief through targeting the parasite need to be guided by this biological backdrop of its life cycle.

2.4. Malaria transmission in South Africa

Limpopo, KwaZulu-Natal, and Mpumalanga are the only provinces (Figure 2.2) where malaria transmission occurs (Maharaj et al., 2019). The Limpopo (Vhembe and Mopani) and Mpumalanga (Ehlanzeni) provinces have a higher burden compared to KwaZulu-Natal (Yael et al., 2019). About 10% of the population in SA is at risk of contracting malaria. Between 2015 – 2019, SA annually recorded 10 000 – 30 000 malaria cases (National Department of Health, 2018). Although the number of confirmed cases decreased drastically, there has been a fluctuating pattern since 2000 (Figure 2.3) (Aide et al., 2019). Most of the malaria burden experienced in these provinces is due to imported cases from neighboring countries like Mozambique and Zimbabwe. The two important malaria transmitting vectors prevalent in SA are *Anopheles arabiensis* and *Anopheles funestus*. These anopheline vectors thrive during the summer rains between September and May (Yael et al., 2019). The most prevalent malaria is falciparum malaria, which is transmitted by *A. arabiensis*.

Figure 2.3. Malaria distribution map of South Africa (National Department of Health, 2018).

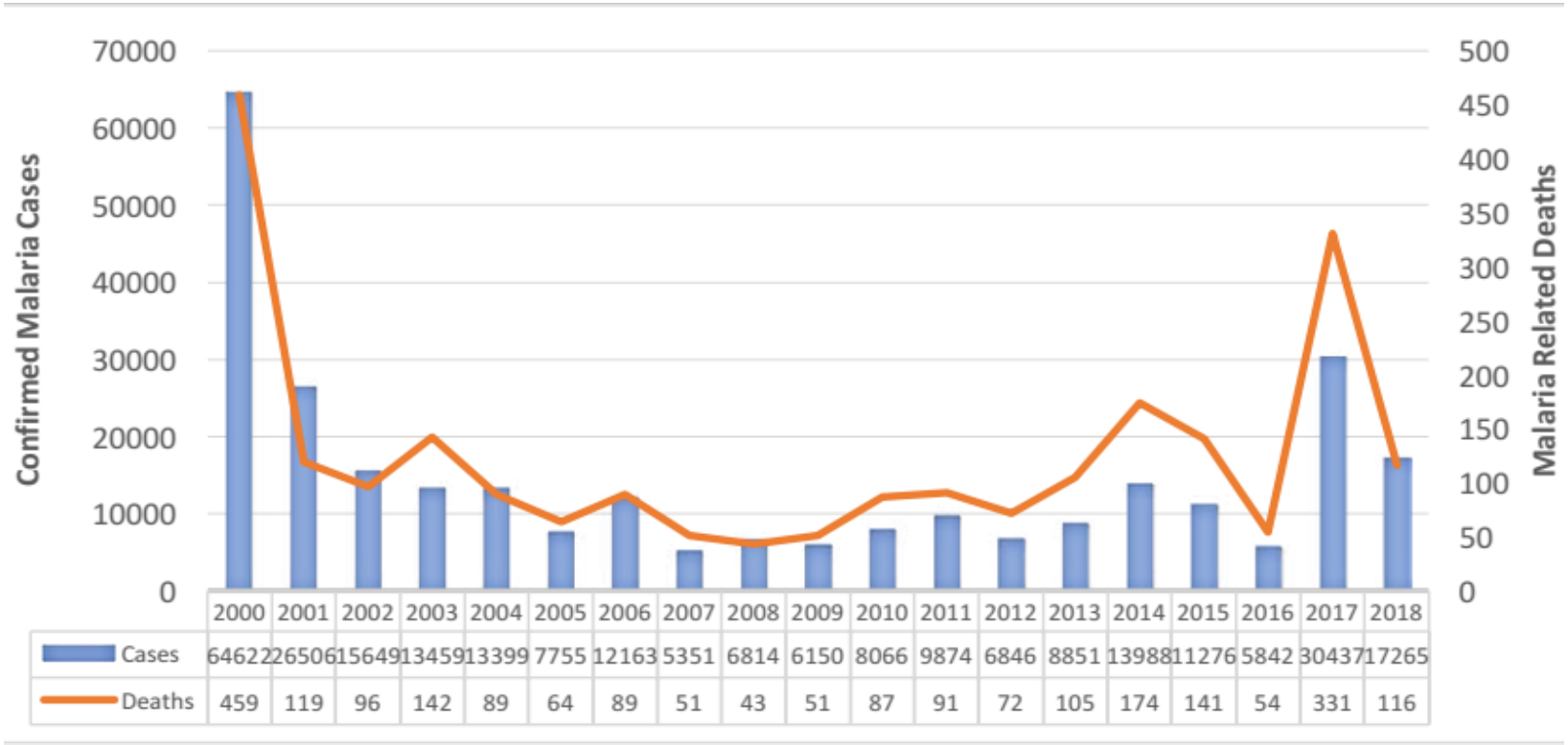

	2000	2001	2002	2003	2004	2005	2006	2007	2008	2009	2010	2011	2012	2013	2014	2015	2016	2017	2018
Cases	64622	26506	15649	13459	13399	7755	12163	5351	6814	6150	8066	9874	6846	8851	13988	11276	5842	30437	17265
Deaths	459	119	96	142	89	64	89	51	43	51	87	91	72	105	174	141	54	331	116

Figure 2.4. Malaria cases in South Africa between 2010 and 2018 (Aide et al., 2019).

The projection made when the malaria elimination strategic plan was launched in 2019 detailing how SA would have eliminated malaria by 2023 may not have been a realistic goal. The COVID-19 pandemic that affected all parts of the globe in late November of 2019 complicated the detection and diagnosis of malaria, thus hindering malaria eradication endeavors (Wilairatana et al., 2021). The SARS-CoV-2 virus, causing the coronavirus disease, presents symptoms like those of malaria-infected persons, has redirected the focus from malaria to COVID-19 (Sherrard-Smith et al., 2020). Through robust screening approaches and working together with its neighboring countries (Eswatini, Mozambique, Botswana, Namibia, Zimbabwe, Zambia, and Angola), SA needs to craft another strategic plan that will factor in the negative effects of the COVID-19 pandemic and implement that to ensure no malaria cases go undetected during the coronavirus pandemic. When waging war against the *Plasmodium* parasite, drug interventions and malaria vaccines targeting different stages of its life cycle are the mainstays.

2.5. Malaria vaccine development and its prospects

Money invested in malaria vaccine development yields promising turnouts (King, 2019; Wilson et al., 2019). A virosomal recombinant CyRPA vaccine, which prevents *P. falciparum* parasites from entering the erythrocytes, has been developed and tested in preclinical trials. The CyPRA vaccine was reported to produce the desired immune response targeting the parasite blood stages (Tamborrini et al., 2020). Another vaccine candidate, the RTS, S malaria vaccine developed by GlaxoSmithKline (GSK), has been rolled out in some African countries like Malawi to treat malaria in young children (Mahase, 2019). The vaccine triggers the immune response against the first stages of post-*P. falciparum* introduction in the bloodstream. It prevents

malaria parasites from infecting the liver cells (Malaria Vaccine Initiative, 2021). There are positive preliminary results from the initial vaccine rollout. However, medical concerns are mounted against the RTS, S, which predisposes injected subjects to cerebral malaria and meningitis (Aaby et al., 2020).

Doshi (2020) argues that international ethical standards were bridged when the RTS, S vaccine doses were administered to young children without informed consent. It is further alleged that the clinical trials did not run for the minimum required time sufficient to establish efficacy and clinical safety beyond reasonable doubt (Doshi, 2020). Therefore, it is expedient that transparency is exercised in vaccine discovery endeavors because such criticisms (if substantive) can easily erode the public's acceptance of vaccines as a viable chemotherapeutic option. Studies conducted by the Malaria Vaccine Initiative (MVI) have carved a clear research path towards discovering effective malaria vaccines by outlining two priority program areas: prevention of infection and transmission-blocking. More research is still ongoing in these priority areas, and further clinical studies are underway to ascertain the effectiveness of different vaccines (Blank et al., 2020).

2.6. Malaria chemotherapy

Drug interventions are the most common chemotherapeutic agents available to prevent and treat malaria (Galatas et al., 2021). Most of these available therapeutic drugs rely on different molecular targets to prevent transmission at different stages of the *Plasmodium* life cycle (Batista et al., 2020; Yadav et al., 2019). Quinine (**1**), isolated from *Cinchona calisaya* Wedd., was the first drug used to remedy malaria (Figure 2.5) (Gisselmann et al., 2018). It is a schizocide and has gametocidal properties against *P. vivax* and *P. Malariae* (Achan et al., 2011). Artemisinin (**2**), derived from *Artemisia*

annua L., (Figure 2.5), is the prescribed drug for treating complicated and uncomplicated malaria. Doxycycline (**3**), atovaquone (**4**), and proguanil (**5**) are also effective malaria prophylaxis drugs (Figure 2.6) used against acute infections caused by *P. falciparum* with limited effectiveness against malaria caused by *P. ovale* and *P. malariae* (Gaillard et al., 2018).

Artemisinin monotherapy (a single drug utilized to treat a disease) had been the gold standard for treating complicated falciparum malaria (Mita et al., 2009). Its success was employing a two-step mechanism of action. Firstly, it gets activated by the heme-iron in the parasite, which cleaves the endoperoxide. Upon cleavage of this endoperoxide, free radicals kill the *Plasmodium* parasite by alkylating it and poisoning its essential malaria proteins (Meshnick et al., 1996). Common artemisinin derivatives (Figure 2.7) that were used to treat malaria include dihydroartemisinin (**6**), artemether (**7**), arteether (**8**), artesunic acid (**9**), and sodium artesunate (**10**) (Patel et al., 2021). These derivatives intrinsically possess a short half-life with low bioavailability levels, thus making them less effective as malaria monotherapy.

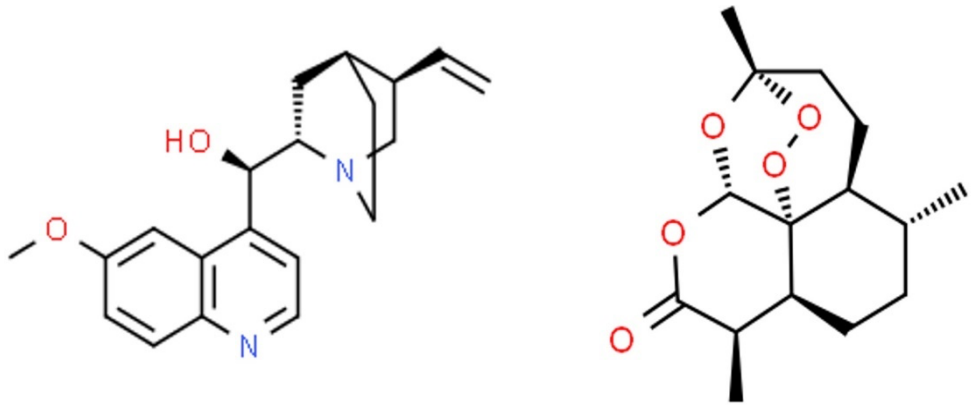

(1) Quinine **(2)** Artemisinin

Figure 2.5. Chemical structures of quinine and artemisinin

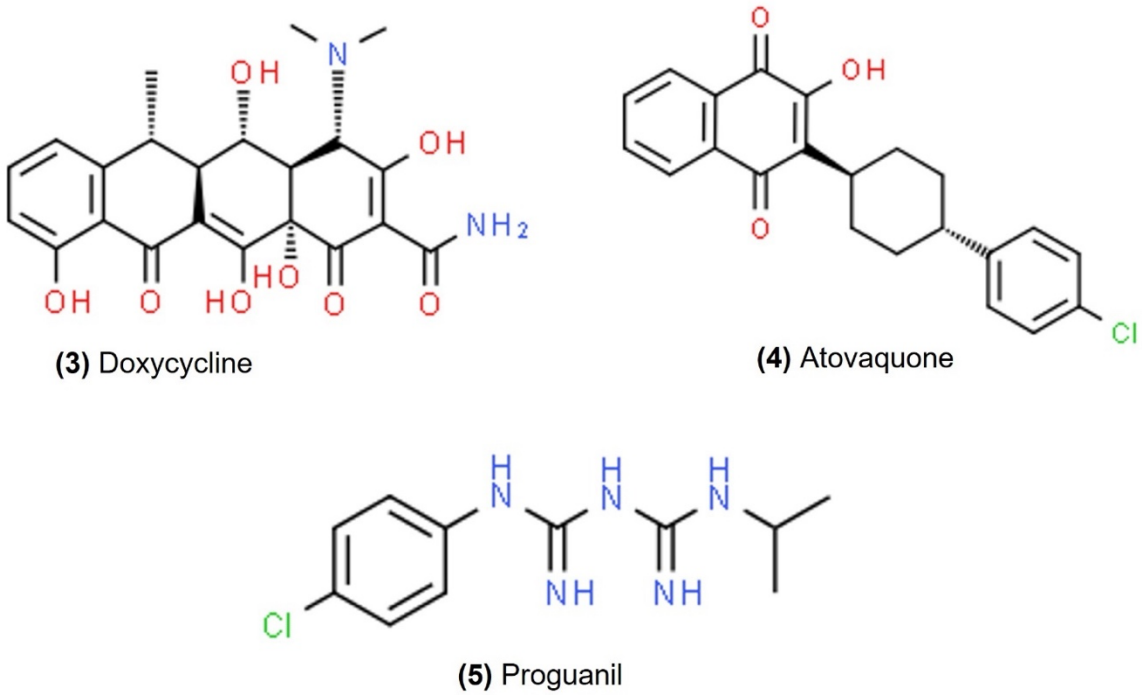

(3) Doxycycline **(4)** Atovaquone

(5) Proguanil

Figure 2.6. Antiplasmodial drugs with limited bioavailability.

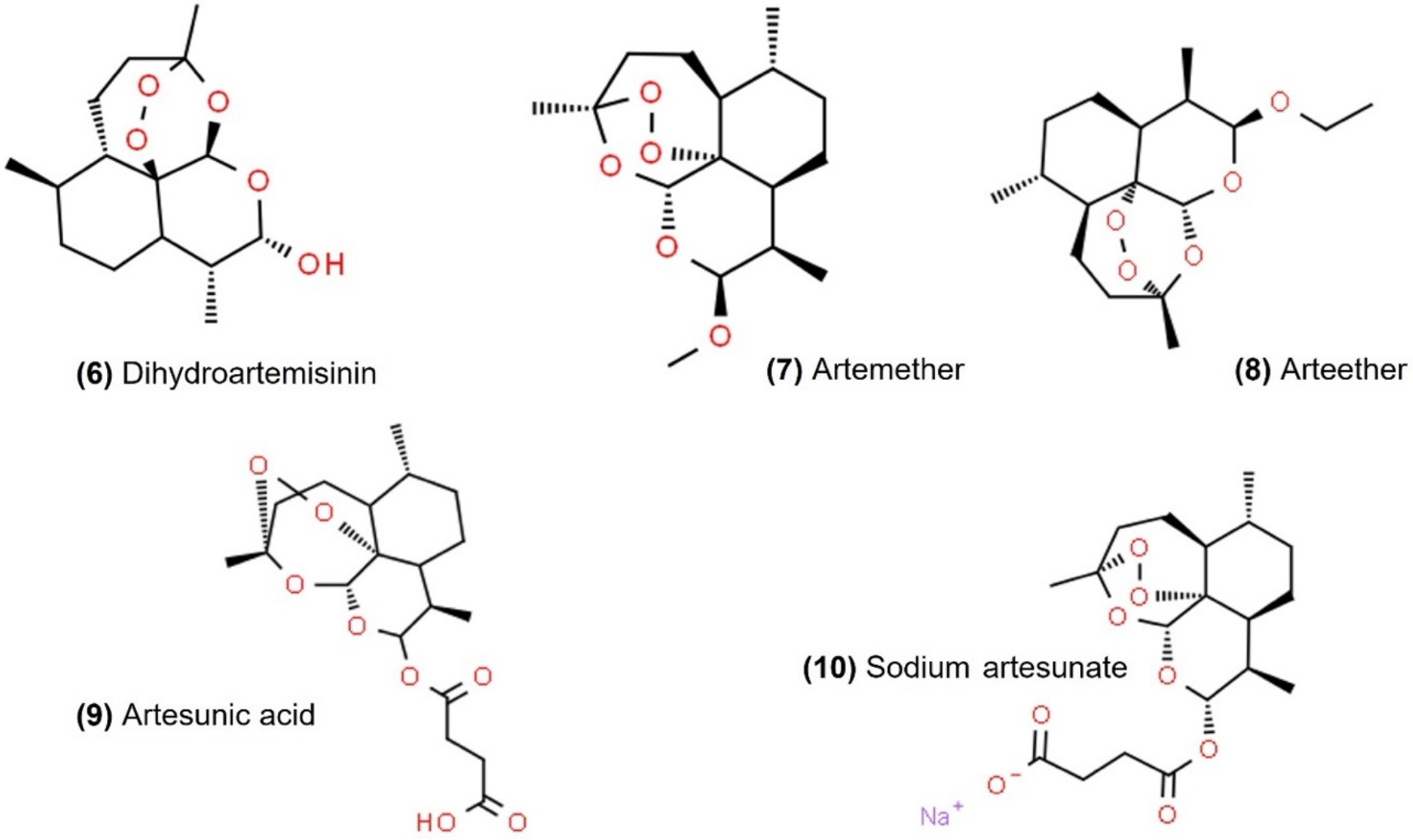

Figure 2.7. Chemical structures of artemisinin derivatives.

Artemisinin-based combination therapies (ACTs) were rolled out in 2005 to enhance the efficacy of artemisinin monotherapies (Arya et al., 2020). These leverage on combining artemisinin derivatives with a companion drug into one tablet to enhance bioavailability and bioactivity. Common companion drugs used with artemisinin include lumefantrine (**11**), mefloquine (**12**), amodiaquine (**13**), pyrimethamine (**14**), piperaquine (**15**), and chlorproguanil (**16**) (Figure 2.8). These ACTs bring together two-drug regimens with different modes of action to outsmart the parasite's proliferative potential in its different life-cycle stages. Studies have shown that sodium artesunate (modified artesunate) and conjugate base capsules of artesunate-heparin have enhanced solubility, thus positively affecting its efficacy (Adebayo et al., 2020). A pharmacokinetic study of primaquine (**17**) has revealed its ability to provide a radical cure when combined with ACT, and this has revolutionized scientific understanding of the significance of combination therapies (Daher et al., 2019). A significant reduction in the malaria burden is a good indicator of these antiplasmodial drug interventions (Rabinovitch et al., 2017). However, complete eradication is still far from being achieved, and consistent resurgences keep occurring quite frequently

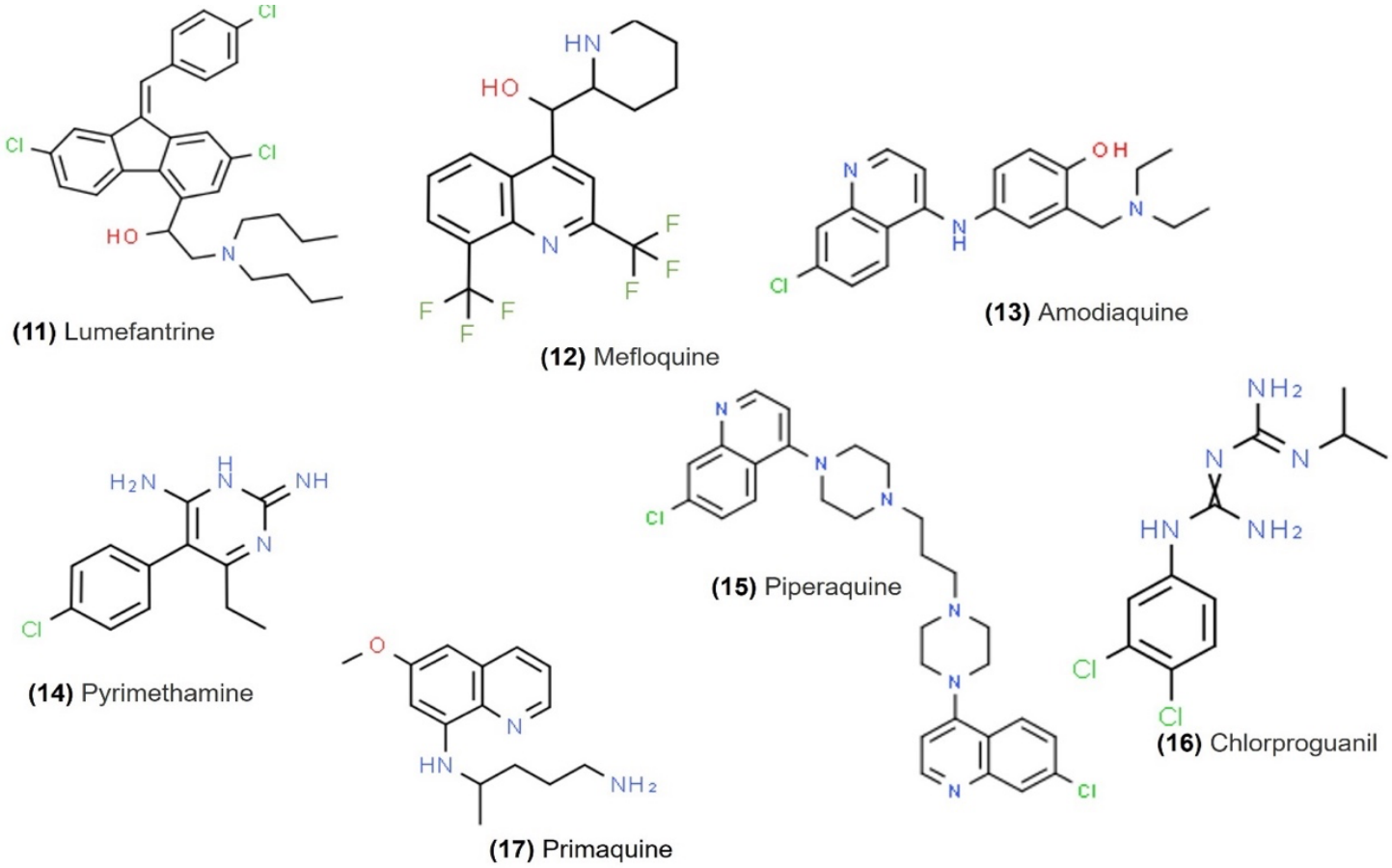

Figure 2.8. Some companion drugs used with artemisinin in ACTs.

Plasmodium parasites exhibit drug resistance, thus rendering the treatment ineffective (Hassett & Roepe, 2021). Malaria drug resistance to both mono- and combination therapies are common to *P. falciparum* and *P. vivax* (Romphosri et al., 2020). The effectiveness of ACTs is increasingly complicated by partner drug resistance (Suresh & Haldar, 2018). The mounting predicament of partner drug resistance has prompted researchers to add a second partner drug that forms a triple combination treatment regime for artemisinin. This triple therapy is believed to function as a stop-gap therapy for multidrug-resistant malaria to buy some time until new antimalarial agents can be discovered (Van der Pluijm et al., 2021). To keep up with the ever-evolving parasite, drugs with different mechanisms of action and diverse chemical structures need to be developed. When searching for sources for new drug leads and even bio-safe insecticides, the botanical kingdom is mostly consulted for solutions (Erhirhie et al., 2021)

2.7. Plants as sources for antimalarial drug leads

Historically, plants have proven to have the capacity to supply drug leads that produce an effective treatment for various diseases (Newman & Cragg, 2016). Plants have been the best sources of healing for humanity since antiquity, and they still do even today. About 80% of the world's population uses medicinal plants for primary health care (Noronha et al., 2020). Their implied safety has granted them acceptability in many indigenous cultural communities. Plant metabolites are preferred entities in the drug discovery processes over synthetic compounds for different reasons (Hao & Xiao, 2020). Phytoconstituents have many chiral centers, a high O_2: N_2 ratio, a lower aromatic ring: atom ratio, and a higher ratio of hydrogen bond donors and acceptor functional groups (Yuliana et al., 2013). These characteristics make plant metabolites

desirable choice drug candidates and *par excellence*. Most of the top currently prescribed drugs originate directly or indirectly from medicinal plant species (Singh et al., 2019).

Recent research endeavors have focused on discovering novel antimalarial drug leads, and plants provide the best sources (Saxena et al., 2003). Many plant extracts have been confirmed to have antiplasmodial activity against some of the most virulent *Plasmodium* species (Bapela et al., 2014; Bero et al., 2009; Kalauni et al., 2006; Kiringe, 2006; Nguta et al., 2010; Portet et al., 2007; Saxena et al., 2003; Ziegler et al., 2002). Most of these plants have not been studied in-depth for their antiplasmodial biological activity. Most of the specific compounds attributed to the antiplasmodial activity have not been isolated and characterized. Antimalarial plant species have not been extensively explored in SA and many other malaria-endemic countries; hence, they need to be studied for novel antimalarial phytoconstituents.

2.8. Taxonomy, distribution, and description of *Pappea capensis*

Pappea capensis Eckl. & Zeyh. (Sapindaceae) is an indigenous, drought-tolerant plant species widely distributed in Africa (Robbertse et al., 2011). Information from the South African National Biodiversity Institute (SANBI) shows that *P.* capensis is not endemic to SA and can be found in all nine provinces (SANBI, 2019). As it is commonly referred to in English, jacket plum includes *P. fulva* Conrath, *P. radlkoferi* Schweinf. ex Penzig, *P. schumanniana* Schinz, *P. ugandensis* Baker f. and *Sapindus pappea* Sond (SANBI, 2019). Taxonomically, *P. capensis* is the only species in the *Pappea* genus. There are 1900 species in the *Pappea* genus distributed among 144 genera. In South Africa, the family is represented by seven genera and 12 species (Buerki et al., 2021).

Pappea capensis is referred to by varying local names among South African ethnic groups. In isiXhosa, it is called *umgqalutye*, *indaba* in isiNdebele, *tshikavhavhe* in Tshivenda, *uzagogwane* in isiZulu, *mongatane/mopsinyugane* in Sesotho, *doppruim* in Afrikaans, and *liletsa* in Siswati (Raimondo et al., 2009; SANBI, 2019). *Pappea* capensis can reach a height of 3.9 m tall in different ecological conditions (Palmer & Pitman, 1972; Venter & Venter, 1996). It has grey/pale stems with choppy branches, which are considered distinguishing characteristics of the plant (Mng'omba et al., 2008). It also has red edible fruits that are considered a delicacy. The leaves are oblong, simple, wavy, and hard-textured. The younger leaves which sprout in spring are easily distinguishable by their pinky-bronze color, and the older leaves have a dark green appearance (Karau et al., 2012).

There are still disagreements regarding the sexuality of *P. capensis*, its structure, and the type of inflorescence. However, there seems to be a consensus that attributes *P. capensis* to be a monoecious plant (Mng'omba et al., 2008). It flowers between December and April, producing male flowers first then female ones at the end of the flowering year. The inflorescence resembles a thyrse of a tiny flower. The male flowers contain five short-lived petals, eight stamens, and a poorly developed pistil. The female flowers have a trilobed ovary, one stigma, and a style with eight staminodes (Robbertse et al., 2011).

2.9. Ethnomedicinal uses of *Pappea capensis*

Pappea capensis presents widespread ethnomedicinal and non-medicinal uses (Karau et al., 2012). African indigenous people harvest *P. capensis* edible fruits to manufacture vinegar, jelly, and jam (Mng'omba et al., 2008). The seeds produce soap, edible oils, and metal lubricating oils (Robbertse et al., 2011; Van Wyk and Wink,

2017). *Pappea capensis* oils can also be utilized as a biodiesel alternative power source. Besides the nutritional benefits, *P. capensis* has been flagged as a major bush encroacher in pasture lands and continuously reducing the quality of grasslands; the fate of *P. capensis* is yet to be determined.

Ethnomedicinally, *P. capensis* is a significant *materia medica*. The Maasai from Kenya crushes the stem bark, soak it in cold or warm water for a few days and drinks the infusion. The infusion boosts the courage of hunters and people watching over the livestock and is also administered for malaria treatment (Watt & Breyer-Brandwijk, 1962). The Machakos and the Makueni in Kenya administer the root and stem bark infusion to treat painful joints (Wambugu et al., 2011). The Ndebele tribes in Southern Africa use the leaf water infusion to treat painful eyes, while the root infusion works to purge cattle (Hutchings & Scott, 1996). Batswana treat venereal diseases using the water infusion from the stem bark and use it as protective sprinkling charms (Hedberg & Staugård, 1989). The Gumuz indigenous people of Ethiopia administer a bark decoction of *P. capensis* to treat malaria and tiredness (Asnake et al., 2016). Table 2.1 summarizes other traditional and ethnomedicinal uses of *Pappea capensis* in the African continent.

Table 2.1. Ethnomedicinal uses of *Pappea capensis.*

Plant part	Preparation	Ethnomedicinal uses
Fruits	Eaten raw	Diarrhea and Vitamin C (Kokwaro, 1976)
Leaf	An infusion is prepared and taken orally.	Eye infection, aphrodisiac, diabetes, and sexually transmitted infections (Hutchings & Scott, 1996)
Stem bark	decoction (oral)	Aphrodisiac for men and stomach problems, protective charms, and whooping cough (Hedberg & Staugård, 1989; Watt & Breyer-Brandwijk, 1962)
Branches/Twigs	Boiled in water and drunk	Malaria (Koch et al., 2005)
Roots	Infusion macerated	Chest pains, enema, cattle purgative (Hedberg & Staugård, 1989; Watt & Breyer-Brandwijk, 1962)
Seeds	A tincture prepared from kernel	Constipation (Venter & Venter, 1996)
Kernel	Oil squeezed from seeds.	*Tinea capitis,* alopecia, hair restorative and ringworms (Hutchings & Scott, 1996)

2.10. Phytochemistry of *Pappea capensis*

Karau et al. (2012) phytochemically profiled and analyzed the leaf and stem bark extracts of *P. capensis,* discovering the presence of alkaloids, steroids, tannins, flavonoids, ascorbic acid, alpha-tocophenol, beta-carotene, beta-cryptoxanthin, thiamine, psi-carotene (lycopene), and nicotinamide were in abundance. Minerals identified include selenium, iron, copper, zinc, manganese, chromium, nickel, vanadium, molybdenum, and cobalt. The observed nutritional and medicinal value of *P. capensis* are attributed to these minerals and phytoconstituents, respectively. Forty-nine compounds were identified using the NIST11 database, and only 13 had unknown chemical structures. Pendota et al. (2017) isolated two flavonoid compounds (Figure 2.9) from *P. capensis* methanol leaf extract: epicatechin (**18**) and quercetin-3-O-rhamnoside (**19**) (Pendota et al., 2009). Antioxidant and antimicrobial biological assays conducted on the isolated compounds produced significant activity. Tajuddeen et al. (2021) successfully isolated epicatechin (**18**), quercetin 3-O-arabinopyranoside (**20**), quercetin 3-O-α-L-rhamnoside (*21*), and kaempferol 3-O-arabinopyranoside (**22**) from *P. capensis* leaf extracts. These were tested on the 3D7 strain of *P. falciparum* and reported *in vitro* antiplasmodial viability (Tajuddeen et al., 2021).

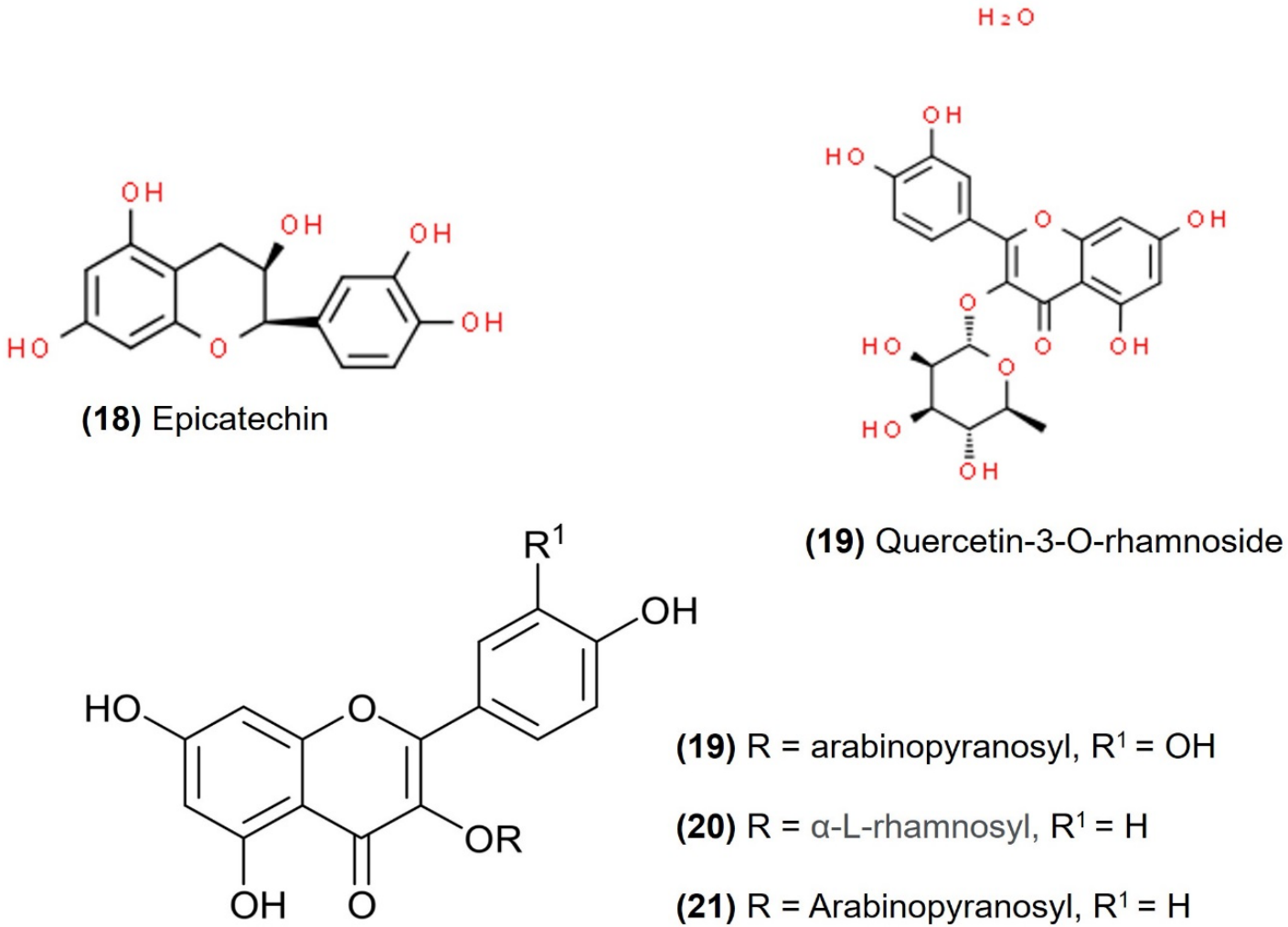

Figure 2.9. Antiplasmodial compounds isolated from *Pappea capensis* (Pendota et al., 2017).

2.11. Pharmacological properties of *Pappea capensis*

The pharmacological properties of *P. capensis* have not been studied broadly and in great detail. However, through bibliometrics, it can be established from the ethnobotanical surveys that it is a tree worth consideration for antiplasmodial drug leads (Bolscher et al., 2015). Some plant parts of *P. capensis* have been tested for different pharmacological responses on different parasites and microbes. The ethyl acetate leaf and bark extracts have demonstrated antimicrobial properties against many pathogenic bacterial strains (Karau, 2014). The presence of phenolic compounds in the plant, which are well known to induce antimicrobial activity, is believed to be responsible for the observed pharmacological response (Okwu & Emenike, 2006). Other pharmacological properties like antiviral, antitumor, antioxidant, and anti-inflammatory have not been reported for *P. capensis*. They can only be inferred to be present by studying phytochemical composition (Karau, 2014). The antiviral, antimicrobial, and antitumor activities of *P. capensis* are attributed to tannin phytoconstituents (Aiyelaagbe & Osamudiamen, 2009; Gulfraz et al., 2011). Flavonoids can be attributed to the anti-inflammatory and antioxidant activity observed in *P. capensis* (Harisaranraj et al., 2009).

2.12. Antiplasmodial activity of *Pappea capensis*

The antiplasmodial activity of *P. capensis* is known to be induced by the polar (methanol and water) and non-polar (dichloromethane) extracts of its leaves, roots, and twigs (Bapela et al., 2014; Mokoka et al., 2013). Three studies validated the antimalarial properties of *P. capensis* crude extracts. Bapela et al. (2014) extracted from the twigs using DCM: 50% methanol (1:1, v/v) and reported a significant antiplasmodial activity from the dichloromethane extract (IC_{50} = 5.47 µg/ml). Mokoka

et al. (2013) extracted the roots and leaves using DCM: MeOH (1:1, v/v), and the antiplasmodial activity ranged from good to moderate (5.30 µg/ml and IC_{50} = 9.67 µg/ml, respectively). Koch et al. (2005) extracted from the plant's inner bark using chloroform, and a low antiplasmodial activity was obtained IC_{50} ≥10 µg/ml. The investigated plant parts were collected from diverse geographical areas, which explains the disparity in the observed bioactivity. The different plant parts differ morphologically and may also result in the discrepancy observed in the antiplasmodial bioactivity observed in the extracts. These factors may have affected the phytoconstituent quality and quantity in the plants, thus resulting in variable antiplasmodial bioactivity in these studies. Although validation of the ethnomedicinal significance of treating malaria using *P. capensis* was confirmed, the phytochemical constituents responsible for the observed antiplasmodial bioactivity in *P. capensis* are still unknown.

2.13. Plant metabolomics and analysis

Natural product research and drug discovery have greatly benefited from cutting-edge plant metabolomics techniques, ushering in comprehensive qualitative/quantitative analysis of plant metabolites (Salem et al., 2020). It measures, qualifies, and quantifies low molecular weight phytoconstituents that traditional methods may not be easily detectable (Clish, 2015). Plants consist of many phytochemicals with varied characteristics at different concentrations, which always complicates the discovery of drugs from plants. There is a need to incorporate techniques to scale up metabolite recovery and enhance global metabolite analysis by increasing the sensitivity to low molecular weight metabolites with low concentrations (Fidele et al., 2013). While metabolomics-based techniques are relatively new, many

publications have been produced in ethnopharmacology (Bapela et al., 2019; Freire et al., 2019; Heyman & Meyer, 2012; Kamal et al., 2017; Lajis et al., 2017; Tawfike et al., 2013; Verpoorte et al., 2007).

2.14. Application of metabolomics in phytomedicine

Metabolomics has broad applicability in phytomedicine, especially quality control (QC), chemotaxonomic studies, and drug discovery (Heyman & Meyer, 2012; Kumar, 2016). The QC or quality assurance of various herbal extracts is paramount, especially for pharmaceutical viability. It is also a prime step towards ensuring the reproducibility of the pharmacological response of herbal products across all batches. Reproducibility can be ensured by standardizing the different herbal formulations to ensure the same active ingredients are present at the same dose and concentration (Heyman & Meyer, 2012). Plant metabolomics affords the possibility of studying small quantity molecules in complex samples and biological systems (Burgess et al., 2014). It is expedient in identifying and isolating low quantity molecules in biological systems (Dayalan et al., 2018). It also permits the authentication of different crude extracts and enhances the understanding of natural medicines, which is essential in drug discovery (Lajis et al., 2017).

2.15. Different types of metabolomics analysis in phytomedicine

Metabolite databases are created to allow the ease, efficiency, and effective identification of low molecular weight phytoconstituents from complex plant samples (Levin et al., 2016). This identification can be carried out in two separate but complementary metabolomics approaches, namely targeted and untargeted metabolomics (Patti et al., 2012). Untargeted metabolomics identifies many

compounds using techniques like gas chromatography (GC) or liquid chromatography (LC) alongside mass spectrometry (MS) and proton NMR (^{1}H NMR) (Wishart, 2016). Bioinformatics tools easily detect over 2000 compounds in an extract in a single run. However, this comes with a huge trade-off in tedious data processing and analysis when identifying phytoconstituents. Targeted metabolomics incorporates measuring specific constituents to confirm the results of an untargeted metabolomics analysis (Khoomrung et al., 2017). This approach uses specific metabolite detection methods that utilize principles of compound specificity, sensitivity, detection, quantification, accuracy, and precision (Khoomrung et al., 2012, 2014). It is thus imperative to first set up and validate a detection method using standard reference material. Quantifying constituents in plant samples can only be conducted after this has been done. (Khoomrung et al., 2013).

2.16. Chemical analytical techniques used in plant metabolomics

Various hyphenated chemical analytical methods used in plant metabolomics include GC-MS, LC-MS, CE-MS, LC-NMR and LC-FTIR. These can allow fast, sensitive, and efficient active hit assessments (Salem et al., 2020; Umar et al., 2021). For example, LC-FTIR was successfully used to evaluate the antioxidant and α-glucosidase inhibitory activities of *Curculigo orchioides* and *C. latifolia* plant species (Umar et al., 2021). This technique also demonstrated the ability to distinguish between the two plant species, thus affirming the significance of its metabolomics acumen in chemotaxonomic studies. However, the major downfall to these techniques is the high costs associated with their usage; the equipment can be pricey and technical to use, thus requiring specialized skills. These can largely hinder the drug discovery

procedure, thus precluding many of these techniques from being efficiently used in different settings.

There is a silver lining; ^{1}H NMR and GC-MS spectroscopy techniques work efficiently, especially when used complementarily to each other. Proton NMR spectroscopy is non-destructive, unbiased, able to quantify metabolites, requires very little or no chromatographic separation, and no sample derivatization is needed (Emwas et al., 2019). Incorporating GC-MS into metabolomics complements ^{1}H NMR spectroscopy shortcomings. There are limitations to using ^{1}H NMR-based metabolomics to study herbal extracts. It has low sensitivity, and signals may overlap, and it is always good practice to rely on different analytical approaches for accuracy (Bhinderwala et al., 2018). The low sensitivity of ^{1}H NMR spectroscopy could affect the integrity of the obtained results and thus further complicate the study of metabolites in the plant sample. However, these limitations may be overcome through optimization and introducing GC-MS to compensate for ^{1}H NMR spectroscopy's shortcomings (Emwas, 2015). Nuclear Magnetic Resonance spectroscopy is incapable of analyzing volatiles; thus, GC-MS is incorporated to cater to this limitation and detect low molecular weight phytoconstituents in complex plant extracts. Gas Chromatography coupled with MS can also be used with another variant of ^{1}H NMR called 2D NMR to study complex plant crude extracts (Guo et al., 2020).

Different scholars have applied metabolomics in bioprospecting plants with antiplasmodial properties to isolate bioactive constituents (Alhadrami et al., 2021; Allman et al., 2016; Bapela et al., 2019; Freire et al., 2019; Kamal et al., 2017). Different analytical techniques and metabolomics approaches have been exploited to understand the antiplasmodial pharmacological value of other plants and isolated

compounds. However, there have not been any studies where ^{1}H NMR has been coupled with GC-MS to study the antiplasmodial properties of crude extracts. This study's burden is to understand the antiplasmodial properties of *P. capensis* crude extracts by employing these two metabolomics approaches.

2.17. References

Aaby, P., Fisker, A.B., Björkman, A., Benn, C.S., 2020. WHO's rollout of malaria vaccine in Africa: can safety questions be answered after only 24 months? The BMJ 368, 1–6.

Achan, J., Talisuna, A.O., Erhart, A., (…), D'Alessandro, U., 2011. Quinine, an old anti-malarial drug in a modern world: role in the treatment of malaria. Malaria Journal 10, 1–12.

Adebayo, J.O., Tijjani, H., Adegunloye, A.P., Ishola, A.A., Balogun, E.A., Malomo, S.O., 2020. Enhancing the antimalarial activity of artesunate. Parasitology Research 119, 2749–2764.

Aide, P., Candrinho, B., Galatas, B., (…), Saúte, F., 2019. Setting the scene and generating evidence for malaria elimination in Southern Mozambique. Malaria Journal 18, 190.

Aiyelaagbe, O.O., Osamudiamen, P.M., 2009. Phytochemical screening for active compounds in *Mangifera indica* leaves from Ibadan, Oyo State. Plant Science Research 2, 11–13.

Alhadrami, H.A., Sayed, A.M., El-Gendy, A.O., (…), Hozzein, W.N., 2021. A metabolomic approach to target antimalarial metabolites in the *Artemisia annua* fungal endophytes. Scientific Reports 2021 11, 1–11.

Allman, E.L., Painter, H.J., Samra, J., Carrasquilla, M., Llinás, M., 2016. Metabolomic profiling of the malaria box reveals antimalarial target pathways. Antimicrobial Agents and Chemotherapy 60, 6635.

Amoah, L.E., Acquah, F.K., Nyarko, P.B., Cudjoe, E., Donu, D., Ayanful-Torgby, R., Sey, F., Williamson, K.C., Awandare, G.A., 2020. Comparative analysis of asexual and sexual stage *Plasmodium falciparum* development in different red blood cell types. Malaria Journal 19, 1–10.

Arya, A., Kojom Foko, L.P., Chaudhry, S., Sharma, A., Singh, V., 2020. Artemisinin-based combination therapy (ACT) and drug resistance molecular markers: a systematic review of clinical studies from two malaria-endemic regions – India and sub-Saharan Africa. International Journal for Parasitology: Drugs and Drug Resistance 15, 43–56.

Ashley, E.A., Pyae Phyo, A., Woodrow, C.J., 2018. Malaria. The Lancet 391, 1608–1621.

Asnake, S., Teklehaymanot, T., Hymete, A., Erko, B., Giday, M., 2016. Antimalarial medicinal plants used by Gumuz people of Mandura Woreda, Benishangul-Gumuz Regional State, Ethiopia. Indian Journal of Traditional Knowledge 15, 546–552.

Bapela, M.J., Heyman, H., Senejoux, F., Meyer, J.J.M., 2019. ^{1}H NMR-based metabolomics of antimalarial plant species traditionally used by Vha-Venda people in Limpopo Province, South Africa, and isolation of antiplasmodial compounds. Journal of ethnopharmacology 228, 148–155.

Bapela, M.J., Meyer, J.J.M., Kaiser, M., 2014. *In vitro* antiplasmodial screening of ethnopharmacologically selected South African plant species used for the treatment of malaria. Journal of Ethnopharmacology 156, 370–373.

Bartoloni, A., Zammarchi, L., 2012. Clinical aspects of uncomplicated and severe malaria. Mediterranean Journal of Hematology and Infectious Diseases 4, e2012026.

Batista, F.A., Gyau, B., Vilacha, J.F., Bosch, S.S., Lunev, S., Wrenger, C., Groves, M.R., 2020. New directions in antimalarial target validation. Expert Opinion on Drug Discovery 15, 189–202.

Bero, J., Frédérich, M., Quetin-Leclercq, J., (…), Quetin-Leclercq, J., 2009. Antimalarial compounds isolated from plants used in traditional medicine. Journal of Pharmacy and Pharmacology 61, 1401–1433.

Bhinderwala, F., Wase, N., Dirusso, C., Powers, R., 2018. Combining mass spectrometry and NMR improves metabolite detection and annotation. Journal of Proteome Research 17, 4017.

Blank, A., Fürle, K., Jäschke, A., (…), Bujard, H., 2020. Immunization with full-length *Plasmodium falciparum* merozoite surface protein 1 is safe and elicits functional cytophilic antibodies in a randomized first-in-human trial. npj Vaccines 5, 1–15.

Bolscher, J.M., Koolen, K.M.J., Van Gemert, G.J., (…), Dechering, K.J., 2015. A combination of new screening assays for prioritization of transmission-blocking antimalarials reveals distinct dynamics of marketed and experimental drugs. Journal of Antimicrobial Chemotherapy 70, 1357–1366.

Buerki, S., Callmander, M.W., Acevedo-Rodriguez, P., (…), Forest, F., 2021. An updated infra-familial classification of Sapindaceae based on targeted enrichment data. American Journal of Botany 108, 1234–1251.

Burgess, K., Rankin, N., Weidt, S., 2014. Metabolomics, in: Handbook of Pharmacogenomics and Stratified Medicine. Elsevier Inc., pp. 181–205.

Clarkson, C., Maharaj, V.J., Crouch, N.R., (…), Folb, P.I., 2004. *In vitro* antiplasmodial activity of medicinal plants native to or naturalized in South Africa. Journal of Ethnopharmacology 92, 177–191.

Clish, C.B., 2015. Metabolomics: an emerging but powerful tool for precision medicine. Cold Spring Harbor Molecular Case Studies 1, a000588.

Daher, A., Aljayyoussi, G., Pereira, D., (…), Lalloo, D.G., 2019. Pharmacokinetics/pharmacodynamics of chloroquine and artemisinin-based combination therapy with primaquine. Malaria Journal 18, 325.

Dayalan, S., Xia, J., Spicer, R.A., Salek, R., Roessner, U., 2018. Metabolome analysis, in: Encyclopedia of Bioinformatics and Computational Biology: ABC of Bioinformatics. Elsevier, pp. 396–409.

Doshi, P., 2020. WHO's malaria vaccine study represents a "serious breach of international ethical standards." The British Medical Journal 368, 1–2.

Emwas, A.H., Roy, R., McKay, R.T., Tenori, L., Saccenti, E., Nagana Gowda, G.A., Raftery, D., Alahmari, F., Jaremko, L., Jaremko, M., Wishart, D.S., 2019. NMR spectroscopy for metabolomics research. Metabolites 9, 1–39.

Emwas, A.H.M., 2015. The strengths and weaknesses of NMR spectroscopy and mass spectrometry with particular focus on metabolomics research. Methods in Molecular Biology 1277, 161–193.

Erhirhie, E.O., Ikegbune, C., Okeke, A.I., Onwuzuligbo, C.C., Madubuogwu, N.U., Chukwudulue, U.M., Okonkwo, O.B., 2021. Antimalarial herbal drugs: a review of their interactions with conventional antimalarial drugs. Clinical Phytoscience 7, 1–10.

Fidele, T., Lizelle, P., Ian, D., 2013. Plant metabolomics: a new frontier in phytochemical analysis. South African Journal of Science 109, 1–11.

Freire, R.T., Bero, J., Beaufay, C., Selegato, D.M., Coqueiro, A., Choi, Y.H., Quetin-Leclercq, J., 2019. Identification of antiplasmodial triterpenes from Keetia species using NMR-based metabolic profiling. Metabolomics 15, 1–11.

Gaillard, T., Boxberger, M., Madamet, M., Pradines, B., 2018. Has doxycycline, in combination with anti-malarial drugs, a role to play in the intermittent preventive treatment of *Plasmodium falciparum* malaria infection in pregnant women in Africa? Malaria Journal 17, 469.

Galatas, B., Nhantumbo, H., Soares, R., (…), Munguambe, K., 2021. Community acceptability to antimalarial mass drug administrations in Magude district, Southern Mozambique: a mixed-methods study. PLOS ONE 16, e0249080.

Gisselmann, G., Alisch, D., Welbers-Joop, B., Hatt, H., 2018. Effects of quinine, quinidine, and chloroquine on human muscle nicotinic acetylcholine receptors. Frontiers in Pharmacology 9, 1339.

Gulfraz, M., Sadiq, A., Imran, M., Qureshi, R., Zeenat, M., 2011. Phytochemical analysis and antibacterial activity of *Eruca sativa* seed skin regeneration. Article in Pakistan Journal of Botany 43, 1351–1359.

Guo, Z. Feng, Bi, G. Ming, Zhang, Y. Hong, Li, J. heng, Meng, D, L., 2020. Rare benzonaphthoxanthenones from Chinese folk herbal medicine *Polytrichum commune* and their anti-neuroinflammatory activities *in vitro*. Bioorganic Chemistry 102, 104087.

Hao, D., Xiao, P., 2020. Pharmaceutical resource discovery from traditional medicinal plants: pharmacophylogeny and pharmacophylogenomics. Chinese Herbal Medicines 12, 104–117.

Harisaranraj, R., Suresh, K., Saravanababu, S., 2009. Evaluation of the chemical composition of *Rauwolfia serpentina* and *Ephedra vulgaris*. Advances in Biological Research 3, 174–178.

Hassen, J., Dinka, H., 2020. Retrospective analysis of urban malaria cases due to *Plasmodium falciparum* and *Plasmodium vivax*: the case of Batu town, Oromia, Ethiopia. Heliyon 6, e03616.

Hassett, M.R., Roepe, P.D., 2021. *In vitro* growth competition experiments suggest consequences of the substandard artemisinin epidemic that may be

accelerating drug resistance in *P. falciparum* malaria. PLOS ONE 16, e0248057.

Hedberg, I., Staugård, F., 1989. Traditional medicine in Botswana: traditional medicinal plants. Ipeleng Publishers, Botswana.

Heyman, H.M., Meyer, J.J.M., 2012. NMR-based metabolomics as a quality control tool for herbal products. South African Journal of Botany 82, 21–32.

Hutchings, Anne., Scott, A.Haxton., 1996. Zulu medicinal plants: an inventory. University of Natal Press, Pietermaritzburg.

Ingstad, B., Munthali, A.C., Braathen, S.H., Grut, L., 2012. The evil circle of poverty: a qualitative study of malaria and disability. Malaria Journal 11, 1–6.

Kalauni, S.K., Awale, S., Tezuka, Y., (…), Kadota, S., 2006. Antimalarial activity of cassane- and norcassane-type diterpenes from *Caesalpinia crista* and their structure-activity relationship. Biological and Pharmaceutical Bulletin 29, 1050–1052.

Kamal, N., Viegelmann, C. v., Clements, C.J., Edrada-Ebel, R.A., 2017. Metabolomics-guided isolation of anti-trypanosomal metabolites from the endophytic fungus *Lasiodiplodia theobromae*. Planta Medica 83, 565–573.

Karau, G.M., 2014. Antidiabetic activities of ethyl acetate and aqueous extracts of *Pappea capensis*, *Senna spectabilis*, *Maytenus obscura*, *Ocimum americanum,* and *Launaea cornuta*. Nairobi.

Karau, G.M., Njagi, E.N.M., Machocho, A.K., Wangai, L.N., 2012. Phytonutrient, mineral composition, and *in vitro* antioxidant activity of leaf and stem bark powders of *Pappea capensis* (L.). Pakistan Journal of Nutrition 11, 123–132.

Khoomrung, S., Chumnanpuen, P., Jansa-Ard, S., Nookaew, I., Nielsen, J., 2012. Fast and accurate preparation of fatty acid methyl esters by microwave-assisted derivatization in the yeast *Saccharomyces cerevisiae*. Applied Microbiology and Biotechnology 2012 94:6 94, 1637–1646.

Khoomrung, S., Chumnanpuen, P., Jansa-Ard, S., Staìšhlman, M., Nookaew, I., Borén, J., Nielsen, J., 2013. Rapid quantification of yeast lipid using microwave-assisted total lipid extraction and HPLC-CAD. Analytical Chemistry 85, 4912–4919.

Khoomrung, S., Raber, G., Laoteng, K., Francesconi, K.A., 2014. Identification and characterization of fish oil supplements based on fatty acid analysis combined with a hierarchical clustering algorithm. European Journal of Lipid Science and Technology 116, 795–804.

Khoomrung, S., Wanichthanarak, K., Nookaew, I., (…), Akarasereenont, P., 2017. Metabolomics and integrative omics for the development of Thai traditional medicine. Frontiers in Pharmacology 8, 474.

Kibret, S., Glenn Wilson, G., Ryder, D., Tekie, H., Petros, B., 2019. Environmental and meteorological factors linked to malaria transmission around large dams at three ecological settings in Ethiopia. Malaria Journal 18, 1–16.

King, A., 2019. Building a better malaria vaccine. Nature 575, S51–S54.

Kiringe, J.W., 2006. A survey of traditional health remedies used by the Maasai of Southern Kaijiado District, Kenya. Ethnobotany Research & Applications 4, 61–73.

Koch, A., Tamez, P., Pezzuto, J., Soejarto, D., 2005. Evaluation of plants used for antimalarial treatment by the Maasai of Kenya. Journal of Ethnopharmacology 101, 95–99.

Kokwaro, J.O., 1976. Medicinal plants of east Africa. East African Literature Bureau, Nairobi.

Kumar, D., 2016. Nuclear magnetic resonance (NMR) spectroscopy for metabolic profiling of medicinal plants and their products. Critical Reviews in Analytical Chemistry 46, 400–412.

Lajis, N., Maulidiani, M., Abas, F., Ismail, I.S., 2017. Metabolomics approach in pharmacognosy, in: Pharmacognosy: Fundamentals, Applications, and Strategy. Elsevier, pp. 597–616.

Levin, N., Salek, R.M., Steinbeck, C., 2016. From databases to big data, in: Metabolic Phenotyping in Personalized and Public Healthcare. Elsevier Inc., pp. 317–331.

MacArayan, E., Papanicolas, I., Jha, A., 2020. The quality of malaria care in 25 low-income and middle-income countries. BMJ Global Health 5, 2023.

Maharaj, R., Seocharan, I., Qwabe, B., Mkhabela, M., Kissoon, S., Lakan, V., 2019. Decadal epidemiology of malaria in KwaZulu-Natal, a province in South Africa targeting elimination. Malaria Journal 18, 368.

Mahase, E., 2019. Malawi launches the first malaria vaccination program for children. The BMJ 365, l1901.

Malaria Vaccine Initiative, 2021. Malaria parasite life cycle [WWW Document]. PATH's Malaria Vaccine Initiative. URL https://www.malariavaccine.org/malaria-and-vaccines/vaccine-development/life-cycle-malaria-parasite (accessed 5.25.21).

Meshnick, S.R., Taylor, T.E., Kamchonwongpaisan, S., 1996. Artemisinin and the antimalarial endoperoxides: from herbal remedy to targeted chemotherapy. Microbiological Reviews 60, 301–315.

Mita, T., Tanabe, K., Kita, K., 2009. Spread and evolution of *Plasmodium falciparum* drug resistance. Parasitology International 58, 201–209.

Medicines for Malaria Venture, 2019. ASMQ (artesunate-mefloquine). [WWW Document]. Malaria Vaccine Initiative. https://www.mmv.org/access/products-projects/asmq-artesunate-mefloquine-treatment-acute-uncomplicated-p-falciparum (accessed 5.25.21).

Mng'omba, S.A., du Toit, E.S., Akinnifesi, F.K., 2008. Plant regeneration through somatic embryogenesis of jacket plum (*Pappea capensis*). New Zealand Journal of Crop and Horticultural Science 36, 137–144.

Mokoka, T.A., Xolani, Peter.K., Zimmermann, S., Hata, Y., Adams, M., Kaiser, M., Moodley, N., Maharaj, V., Koorbanally, N.A., Hamburger, M., Brun, R., Fouche, G., 2013. Antiprotozoal screening of 60 South African plants, and the identification of the antitrypanosomal germacranolides schkuhrin I and II. Planta Medica 79, 1380–1384.

Mota, M.M., Mello-Vieira, J., 2019. Parasitism: *Anopheles* mosquitoes and *Plasmodium* parasites share resources. Current Biology 29, R632–R634.

Mukhtar, A.Y.A., Munyakazi, J.B., Ouifki, R., 2020. Assessing the role of human mobility on malaria transmission. Mathematical Biosciences 320, 108304.

National Department of Health, 2018. Malaria risk map for South Africa 2018 [WWW Document]. The South African National Travel Health Network. URL https://www.santhnet.co.za (accessed 7.31.19).

Newman, D.J., Cragg, G.M., 2016. Natural products as sources of new drugs from 1981 to 2014. Journal of Natural Products 79, 629–661.

Nguta, J.M., Mbaria, J.M., Gakuya, D.W., Gathumbi, P.K., Kiama, S.G., 2010. Antimalarial herbal remedies of Msambweni, Kenya. Journal of Ethnopharmacology 128, 424–432.

Noronha, M., Pawar, V., Prajapati, A., Subramanian, R.B., 2020. A literature review on traditional herbal medicines for malaria. South African Journal of Botany 128, 292–303.

Obebe, O.O., Falohun, O.O., 2021. Epidemiology of malaria among HIV/AIDS patients in sub-Saharan Africa: a systematic review and meta-analysis of observational studies. Acta Tropica 215, 105798.

Okwu, D., Emenike, I., 2006. Evaluation of the nutrients and vitamins content of citrus fruits. International Journal of Molecular Medicine and Advanced Sciences 2, 1–6.

Palmer, E., Pitman, N., 1972. Trees of Southern Africa: covering all known indigenous species in the Republic of South Africa, South-West Africa, Botswana, Lesotho & Swaziland. Balkema, Cape Town.

Patel, O.P.S., Beteck, R.M., Legoabe, L.J., 2021. Exploration of artemisinin derivatives and synthetic peroxides in antimalarial drug discovery research. European Journal of Medicinal Chemistry 213, 113193.

Patti, G.J., Yanes, O., Siuzdak, G., 2012. Metabolomics: the apogee of the omics trilogy. Nature Reviews Molecular Cell Biology 13, 263–269.

Pendota, S.C., Aderogba, M.A., Moyo, M., McGaw, L.J., Mulaudzi, R.B., van Staden, J., 2017. Antimicrobial, antioxidant, and cytotoxicity of isolated compounds from leaves of *Pappea capensis*. South African Journal of Botany 108, 272–277.

Pendota, S.C., Grierson, D.S., Afolayan, A.J., 2009. Antimicrobial activity of *Hippobromus pauciflorus*: a medicinal plant used for the treatment of eye infections in the Eastern Cape, South Africa. Pharmaceutical Biology 47, 309–313.

Portet, B., Fabre, N., Roumy, V., (…), Moulis, C., 2007. Activity-guided isolation of antiplasmodial dihydrochalcones and flavanones from *Piper hostmannianum* var. *berbicense*. Phytochemistry 68, 1312–1320.

Rabinovitch, R.N., Drakeley, C., Djimde, A.A., (…), Alonso, P.L., 2017. malERA: an updated research agenda for malaria elimination and eradication. PLoS Medicine 14, 1–17.

Raimondo, D., Staden, L., Foden, W., Victor, J.E., Helme, N.A., Turner, R.C., Kamundi, D.A., Manyama, P.A., others, 2009. Red list of South African plants 2009. South African National Biodiversity Institute, Pretoria.

Robbertse, P.J., du Toit, E.S., Cloete, M.O., 2011. Gender expression and inflorescence structure of *Pappea capensis* Eckl. and Zeyh. (Sapindaceae). South African Journal of Botany 77, 425–429.

Romphosri, S., Changruenngam, S., Chookajorn, T., Modchang, C., 2020. Role of a concentration gradient in malaria drug resistance evolution: a combined within- and between-hosts modeling approach. Scientific Reports 10, 1–13.

Salem, M.A., de Souza, L.P., Serag, A., Fernie, A.R., Farag, M.A., Ezzat, S.M., Alseekh, S., 2020. Metabolomics in the context of plant natural products research: from sample preparation to metabolite analysis. Metabolites 10, 1–30.

SANBI, 2019. Threatened species program | SANBI Red List of South African Plants [WWW Document].

Sato, S., 2021. *Plasmodium*—a brief introduction to the parasites causing human malaria and their basic biology. Journal of Physiological Anthropology 40, 1–13.

Saxena, S., Pant, N., Jain, D.C., Bhakuni, R.S., 2003. Antimalarial agents from plant sources. Current Science 85, 1314–1329.

Schneider, P., Reece, S.E., 2021. The private life of malaria parasites: Strategies for sexual reproduction. Molecular and Biochemical Parasitology 244.

Shapiro, L.L.M., Whitehead, S.A., Thomas, M.B., 2017. Quantifying the effects of temperature on mosquito and parasite traits that determine the transmission potential of human malaria. PLoS Biology 15, e2003489.

Sherrard-Smith, E., Hogan, A.B., Hamlet, A., (…), Churcher, T.S., 2020. The potential public health consequences of COVID-19 on malaria in Africa. Nature Medicine 26, 1411–1416.

Singh, Satendra, Singh, D.B., Singh, Shivani, Shukla, R., Ramteke, P.W., Misra, K., 2019. Exploring medicinal plant legacy for drug discovery in the post-genomic era. Proceedings of the National Academy of Sciences India Section B - Biological Sciences 89, 1141–1151.

Stresman, G.W.C., Slater, H.C., Bousema, T., Cook, J., 2020. Quantifying *Plasmodium falciparum* infections clustering within households to inform household-based intervention strategies for malaria control programs: an observational study and meta-analysis from 41 malaria-endemic countries. PLoS Medicine 29, e1003370.

Suresh, N., Haldar, K., 2018. Mechanisms of artemisinin resistance in *Plasmodium falciparum* malaria. Current Opinion in Pharmacology 42, 46–54.

Tajuddeen, N., Swart, T., Hoppe, H.C., van Heerden, F.R., 2021. Antiplasmodial and cytotoxic flavonoids from *Pappea capensis* (Eckl. & Zeyh.) leaves. Molecules 26, 3875.

Tamborrini, M., Hauser, J., Schäfer, A., Amacker, M., Favuzza, P., Kyungtak, K., Fleury, S., Pluschke, G., 2020. Vaccination with virosomally formulated

recombinant CyRPA elicits protective antibodies against *Plasmodium falciparum* parasites in preclinical in vitro and in vivo models. npj Vaccines 5, 1–8.

Tawfike, A.F., Viegelmann, C., Edrada-Ebel, R., 2013. Metabolomics and dereplication strategies in natural products. Methods in Molecular Biology 1055, 227–244.

Tougan, T., Edula, J.R., Morita, M., Takashima, E., Honma, H., Tsuboi, T., Horii, T., 2020. The malaria parasite *Plasmodium falciparum* in red blood cells selectively takes up serum proteins that affect host pathogenicity. Malaria Journal 19, 1–13.

Traoré, B., Koutou, O., Sangaré, B., 2020. A global mathematical model of malaria transmission dynamics with structured mosquito population and temperature variations. Nonlinear Analysis: Real World Applications 53, 103081.

Umar, A.H., Ratnadewi, D., Rafi, M., Sulistyaningsih, Y.C., 2021. Untargeted metabolomics analysis using FTIR and UHPLC-Q-Orbitrap HRMS of two Curculigo species and evaluation of their antioxidant and α-glucosidase inhibitory activities. Metabolites 11, 1–17.

Van der Pluijm, R.W., Amaratunga, C., Dhorda, M., Dondorp, A.M., 2021. Triple artemisinin-based combination therapies for malaria – a new paradigm? Trends in Parasitology 37, 15–24.

Van Wyk, B.-E., Wink, M., 2017. Medicinal plants of the world: an illustrated scientific guide to important medicinal plants and their uses. C.A.B. International, Wallingford.

Varo, R., Chaccour, C., Bassat, Q., 2020. Update on malaria. Medicina Clinica 155, 395–402.

Venter, F., Venter, J.-A., 1996. Making the most of indigenous trees. Briza Publications, Pretoria.

Verpoorte, R., Choi, Y.H., Kim, H.K., 2007. NMR-based metabolomics at work in phytochemistry. Phytochemistry Reviews 6, 3–14.

Wambugu, S.N., Mathiu, P.M., Gakuya, D.W., Kanui, T.I., Kabasa, J.D., Kiama, S.G., 2011. Medicinal plants used in the management of chronic joint pains in Machakos and Makueni counties, Kenya. Journal of Ethnopharmacology 137, 945–955.

Wang, Q., Yu, C., Zhang, H., Zheng, S., Song, J., Deng, C., 2021. China's foreign aid for global poverty alleviation: artemisinin-based combination therapies against malaria in Togo. Global Health Journal 5, 144–148.

Watt, M.J. and, Breyer-Brandwijk, M.G., 1962. The Medicinal and poisonous plants of Southern and Eastern Africa being an account for their medicinal and other uses, chemical composition, pharmacological effects, and toxicology in man and animal. E. & S. Livingstone Limited, Edinburgh.

WHO, 2021. World malaria report 2021 [WWW Document]. URL https://www.who.int/publications/i/item/9789240040496 (accessed 12.13.21).

WHO, 2020. Malaria [WWW Document]. World Health Organization, Geneva. URL https://www.who.int/news-room/fact-sheets/detail/malaria (accessed 11.22.19).

WHO, 2019. World malaria report 2019. Geneva.

Wilairatana, P., Masangkay, F.R., Kotepui, K.U., Milanez, G.D.J., Kotepui, M., 2021. Prevalence and characteristics of malaria among COVID-19 individuals: a systematic review, meta-analysis, and analysis of case reports. PLOS Neglected Tropical Diseases 15, e0009766.

Wilson, K.L., Flanagan, K.L., Prakash, M.D., Plebanski, M., 2019. Malaria vaccines in the eradication era: current status and future perspectives. Expert Review of Vaccines.

Wishart, D.S., 2016. Emerging applications of metabolomics in drug discovery and precision medicine. Nature Reviews Drug Discovery 15, 473–484.

Yadav, D.K., Kumar, S., Teli, M.K., Yadav, R., Chaudhary, S., 2019. Molecular targets for malarial chemotherapy: a review. Current Topics in Medicinal Chemistry 19, 861–873.

Yael, D.-M., Eunice, J., Allison, G., (…), Basil, B., 2019. Malaria surveillance report, South Africa, January - December 2018. Johannesburg.

Yuliana, N.D., Jahangir, M., Verpoorte, R., Choi, Y.H., 2013. Metabolomics for the rapid dereplication of bioactive compounds from natural sources. Phytochemistry Reviews 12, 293–304.

Ziegler, H.L., Staerk, D., Christensen, J., (…), Jaroszewski, J.W., 2002. *In vitro Plasmodium falciparum* drug sensitivity assay: inhibition of parasite growth by incorporation of stomatocytogenic amphiphiles into the erythrocyte membrane. Antimicrobial Agents and Chemotherapy 46, 1441–1446.

CHAPTER 3: ANTIPLASMODIAL ACTIVITY OF *PAPPEA CAPENSIS* ECKL. & ZEYH. (SAPINDACEAE) TWIGS

3.1. Introduction……..57

3.2. Materials and methods……..58

3.2.1. General……58

3.2.2. Plant sample collection……...58

3.2.3. Extraction of plant samples……...58

3.2.4. Column chromatography of crude extracts of *Pappea capensis*……59

3.2.5. *In vitro* antiplasmodial assay……..60

3.2.6. Cytotoxicity assay of *Pappea capensis* crude extracts……..60

3.2.7. 1H NMR spectroscopy analysis of *Pappea capensis* crude extracts……61

3.2.8. GC-MS analysis of Pappea capensis crude extracts……62

3.3. Results and discussions……62

3.4. Conclusion……...76

3.5. References……...76

3.1. Introduction

Pappea capensis (Sapindaceae) has been a valuable plant species for medicinal and non-medicinal purposes. (Karau et al., 2012; Mng'omba et al., 2008). It has been one of the trusted plant species for treating malaria and its related symptoms across many African communities (Asnake et al., 2016; Clarkson et al., 2004). Water-based decoctions from *P.* capensis twigs have been vouched for by indigenous people in Venda, with a long-standing history of interacting with the plant (Bapela et al., 2014). With that backdrop, ethnobotanical and ethnopharmacological researchers are burdened with ascertaining this anecdotal evidence (Alebie et al., 2017). It allows researchers to discover new plants with desired biological activities for different diseases. Studies conducted indicate that the antiplasmodial activity of *P. capensis* is largely attributed to its organic extracts, and a lesser extent, the polar ones (Bapela et al., 2014; Koch et al., 2005; Mokoka et al., 2013).

It is generally observed that organic extracts tend to display high biological activity and are accompanied by high cytotoxicity in most instances, and this hinders drug discovery and bioprospecting as further studies on pharmaceutical delivery cannot be conducted on cytotoxic substances. However, chemical derivatization renders the active cytotoxic extracts pharmacologically significant, thus salvaging the situation (Choi & Dong, 2005). Fortunately, organic crude extracts of *P. capensis* are not cytotoxic and can be further studied in great depth for antimalarial drug lead discovery. There are not many ethnopharmacological studies conducted on *P. capensis* antimalarial properties. The few that have been conducted barely scratch the surface when it comes to a full understanding of the plant's pharmacological properties.

Antiplasmodial and cytotoxicity studies on *P. capensis* have mostly focused on the biological activity of the crude extracts (Bapela et al., 2014; Koch et al., 2005; Mokoka et al., 2013). One study has recently reported on the antiplasmodial activity and cytotoxicity of the methanol leaf extract of *P.* capensis with its isolated constituents (Tajuddeen et al., 2021). There remains much research to be conducted on *P. capensis* extracts, and it is against this backdrop that this chapter aims to explore in detail the antiplasmodial activity and cytotoxicity of *P. capensis* twigs.

3.2. Materials and methods

3.2.1. General

The chemical profiles of extracts and fractions were analyzed on silica pre-coated thin layer chromatography (TLC) plates at room temperature (MERCK, silica gel 60 F254 0.2 mm thickness). Spots on the TLC were observed under UV light with a spectrum ranging from 254 nm to 366 nm. Silica gel was used as a stationary phase for column chromatography (CC). The various eluting solvents used were all of the analytical grades.

3.2.2. Plant sample collection

Pappea capensis twigs were collected from Sekhukhune, Limpopo, South Africa, and a voucher specimen (120331) was made and submitted to the H.G.W.J. Schweickerdt Herbarium (University of Pretoria). The plant twigs were dried at room temperature ground to powder in an Ultracentrifugal Mill (ZM, 200, Retsch®, Germany).

3.2.3. Extraction of plant samples

About 5L of water was used to extract 2.5 kg of plant material using dichloromethane (DCM): 50% methanol (MeOH) in a 1:1 (v/v) ratio. The solution was filtered using Whatman's No. 1 filter paper, and extractions were repeated three times. Filtrates were evaporated in a vacuum yielding DCM (I = 60 g) and aqueous extracts (Choi et al., 2005). The aqueous extract (II) was freeze-dried (Virtis) to yield 287 g. The DCM extract (I) was further partitioned between DCM: MeOH (1:1, v/v), separated, concentrated under vacuum, and resulted in DCM (III) and MeOH (IV) extracts, which weighed 40 g and 15 g, respectively. Non-polar extracts were dried in a vacuum at 30ºC. Methanol from the aqueous extracts was vaporized using a rotary vapor water bath (Buchi, R - 200, Switzerland) at 40ºC, and the aqueous extracts were then freeze-dried (Virtis). A decoction extract (V = 10 g) was prepared to simulate the traditional method used by indigenous people to establish the clinical relevance of the traditional use of *P. capensis*. The water-based decoction was prepared from 500 g of ground *P.* capensis twigs boiled at 100°C for about 45 minutes to an hour. All polar and organic extracts were analyzed independently.

3.2.4. Column chromatography of crude extracts of *Pappea capensis*

Crude extracts II (15 g), III (20 g), and IV (15 g) were subjected to silica gel column chromatography. Extract II was eluted with ethyl acetate (EtOAc): MeOH, MeOH: distilled water (dH_2O) at ratios of 1:10→10:1. Extract III was chromatographed using hexane (H): DCM, DCM: EtOAc, EtOAc: MeOH, and MeOH: dH_2O at ratios of 1:10→10:1 for each solvent system. Extract IV was chromatographed eluting with DCM: EtOAc, EtOAc: MeOH, and MeOH:dH_2O at solvent ratios 1:10→10:1. All fractions collected from the different crude extracts were analyzed using TLC. Extract II was analyzed using EtOAc: MeOH, MeOH:dH2O, at solvent ratios 1:10→10:1.

Extract III employed solvent ratios 1:10→10:1 for solvents H: DCM, DCM: EtOAc, EtOAc: MeOH, and MeOH:dH_2O. Extract IV was analyzed using DCM: EtOAc, EtOAc: MeOH, and MeOH:dH_2O at solvent ratios 1:10→10:1. All fractions that displayed chemical profile similarities were pooled together to yield 25 bits. Extracts II, III, and IV lost 8 (R-Y), 9 (A-I), and 8 (J-Q) fractions, respectively.

3.2.5. *In vitro* antiplasmodial assay

In vitro, antiplasmodial screening of all extracts and fractions employed the [^{3}H] hypoxanthine incorporation assay (Desjardins et al., 1979; Matile et al., 1990). The parasite strain used was *Plasmodium falciparum* (NF54) and chloroquine (Sigma C6628) as the standard drug (Ponnudurai et al., 1981). Dimethyl sulfoxide (DMSO) was used to dissolve all samples before parasite culturing and incubation in RPMI 1640 without hypoxanthine. Some HEPES was added to the RPMI 1640 growth medium (5.94 g/l), $NaHCO_3$ (2.1 g/l), neomycin (100 U/ml), AlbumaxR (5 g/l) and human red blood cells A+ at 25% haematocrit (0.3% parasitaemia). Serial drug dilution of eleven 3-fold dilution steps covering the range of 100 – 0.002 ug/ml was prepared in 96 well plates, then incubated in a humidified environment at 37ºC, 4% CO_2, 3% O_2, and 93% N_2. A measure of 50 µl of [^{3}H] hypoxanthine was added to each well after an hour, and the plates were incubated for 24 hrs before the cells were harvested using a BetaplateTM cell harvester (Wallac). Red blood cells were transferred onto a glass fiber filter for rinsing with dH_2O. A plastic foil with dry glass filters inserted with 10 ml of scintillation fluid was counted using the BetaplateTM liquid scintillation counter (Wallac). The different IC_{50} values for all test samples were computed and presented in an excel (Microsoft Office 365) spreadsheet (Huber & Koella, 1993).

3.2.6. Cytotoxicity assay of *Pappea capensis* crude extracts

Cytotoxicity screening to determine the toxicity or safety of the assayed plant samples was done on rat skeletal cells. Microtiter plates (96-wells) with 100 ul of RPMI 1640 medium supplemented with 1% L-glutamine (200 nM), 10% fetal bovine serum, and 4000 rat skeletal cell lines (Ahmed et al., 1994). Serial drug dilution of eleven 3-fold dilution steps spanning the range of 100 – 0.002 µg/ml was prepared, and after 70 hrs had lapsed, the incubated plates were observed under an inverted microscope. It was done to ensure the growth of the experimental control (podophyllotoxin) and the sterility of the conditions. Alamar Blue at a concentration of 10 µg/ml was then added to each well, and the plates were further incubated for 2 hrs. After the incubation time had lapsed, the plates were read with a Spectramax Gemini XS microplate fluorometer (Molecular Devices Corporation, United States of America) at an excitation wavelength of 536 nm and an emission wavelength of 588 nm. The IC_{50} values were computed using linear regression from the sigmoidal curves using the SoftmaxPro software (Molecular Devices Corporation, United States of America) (Huber & Koella, 1993).

3.2.7. ^{1}H NMR spectroscopy analysis of *Pappea capensis* crude extracts

Proton NMR analysis was conducted to identify the different classes of compounds in the crude extracts. These are identified by carefully studying the chemical profiles represented by the various spectral chemical shifts for the other crude extracts. Each natural extract was reconstituted in deuterated dimethyl sulfoxide (DMSO-d_6) to 15 mg/ml. About 700 µl was transferred into a 5mm NMR tube (Wilmad, Sigma-Aldrich). Extracts were measured using the Varian 200 MHz ^{1}H NMR spectrometer, and fractions using the 400 MHz spectrometer ran at 25 ºC. The spectral width of each spectrum was 14 ppm, and the acquired scans were 512 per sample. The obtained spectral data were referenced to the DMSO-d_6 solvent peak (2.5000

ppm), manually phase-corrected, and automatically baseline corrected using the Whittaker smoother (Eilers, 2003).

3.2.8. GC-MS analysis of *Pappea capensis* crude extracts

The crude extracts were also subjected to GC-MS analysis to identify different phytoconstituents attributed to the observed antiplasmodial activity. All polar extracts were redissolved in methanol, and the lipophilic ones were reconstituted in distilled dichloromethane. Each sample was homogenized by sonication for 30 minutes at 30 ºC and prepared to a final 1 µg/ml concentration. All prepared extracts were transferred into 1.5 ml short thread vials (La-Pha-Pack, Separations). Gas chromatography and mass spectrometry analysis were conducted on the GCMS-QP2010SE (Shimadzu, Japan) machine, and an AOC-20i/s autosampler was used to inject the sample into the machine. The start temperature was 30 ºC, and the end temperature was 230 ºC. The splitless injection technique was carried out for all fractions, and the injection volume was 1 µl. For the MS analysis, the ion source temperature was 230 ºC, the interphase temperature was 250 ºC, and the solvent cut time was 1.5 minutes. The detector voltage was set to 0.1 kV and adjusted to a tuning result. The start time was set to 4.5 minutes and the end time was 30 minutes. The acquisition mode was calibrated to the scan mode, running at 2500. The mass range was 40 – 650 m/z. Compounds were tentatively identified based on comparing their relative mass spectral data with those of the National Institute for Standards and Technology (NIST) database (NIST, 2020).

3.3. Results and discussions

In vitro antiplasmodial and cytotoxicity screening was conducted on 30 samples acquired from the twigs of *P. capensis*. Five crude extracts (I, II, III, IV, and V) and 25

fractions (A – Y) recovered from the column chromatography of extracts II, III, and IV were tested against *P. falciparum* NF54 strain, and for cytotoxicity screens, they were run on L-6 rat skeletal myoblast cell lines. Selectivity index (SI) values represent the quotient of the antiplasmodial and cytotoxicity IC_{50} values (cytotoxicity IC_{50} value is divided by the antiplasmodial IC_{50} value to obtain the SI). In this study, a sample was regarded as a potential candidate when the concentration inhibited 50% of the parasite proliferation (IC_{50} was ≤ 5 µg/ml with the SI ≥ 10 units). A sample's high parasite selectivity is not equivalent to high antiplasmodial efficacy. An extract's antiplasmodial efficacy is not a result of its *in vitro* cytotoxicity when the SI ≥ 10 (Ndjakou et al., 2007). Table 3.1 shows the IC_{50} values of all samples that displayed significantly high antiplasmodial activity with their respective selectivity index (SI) values. A total of 30 samples were tested for antiplasmodial efficacy, and only 14 showed high antiplasmodial activity and parasite selectivity (SI > 10) to the NF54 strain of *P. falciparum*.

Table 3.1. The antiplasmodial activity (IC_{50} values (µg/ml)) and cytotoxicity of *Pappea capensis* crude extracts and fractions with a selectivity index (SI) value were computed. Mean values were calculated for two independent experiments conducted in duplicate.

Sample ID	Solvent	IC50 (µg/ml)	Cytotoxicity (µg/ml)	Selectivity Index (SI)
I	DCM	2.93 ± 0.66	40.3 ± 6.36	14
II	dH_2O	24.25 ± 10.11	>100	ND
III	DCM	2.59 ± 0.51	55.3 ± 3.75	21
IV	MeOH	3.56 ± 0.31	45.1 ± 3.32	13
V	H_2O	40.40 ± 0.00	65.3 ± 3.11	2
A	DCM	7.90 ± 1.17	>100	ND
B	DCM	2.98 ± 0.31	61.0 ± 8.27	20
C	DCM	1.12 ± 0.02	21.0 ± 2.33	18
D	DCM	0.85 ± 0.03	31.5 ± 16.62	37
E	DCM	0.91 ± 0.00	26.9 ± 11.09	30
F	DCM	2.37 ± 0.08	54.0 ± 1.41	23
G	DCM	3.18 ± 1.27	61.9 ± 6.22	19
H	DCM	11.27 ± 2.87	15.9 ± 1.20	1

I	DCM	2.81 ± 0.63	51.5 ± 7.14	18
J	MeOH	38.80 ± 1.82	>100	ND
K	MeOH	3.90 ± 1.15	39.0 ± 13.72	10
L	MeOH	4.84 ± 0.35	56.1 ± 2.69	12
M	MeOH	1.56 ± 0.80	56.5 ± 0.07	36
N	MeOH	0.60 ± 0.48	54.3 ± 2.40	91
O	MeOH	21.80 ± 0.14	40.4 ± 15.13	2
P	MeOH	4.09 ± 1.77	50.5 ± 4.60	12
Q	MeOH	24.45 ± 0.64	>100	ND
R	dH_2O	22.20 ± 1.13	48.2 ± 5.94	2
S	dH_2O	28.75 ± 0.78	53.0 ± 0.00	2
T	dH_2O	25.75 ± 18.03	>100	ND
U	dH_2O	33.95 ± 21.14	>100	ND
V	dH_2O	20.60 ± 8.63	>100	ND
W	dH_2O	20.50 ± 0.00	>100	ND
X	dH_2O	20.70 ± 0.00	>100	ND
Y	dH_2O	22.55 ± 6.72	59.3 ± 0.57	3

Chloroquine	0.0035	
Podophyllotoxin		0.011

***Pf*-NF54**: *Plasmodium falciparum* NF54 strain

L6-Cells: Rat skeletal myoblast cells

dH_2O: Distilled water

DCM: Dichloromethane

MeOH: Methanol

ND: Not detectable

Of the five assayed crude extracts, three (I, III, and IV) exhibited significant antimalarial activity at IC_{50} = 2.93, 2.59, and 3.56 µg/ml, and their SI values were 14, 21, and 13, respectively (Table 3.1). These results are comparable with those reported in previous *in vitro* antiplasmodial activity studies on *P. capensis*. For example, Bapela et al. (2014) reported moderate antiplasmodial activity (IC_{50} = 5.47 µg/ml; SI = 9.89) from DCM extract of the twigs. Mokoka et al. (2013) reported significant antiplasmodial activity (IC_{50} = 5.30 µg/ml; SI = 16) from DCM extracts of the leaves and roots. The noticeable disparities in the results can be explained by the differing spatial geographic distribution, seasonality, plant part used, and solvent of extraction, which plays a critical role in varying the observed antiplasmodial activity.

Research on *Aloe vera* collected in India reported that those from colder climatic regions recorded higher antiplasmodial activity than those from warmer areas (Kumar et al., 2017). Different plant parts assayed for antiplasmodial activity contain different chemical profiles that yield different antiplasmodial results. The stem bark assayed by Koch et al. (2005) showed poor inhibitory effects (IC_{50} >10 µg/ml), while the twigs and root extracts assayed by Bapela et al. (2014) and Mokoka et al. (2013) displayed high activity. The methanolic crude extract IV demonstrated a significant parasite inhibitory effect at IC_{50} = 3.56 µg/ml, and the SI of 13 indicates the non-toxicity of the extract when tested on rat skeletal myoblast L6 cell lines (Table 3.1). The methanolic leaf crude extract assayed by Tajuddeen et al. (2021) reported poor antiplasmodial activity at lower concentrations (10 µg/ml) and more than 80% viability at 50 µg/ml when tested on *P. falciparum* 3D7 strain. The disparities between our observed results on the antiplasmodial activity of the methanolic extract IV and those reported by Tajuddeen et al. (2021) can result from differing parasite strains used or the biological assay methods. Although there has not been extensive research conducted on the

antiplasmodial activity of *P. capensis* polar extracts, *in vivo* studies on *Paullinia pinnata* L. (Sapindaceae) share the same taxonomic botanical family as *Pappea capensis*, reported poor antiplasmodial inhibitory effects of its methanol leaf extract (Adeyemo-Salami et al., 2014). On the contrary, this study demonstrates the pharmacological potential of the methanol extract, thus permitting the discovery of potential antimalarial drug leads. The antiplasmodial activity of the crude extracts is comparable with results obtained from ^{1}H NMR and GC -MS analyses.

The ^{1}H NMR spectral data correlates with the observed biological activity for extracts I, III, and IV. There are some noticeable similarities in their ^{1}H NMR spectral region of 0.5 – 2.0 ppm (Figure 3.1), alluding to a similar class of compounds attributed to observed antiplasmodial bioactivity. Table 3.2 shows the compounds found in each *P. capensis* crude extract. Crude extracts I, III and IV that displayed the best antiplasmodial activity contain aliphatic, hydrocarbon, and alcohol-based classes of constituents in abundance. Extracts II and V, which have poor antiplasmodial bioactivity, include hydrocarbon and an alkyl-based type of constituents in the lot, as shown in Table 3.2. Extracts II and V also have unknown classes of constituents compared to I, III, and IV (Table 3.2). For dereplicating novel compounds with antiplasmodial activity, extract II and IV would best be prioritized. When the crude extracts I – V were stacked and the ^{1}H NMR spectra analyzed, the terpenoids' most prevalent constituents were the terpenoids (Figure 3.1). It was further validated through comparisons made with other studies where terpenoids were analyzed using ^{1}H NMR, and the correlation was established (Kadyrov & Rosiak, 2011; Monakhova et al., 2011).

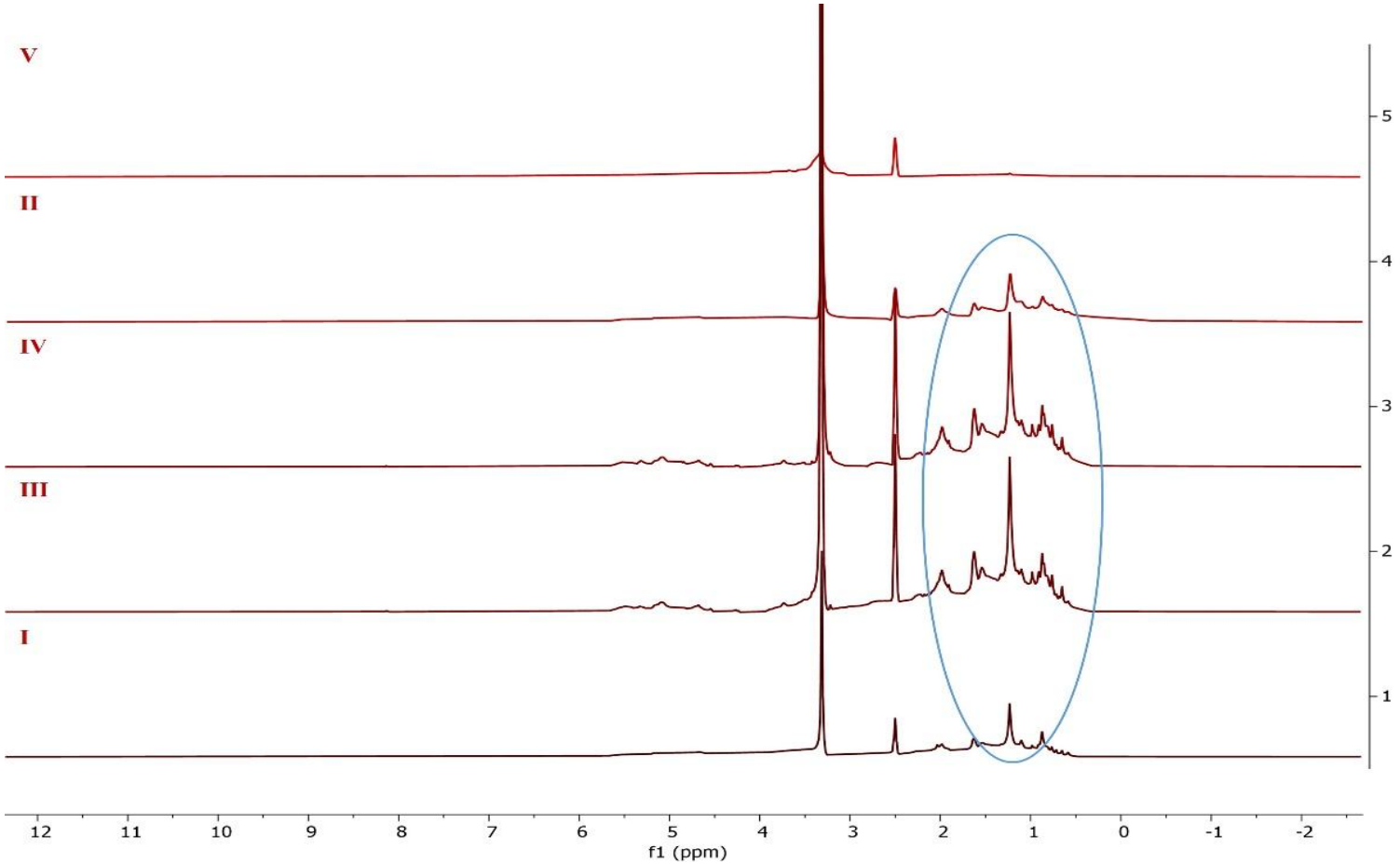

Figure 3.1. Stacked ^{1}H NMR spectra of *Pappea capensis* crude fractions showing the different chemical shift similarities highlighted.

Table 3.2. The percentage proportion of constituent classes identified in the individual extracts of *Pappea capensis* using GC-MS.

Class	**I**	**II**	**III**	**IV**	**V**
Acids	3.15	3.45	2.82	7.51	1.46
Alcohols	10.54	-	8.49	4.06	-
Alkyl	0.85	25.79	0.24	1.51	33.59
Epoxides	-	-	-	0.43	-
Esters	1.3	-	-	2.52	-
Ethers	-	5.2	-	0.43	-
Furan	0.33	-	0.46	0.5	-
Hydrocarbons	36.16	55.07	38.27	16.49	15.43
Sugars	1.52	-	1.24	4.42	38.52
Aliphatic	44.01	-	47.91	62.10	1.53
Unknown	2.14	10.5	0.58	0.03	9.47

The analysis of extracts I, III, and IV using GC-MS identified the most common constituents, lupan-3-one, lupeol acetate, α-amyrin, and β-amyrin (Figure 3.2) (NIST, 2020). Extracts I, III, and IV have different forms of amyrin (extract I and IV contain α-amyrin and III has β-amyrin), which are generally abundant in other plant species (Figure 3.2). Lupeol, lupan-3-one, and lupeol acetate have been reported to possess poor antiplasmodial activity (IC_{50} >10 µg/ml); however, they have been reported to have a significant anti-inflammatory activity which is an important malaria-related symptom (Liu et al., 2021; Mwangi et al., 2010). α-amyrin and β-amyrin both have established antiplasmodial activities against varying strains of the *Plasmodium* parasite at IC_{50} values of 0.96 and 2.65 µg/ml, respectively (Chung et al., 2009). These constituents in *P. capensis* crude extracts can be attributed to its observed

antiplasmodial biological activity. Thus, the observed antiplasmodial bioactivity in extracts I, III, and IV correlates with GC-MS and ^{1}H NMR findings. Extract V exhibited poor antiplasmodial activity (Table 3.1), yet indigenous people rely on its decoctions to remedy malaria. Analyzing extract V using GC-MS reveals the presence of lupeol, a compound with established antiplasmodial activity (Chung et al., 2009). This compound exists in low concentrations in extract V, and at higher concentrations, it would exhibit the desired antiplasmodial activity. Thus, the presence of lupeol revealed by the GC-MS technique validates the traditional use of *P. capensis* twigs to treat malaria.

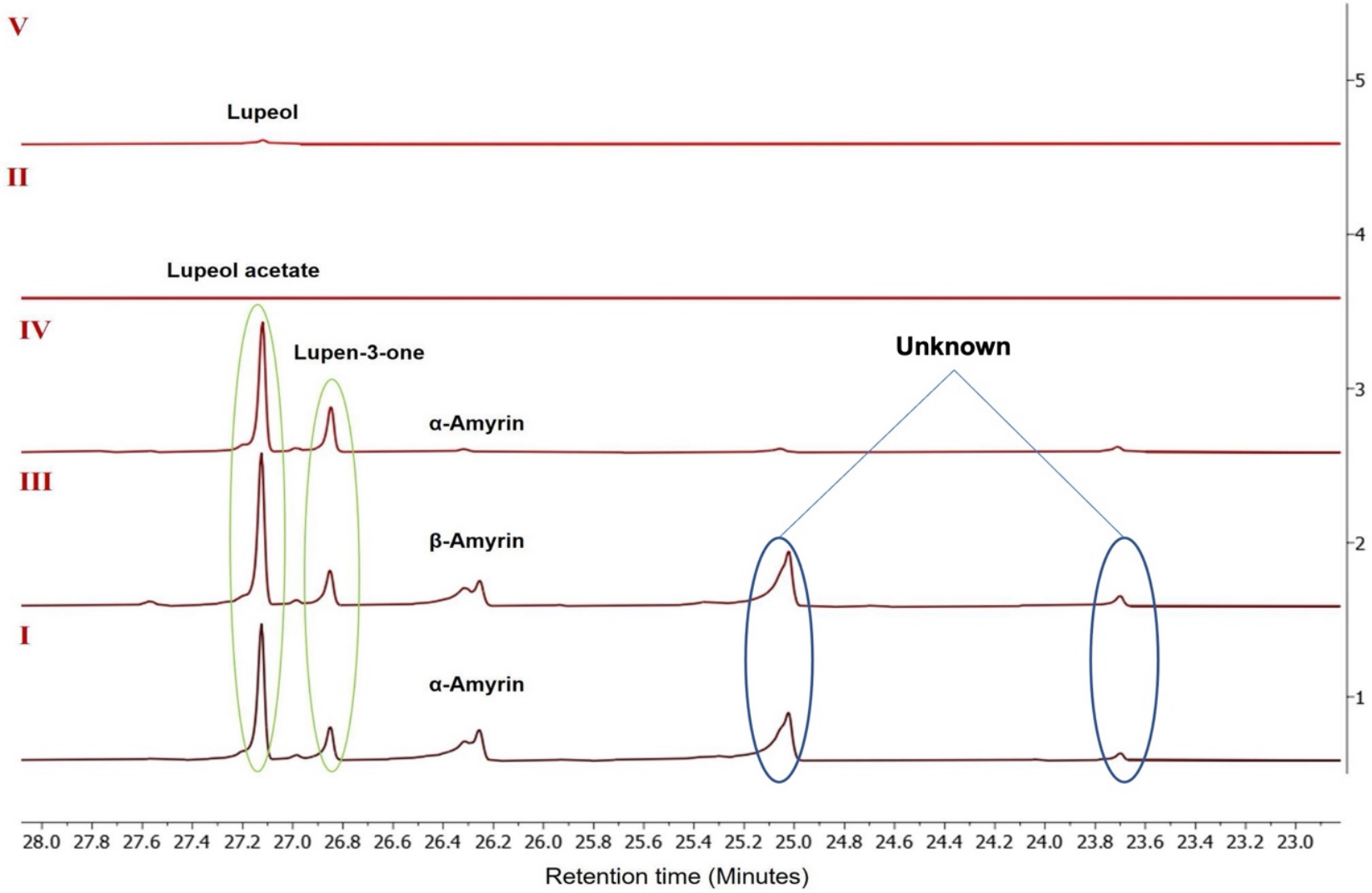

Figure 3.2. The GC-MS spectra of *Pappea capensis* crude extracts. The major phytoconstituents have been highlighted.

All fractions recovered from the chromatographic fractionation of extracts II, III, and IV were subjected to antiplasmodial and cytotoxicity screening. Of the 25 tested subfractions, only 13 exhibited potential antiplasmodial antiproliferative inhibitory effects against the NF54 strain of *P. falciparum* (IC_{50} ≤ 5 µg/ml and SI ≥ 10 (Table 3.1). Dichloromethane samples accounted for 61% of the active fractions, and the remaining were methanol fractions. None of the water crude extract (Extract II) fractions displayed antiplasmodial activity. Fractions N, D, and E showed high antiplasmodial activity at IC_{50} of 0.60, 0.85, and 0.91 µg/ml, respectively. The ^{1}H NMR spectra of fractions N, D, and E were stacked, and the regions where the spectra showed similar chemical shifts were integrated to correlate to the fatty acid-containing phytoconstituents class of compounds (Figure 3.3). Some fatty acids have established antiplasmodial activity and have been reported to be active against different strains of *Plasmodium* (Carballeira, 2008). Gas chromatography-mass spectrometry was also used for comparative analysis among fractions N, D, and E to check for similar trends observed in the ^{1}H NMR analysis. Fractions N, D, and shared identical phytoconstituents at 15.0 and 17.0 mins (Figure 3.4). These were also identified as myristic acid and palmitic acid (NIST, 2020). These two fatty acids were isolated from *Sonchus arvensis* L., a plant with established antiplasmodial activity (Dwi et al., 2020; Wahyuni et al., 2021). The respective compounds have not been studied for their antiplasmodial activity. However, their occurrence in antimalarial plants suggests they can potentially possess the desired antiplasmodial pharmacological activity. Further antiplasmodial bioactivity tests of myristic and palmitic fatty acids would need to be conducted.

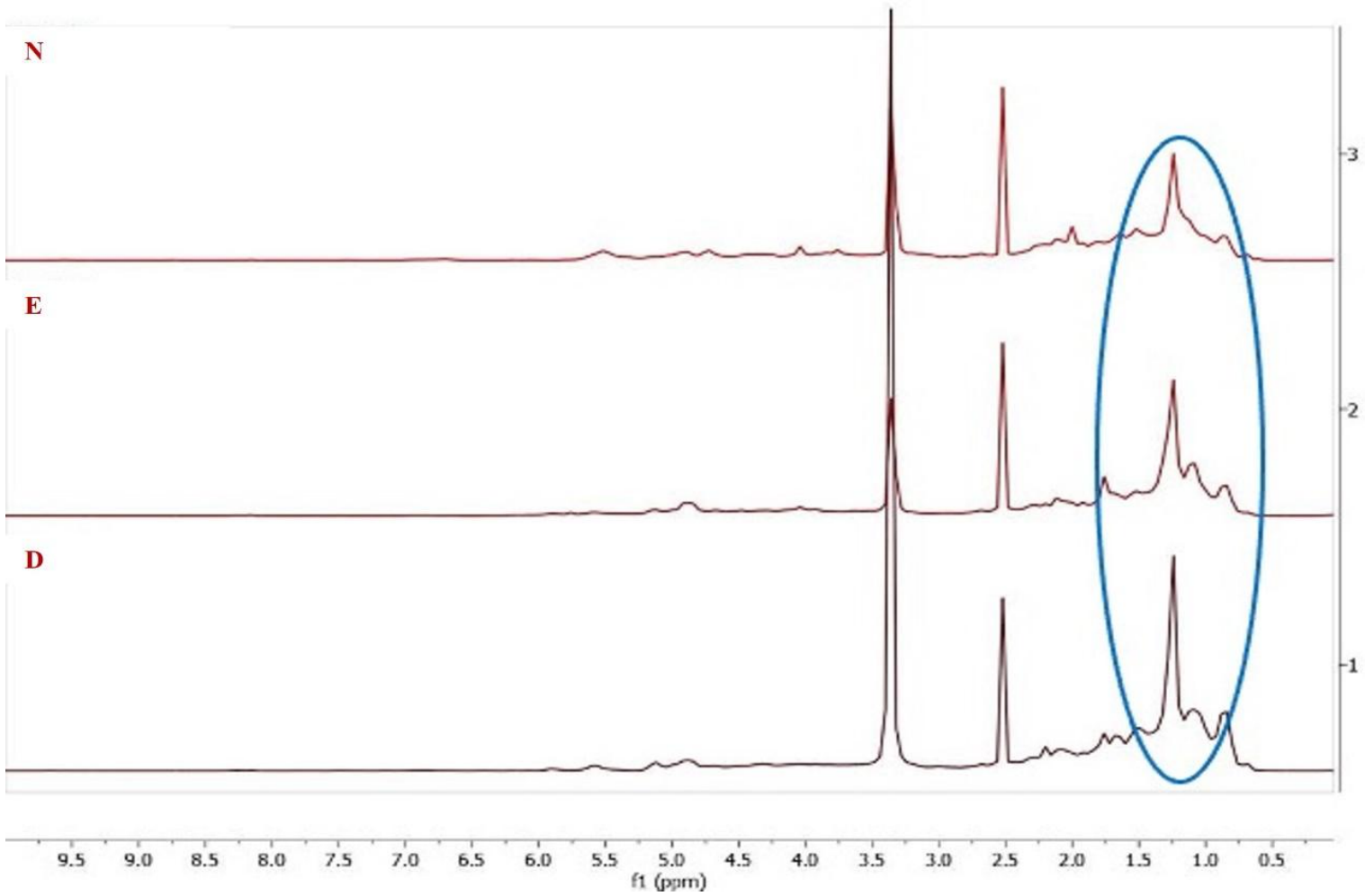

Figure 3.3. ^{1}H NMR spectra of the most active fractions of *Pappea capensis*.

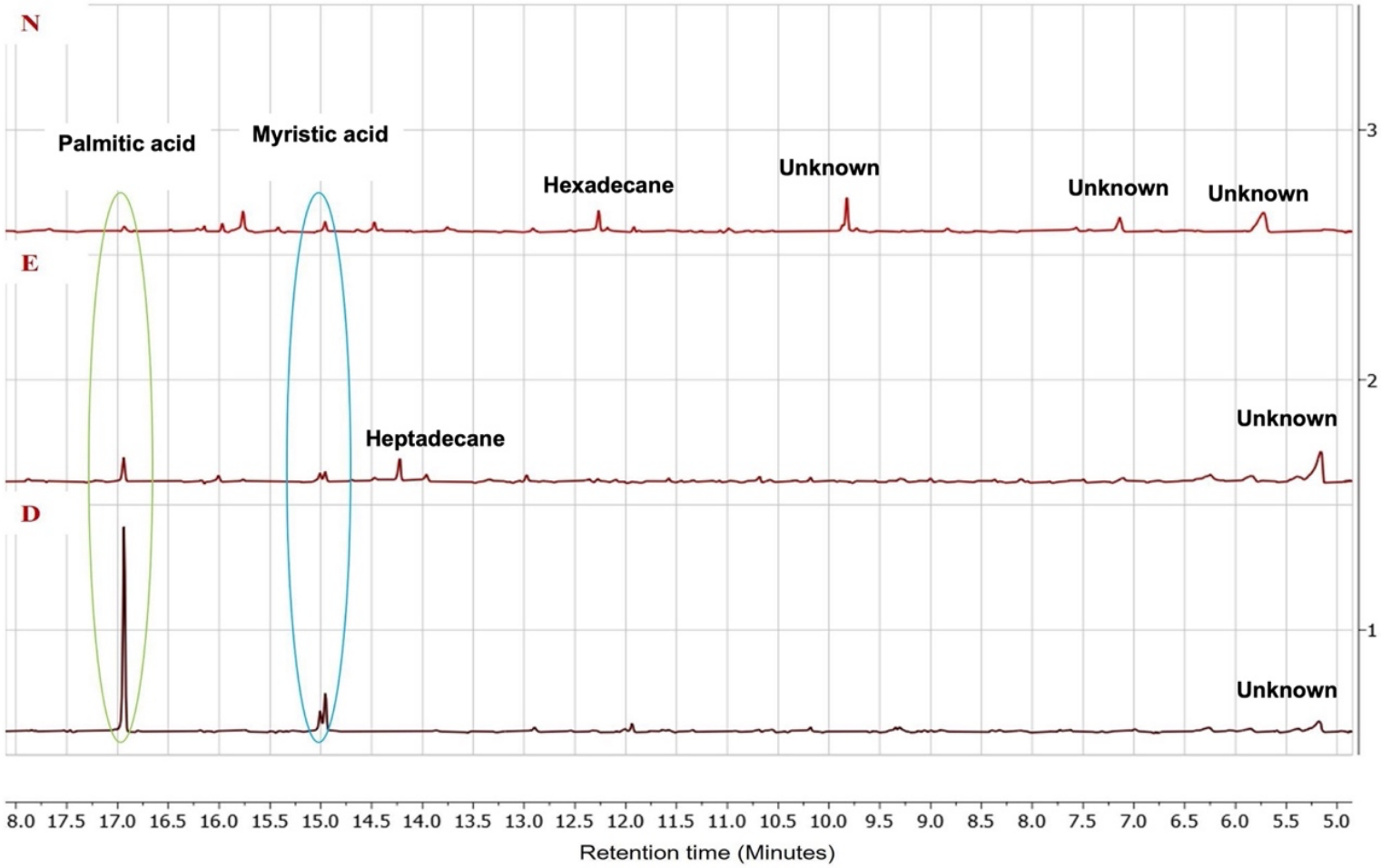

Figure 3.4. Stacked GC-MS spectra of the most active fractions of *Pappea capensis* showing myristic acid and palmitic acid.

Phytochemical studies conducted on *P. capensis* reported the occurrence of many constituent classes like terpenes, phenolics, saponins, tannins, flavonoids, and alkaloids (Karau et al., 2012). Constituent classes like alkaloids, terpenoids, flavonoids, and saponins have been reported in previous studies to have antiplasmodial activity (Akanbi, 2015; Bekono et al., 2020; Ganesh et al., 2012; Uzor, 2020). The observed antiplasmodial activity in *P. capensis* can be attributed to the terpenoids and fatty acid-compounds. The results also suggest that the observed antiplasmodial activity may be attributed to a single or many pure compounds. The observed improvement in Plasmodium inhibitory effects can be explained and extrapolated when *P. capensis* crude extracts were purified to less complex fractions. When extract I was reduced to II by liquid-liquid separation, antiplasmodial activity increased from 2.93 to 2.59 µg/ml (Table 3.1). A similar trend was observed when extract III and IV were further purified through column chromatographic fractionation, resulting in D, E, and N, which showed significant improvement in antiplasmodial activity. It may explain that individual phytoconstituents could be major antiplasmodial activity contributors in *P. capensis*.

3.4. Conclusion

The study validates the ethnomedicinal use of *P. capensis* in treating malaria. The findings also highlight the pharmacological potential of *P. capensis* as a botanical entity worth further exploration for new malaria drug interventions, especially the methanolic extract and some of its chromatographic fractions. Unknown constituents in active extracts will be prioritized for isolation and testing for antiplasmodial pharmacological viability to dereplicate unknown from known compounds with established antiplasmodial activity.

3.5. References

Adeyemo-Salami, O A, Farombi, E.O., Ademowo, O.G., 2014. An investigation into the antimalarial effect of methanolic extract of *Paullinia pinnata* leaves in *Plasmodium berghei* infected mice and course of infection. African Journal of Medicine and Medical Sciences 43, 93–100.

Ahmed, S.A., Gogal, R.M., Walsh, J.E., 1994. A new rapid and simple non-radioactive assay to monitor and determine the proliferation of lymphocytes: an alternative to [^{3}H]thymidine incorporation assay. Journal of Immunological Methods 170, 211–224.

Akanbi, O.A., 2015. Structural and institutional determinants of poverty in sub-Saharan African countries. Journal of Human Development and Capabilities 16, 122–141.

Alebie, G., Urga, B., Worku, A., 2017. A systematic review on traditional medicinal plants used for the treatment of malaria in Ethiopia: trends and perspectives. Malaria Journal 16, 307.

Asnake, S., Teklehaymanot, T., Hymete, A., Erko, B., Giday, M., 2016. Antimalarial medicinal plants used by Gumuz people of Mandura Woreda, Benishangul-Gumuz Regional State, Ethiopia. Indian Journal of Traditional Knowledge 15, 546–552.

Bapela, M.J., Meyer, J.J.M., Kaiser, M., 2014. *In vitro* antiplasmodial screening of ethnopharmacologically selected South African plant species used to treat malaria. Journal of Ethnopharmacology 156, 370–373.

Bekono, B.D., Ntie-Kang, F., Onguéné, P.A., Lifongo, L.L., Sippl, W., Fester, K., Owono, L.C.O.O., 2020. The potential of anti-malarial compounds derived from African medicinal plants: a review of pharmacological evaluations from 2013 to 2019. Malaria Journal 19, 183.

Carballeira, N.M., 2008. New advances in fatty acids as antimalarial, antimycobacterial, and antifungal agents. Progress in Lipid Research 47, 50.

Choi, C.K., Dong, M.W., 2005. Sample preparation for HPLC analysis of drug products. Separation Science and Technology 6, 123–144.

Chung, I.M., Kim, M.Y., Park, S.D., Park, W.H., Moon, H.I., 2009. *In vitro* evaluation of the antiplasmodial activity of *Dendropanax morbifera* against chloroquine-sensitive strains of *Plasmodium falciparum*. Phytotherapy Research 23, 1634–1637.

Clarkson, C., Maharaj, V.J., Crouch, N.R., Grace, O.M., Pillay, P., Matsabisa, M.G., Bhagwandin, N., Smith, P.J., Folb, P.I., 2004. *In vitro* antiplasmodial activity of medicinal plants native to or naturalized in South Africa. Journal of Ethnopharmacology 92, 177–191.

Desjardins, R.E., Canfield, C.J., Haynes, J.D., Chulay, J.D., 1979. Quantitative assessment of antimalarial activity *in vitro* by a semiautomated microdilution technique. Antimicrobial Agents and Chemotherapy 16, 710–718.

Dwi, K.W., Hery Purnobasuki, Eko Prasetyo Kuncoro, Eko Prasetyo Kuncoro, 2020. Callus induction of *Sonchus arvensis* L. and its antiplasmodial activity. African Journal of Infectious Diseases 14, 1–7.

Eilers, P.H.C., 2003. A perfect smoother. Analytical Chemistry 75, 3631–3636.

Ganesh, D., Fuehrer, H.-P.P., Starzengrüber, P., Swoboda, P., Khan, W.A., Reismann, J.A.B.B., Mueller, M.S.K.K., Chiba, P., Noedl, H., 2012. Antiplasmodial activity of flavonol quercetin and its analogs in *Plasmodium falciparum*: evidence from clinical isolates in Bangladesh and standardized parasite clones. Parasitology Research 110, 2289–2295.

Huber, W., Koella, J.C., 1993. A comparison of three methods of estimating EC50 in studies of drug resistance of malaria parasites. Acta Tropica 55, 257–261.

Kadyrov, R., Rosiak, A., 2011. Synthesis of Ru alkylidene complexes. Beilstein Journal of Organic Chemistry 7, 104.

Karau, G.M., Njagi, E.N.M., Machocho, A.K., Wangai, L.N., 2012. Phytonutrient, mineral composition, and *in vitro* antioxidant activity of leaf and stem bark powders of *Pappea capensis* (L.). Pakistan Journal of Nutrition 11, 123–132.

Koch, A., Tamez, P., Pezzuto, J., Soejarto, D., 2005. Evaluation of plants used for antimalarial treatment by the Maasai of Kenya. Journal of Ethnopharmacology 101, 95–99.

Kumar, R., Bohra, A., Pandey, A.K., Pandey, M.K., Kumar, A., 2017. Metabolomics for plant improvement: status and prospects. Frontiers in Plant Science 8, 1302.

Liu, K., Zhang, X., Xie, L., Deng, M., Chen, H., Song, J., Long, J., Li, X., Luo, J., 2021. Lupeol and its derivatives as anticancer and anti-inflammatory agents: molecular mechanisms and therapeutic efficacy. Pharmacological Research 164, 105373.

Matile, H., Richard, J., Pink, L., 1990. *Plasmodium falciparum* malaria parasite cultures and their use in immunology, in: Immunological Methods. Elsevier, pp. 221–234.

Mng'omba, S.A., du Toit, E.S., Akinnifesi, F.K., 2008. Plant regeneration through somatic embryogenesis of jacket plum (*Pappea capensis*). New Zealand Journal of Crop and Horticultural Science 36, 137–144.

Mokoka, T.A., Xolani, Peter.K., Zimmermann, S., Hata, Y., Adams, M., Kaiser, M., Moodley, N., Maharaj, V., Koorbanally, N.A., Hamburger, M., Brun, R., Fouche, G., 2013. Antiprotozoal screening of 60 South African plants, and the identification of the antitrypanosomal germacranolides schkuhrin I and II. Planta Medica 79, 1380–1384.

Monakhova, Y.B., Kuballa, T., Lachenmeier, D.W., 2011. Rapid determination of total thujone in absinthe using ^{1}H NMR spectroscopy. International Journal of Spectroscopy 2011, 1–5.

Mwangi, E.S.K., Keriko, J.M., Machocho, A.K., Wanyonyi, A.W., Malebo, H.M., Chhabra, S.C., Tarus, P.K., 2010. Antiprotozoal activity and cytotoxicity of metabolites from leaves of *Teclea trichocarpa*. Journal of Medicinal Plants Research 4, 726–731.

Ndjakou, L.B., C., V.-S., R., F.S., Tantangmo, F., Ngouela, S., Kaiser, M., Tsamo, E., Anton, R., Weniger, B., 2007. *In vitro* antiprotozoal activities and cytotoxicity of some selected Cameroonian medicinal plants. Journal of Ethnopharmacology 111, 8–12.

NIST, 2020. National Institute of Standards and Technology [WWW Document]. URL https://www.nist.gov/ (accessed 1.3.21).

Ponnudurai, T., Leeuwenberg, D.E.M., Meuwissen Th., J.H.E., Leeuwenberg, A.D., Meuwissen, J.H., 1981. Chloriquine sensitivity of isolates of *Plasmodium falciparum* adapted to *in vitro* culture. Tropical and Geographical Medicine 33, 50–54.

Tajuddeen, N., Swart, T., Hoppe, H.C., van Heerden, F.R., 2021. Antiplasmodial and cytotoxic flavonoids from *Pappea capensis* (Eckl. & Zeyh.) Leaves. Molecules 26, 3875.

Uzor, P.F., 2020. Alkaloids from plants with antimalarial activity: a review of recent studies. Evidence-based Complementary and Alternative Medicine 2020.

Wahyuni, D.K., Rahayu, S., Zaidan, A.H., Ekasari, W., Prasongsuk, S., Purnobasuki, H., 2021. Growth, secondary metabolite production, and *in vitro* antiplasmodial activity of Sonchus arvensis L. callus under dolomite [$CaMg(CO_3)_2$] treatment. PLOS ONE 16, e0254804.

CHAPTER 4: THE APPLICATION OF ^{1}H NMR AND GC – MS METABOLOMICS TO DEREPLICATE ANTIMALARIAL CONSTITUENTS FROM *PAPPEA CAPENSIS* ECKL. & ZEYH. (SAPINDACEAE) TWIGS

4.1. Introduction……....83

4.2. Materials and methods……..84

4.2.1. Plant sample collection……...85

4.2.2. Extraction of plant samples……85

4.2.3. Column chromatography of *Pappea capensis* extracts……....86

4.2.4. ^{1}H NMR spectroscopy of *Pappea capensis* fractions……86

4.2.5. GC-MS analysis of *Pappea capensis* fractions……..87

4.2.6. Statistical analysis using multivariate data analysis (MDA)……....88

4.3. Results and discussion……....88

4.4. Conclusion……..97

4.5. References……98

4.1. Introduction

Ethnopharmacology has led to the delivery of many prescribed drugs like artemisinin and quinine (Sadiq et al., 2014; Wan et al., 2020). These drugs are synthetically produced and are inspired by natural products (Skwarecki et al., 2020). Given the availability of different drug discovery approaches, ethnopharmacological bioprospecting ranks top of the list. Natural products exhibit many advantages, rendering them choice sources for novel drug discovery (Verpoorte et al., 2007). The availability of a vast continuum of phytochemicals with diverse chemical structures is mainly why medicinal plants are choice sources for novel drug leads (Beutler, 2009). Antimalarial drug development from medicinal plants is plagued with numerous challenges and impediments. The metabolites are subject to environmental and ecological factors which influence the metabolite quality and quantity (Uthe et al., 2020). Metabolite physiology and biochemical diversity further complicate drug discovery from plant precursors (Peters et al., 2019).

Although the World Health Organization (WHO) approves the usage of standardized antimalarial extracts with known phytoconstituents, pure compounds have higher antiplasmodial bioactivity than crude extract. The traditional conventional approach to constituent isolation is time-consuming, labor-intensive, and cost-inefficient (Zhang et al., 2018). Isolating known phytoconstituents with already established activity is regressive in discovering novel antimalarial drugs. Applying cutting-edge metabolomics techniques incorporating different spectroscopy approaches alongside multivariate data analysis (MDA) demonstrates robustness in overcoming these challenges (Demarque et al., 2020; Heyman & Meyer, 2012). Metabolomics using varying spectroscopy techniques affords the possibility to study

the constituent composition of crude extracts to dereplicate known and unknown phytoconstituents. Such is expedient in searching for novel antimalarial leads by reducing the time, money, and efforts invested in isolating compounds that have already been characterized and have established antiplasmodial activity.

Specific unknown compounds can be targeted and assessed for antiplasmodial and cytotoxic activity. It is the most efficient approach to discovering new and novel compounds with different modes of action to be used in the antiplasmodial drug discovery endeavor. This study has two primary objectives: firstly, to test the robustness of ^{1}H NMR-based metabolomics and GC-MS-based metabolomics when discriminating classes of phytoconstituent responsible for the observed antiplasmodial bioactivity of active *P. capensis* crude extracts. It is significant when crafting a rapid throughput screening technique for antiplasmodial activity. Secondly, to dereplicate compounds with known bioactivity to focus on unknown compounds to discover new compounds with antiplasmodial activity.

4.2. Materials and methods

The ^{1}H NMR and GC-MS metabolomics analysis of all 25 fractions acquired from the fractionation of *Pappea capensis* crude extracts (II, III, and IV) were conducted following the methodology summarized below (Figure 4.1).

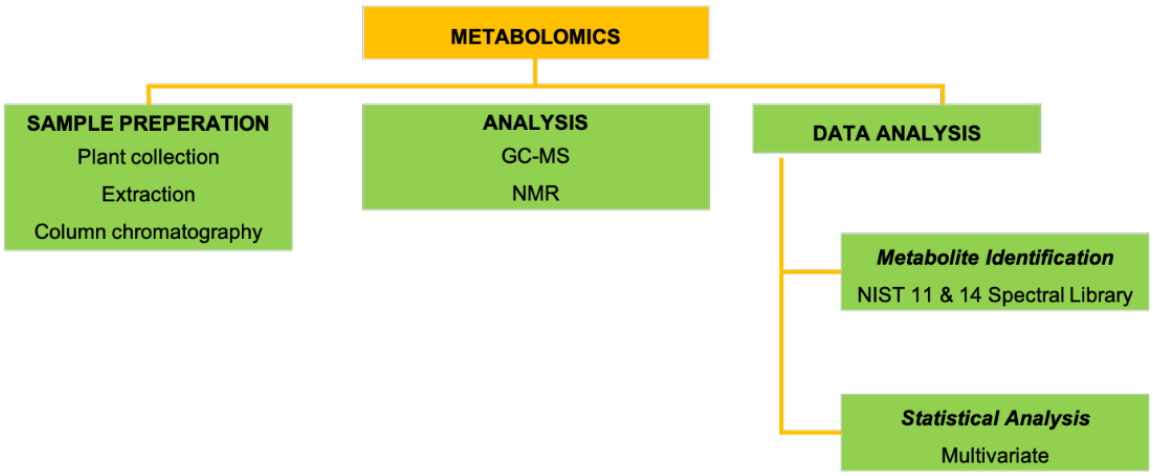

Figure 4.1. The summarized steps followed in metabolomics analysis of *Pappea capensis*.

4.2.1. Plant sample collection

Pappea capensis Eckl. & Zeyh. twigs were collected from Sekhukhune, Limpopo, South Africa. A voucher specimen (12033) was prepared and deposited in the H.G.W.J. Schweickerdt herbarium of the University of Pretoria.

4.2.2. Extraction of plant samples

About 5L of water was used to extract 2.5 kg of plant material using dichloromethane (DCM): 50% methanol (MeOH) in a 1:1 (v/v) ratio. The solution was filtered using Whatman's No. 1 filter paper, and extractions were repeated three times. Filtrates were evaporated in a vacuum yielding DCM (I = 60 g) and aqueous extracts. The aqueous extract (II) was freeze-dried (Virtis) to yield 287 g. The DCM extract (I) was further partitioned between DCM: MeOH (1:1, v/v), separated, concentrated under vacuum, and resulted in DCM (III) and MeOH (IV) extracts, which weighed 40 g and 15 g, respectively. Non-polar extracts were dried in a vacuum at 30ºC. Methanol from the aqueous extracts was vaporized using a rotary vapor water bath (Buchi, R - 200, Switzerland) at 40ºC, and the aqueous extracts were then freeze-dried (Virtis). A

decoction extract (V = 10 g) was prepared to simulate the traditional method used by indigenous people to establish the clinical relevance of the traditional use of *P. capensis*. The water-based decoction was prepared from 500 g of ground *P.* capensis twigs boiled at 100°C for about 45 minutes to an hour. All polar and organic extracts were analyzed independently.

4.2.3. Column chromatography of *Pappea capensis* extracts

Crude extracts II (15g), III (20g), and IV (15g) were subjected to silica gel column chromatography. Extract II was eluted with ethyl acetate (EtOAc): MeOH, MeOH: distilled water (dH_2O) at ratios of 1:10→10:1. Extract III was chromatographed using hexane (H): DCM, DCM: EtOAc, EtOAc: MeOH, and MeOH: dH_2O at ratios of 1:10→10:1 for each solvent system. Extract IV was chromatographed eluting with DCM: EtOAc, EtOAc: MeOH, and MeOH:dH_2O at solvent ratios 1:10→10:1. All fractions collected from the different crude extracts were analyzed using TLC. Extract II was analyzed using EtOAc: MeOH, MeOH:dH_2O, at solvent ratios 1:10→10:1. Extract III employed solvent ratios 1:10→10:1 for solvents H: DCM, DCM: EtOAc, EtOAc: MeOH, and MeOH:dH_2O. Extract IV was analyzed using DCM: EtOAc, EtOAc: MeOH, and MeOH:dH_2O at solvent ratios 1:10→10:1. All fractions that displayed chemical profile similarities were pooled together to yield 25 fractions. Extracts II, III, and IV lost 8 (R-Y), 9 (A-I), and 8 (J-Q) fractions, respectively.

4.2.4. ^{1}H NMR spectroscopy of *Pappea capensis* fractions

All fractions (A – Y) were subjected to ^{1}H NMR analysis to compare their chemical profiles based on their different spectral chemical shifts. Each fraction was reconstituted in deuterated dimethyl sulfoxide (DMSO-d_6) to a concentration of

15mg/ml. About 700 µl was transferred into a 5mm NMR tube (Sigma-Aldrich, United States of America). The Varian 400 MHz NMR was used to obtain the different spectra. The ^{1}H NMR spectroscopy operated at a proton frequency of 400 MHz and ran at a temperature of 25 ºC. The spectral width was 14 ppm, and the acquired scans were 64 per sample. Trimethylsilyl (TMS) was used to reference the spectra, phase correction was manually done, and automatic baseline correction using the Whittaker smoother was carried out (Eilers, 2003).

4.2.5. GC-MS analysis of *Pappea capensis* fractions

The chromatography fractions were subjected to GC-MS analysis to identify different constituents attributed to the observed antiplasmodial activity. All polar fractions were redissolved in distilled methanol, and the lipophilic ones were reconstituted in distilled dichloromethane. Each sample was homogenized by sonication in an ultrasonic water bath (Labotec, Midrand) for 30 minutes at 30 ºC and prepared to a final concentration of 1µg/ml. All prepared extracts were transferred into 1.5 ml short thread vials (Separations, Randburg). Gas chromatography and mass spectrometry analysis were conducted on the GCMS-QP2010SE (Shimadzu, Japan) machine, and an AOC-20i/s autosampler was used to inject the sample into the machine. The start temperature was 30 ºC, and the end temperature was 230 ºC. The splitless injection technique was carried out for all fractions, and the injection volume was 1 µl. For the MS analysis, the ion source temperature was 230 ºC, the interphase temperature was 250 ºC, and the solvent cut time was 1.5 minutes. The detector voltage was set to 0.1 kV and adjusted to a tuning result. The start time was set to 4.5 minutes and the end time was 30 minutes. The acquisition mode was calibrated to the scan mode, running at 2500. The mass range was 40 – 650 m/z. Compounds were

tentatively identified based on comparing their relative mass spectral data with those in the National Institute for Standards and Technology (NIST) database (NIST, 2020). The percentage probability for the NIST search was set at 70 to factor in small spectral differences and negligible discrepancies. A benchmark of ≥ 70% similarity when screening constituents in the different extracts was maintained throughout the analysis.

4.2.6. Statistical analysis using multivariate data analysis (MDA)

The spectral data (^{1}H NMR and GC-MS) was manipulated to ASCII files was conducted on MesteRNova 8.1.1 (Mestrelab Research, United Kingdom). The spectra were normalized and scaled to 0.1 % of trimethylsilyl **(**TMS). The region of 0.00 – 14.00 ppm was binned to 0.04 ppm bins yielding 350 variables. Microsoft Excel Version 356 imported the ASCII files before opening in SIMCA-P 13.0.0 (Umetrics, Umea, Sweden). Pareto scaling before MDA analysis was done to reduce peak interference (Hendriks et al., 2011).

4.3. Results and discussion

Metabolomics using ^{1}H NMR and GC-MS were conducted on 25 polar and non-polar fractions obtained from *P. capensis* crude extracts (II, III, and IV). The ^{1}H NMR spectral data was manipulated to exclude solvent peak regions (2.36 – 2.64 ppm and 3.28 – 3.60 ppm). It was done to reduce false or exaggerated clustering of test samples because of the shared similarity of water solvent peaks. To facilitate data dimensionality, identify outliers and visualize sample clustering, unsupervised PCA score plots were performed on the ^{1}H NMR and GC-MS data, and there was no obvious clustering between the selective and non-selective sample groups (Figure 4.2

A and B). Upon applying the Distance to Model X (DMod[X]), Hotelling's T2Range plot and visualizing the PCA score plots, samples B (Figure 4.2 and 4.2B) and S (Figure 4.2B) were flagged outside the 95% confidence interval region (Hotelling T2 ellipse). These outliers were carefully studied and not excluded from the analysis. The derived PCA score plots failed to discriminate based on observed antiplasmodial activity (Chapter 3). Such could have resulted from the many variations in the biochemical nature of the constituents or that the experimental antimalarial activity results from different phytoconstituents classes. To increase the model's goodness of fit, OPLS-DA, which tells which variables have the largest discriminatory power, was applied to the ^{1}H NMR and GC-MS datasets. Classes were assigned to the different sample groups, and observations were made to assess clustering according to the observed antiplasmodial bioactivity. Clear clustering patterns were observed upon applying the supervised algorithm (Figure 4.3A & C). The OPLS-DA plot discriminated between the selective and non-selective employing Principal Component (PC) 1 (t[1]), while PC2 (t[2]) displayed the variations occurring among secondary metabolites within a class of phytoconstituents (Figure 4.3A & C). The post realignment of the previously observed B (Figure 4.3C) outlier corresponds to the reported antiplasmodial bioactivity.

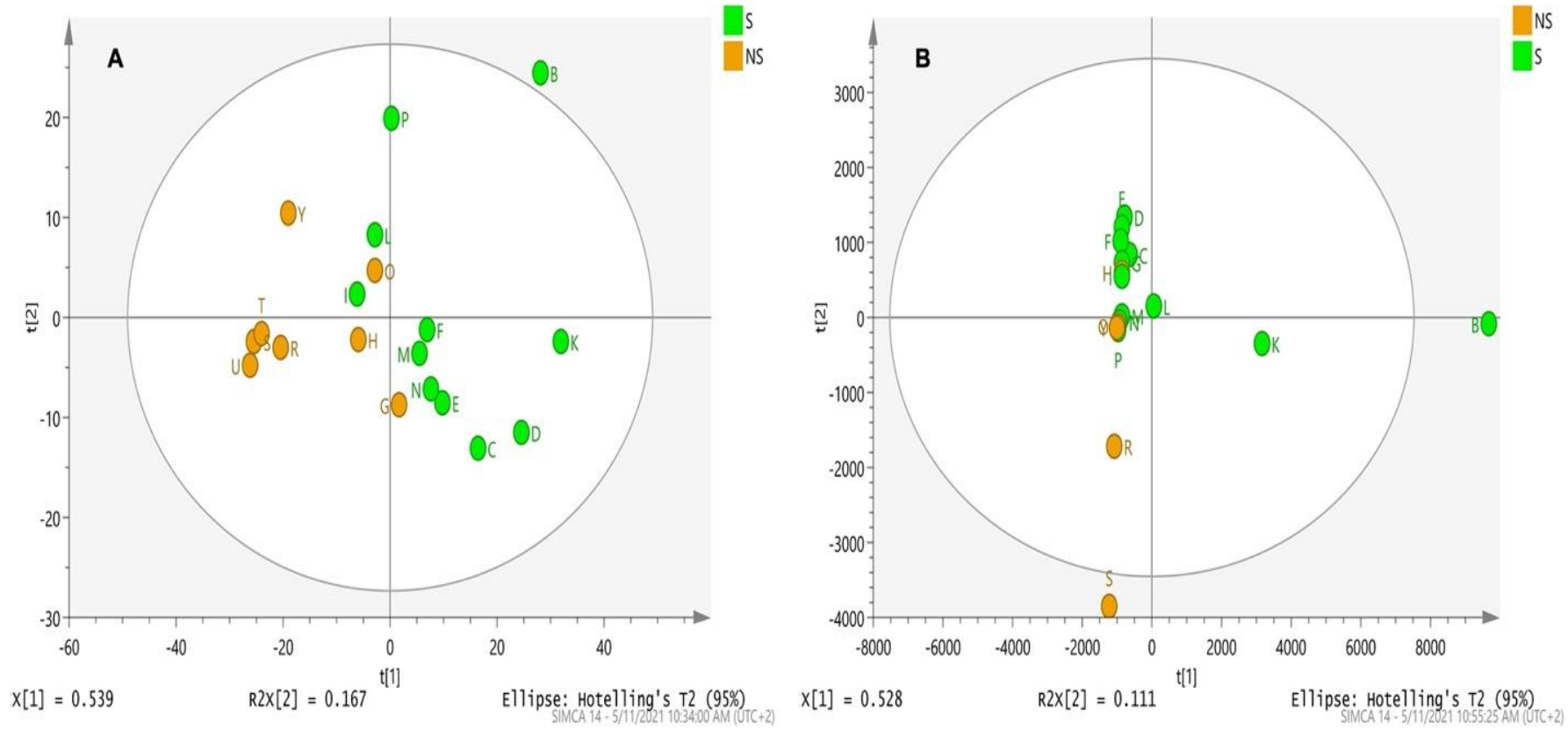

Figure 4.2. Principal Component Analysis (PCA) score plots of *Pappea capensis* fractions generated from GC-MS (A) and (B) ^{1}H NMR spectral datasets: S – Selective and NS – Non-selective.

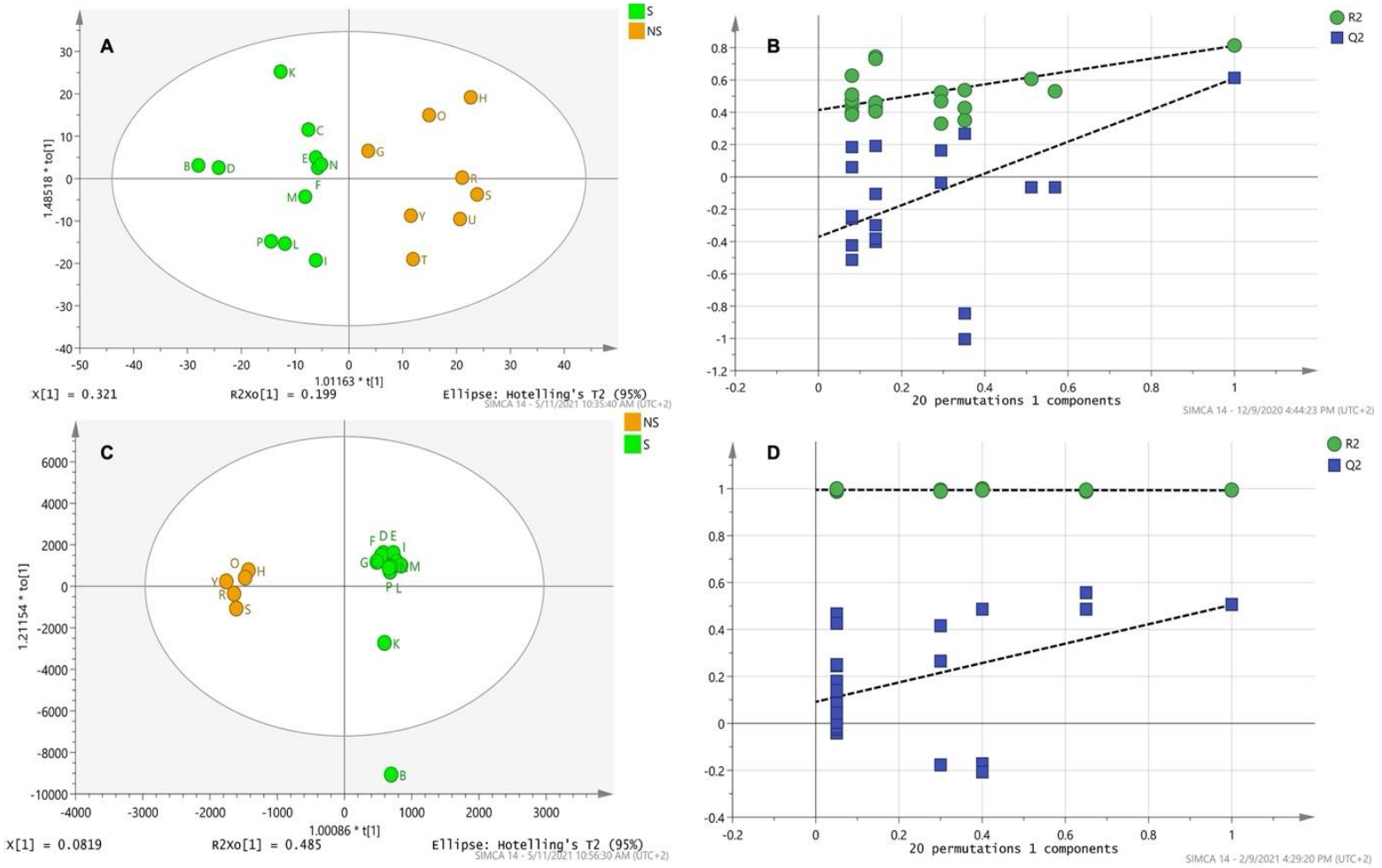

Figure 4.3. (A) The OPLS-DA score plots for *Pappea capensis* fractions were generated from ^{1}H NMR. (B) Permutation score plots validating the OPLS-DA generated from ^{1}H NMR data. (C) The OPLS-DA plots for *Pappea capensis* fractions were generated from GC-MS data. (D) Permutation score plot validating the OPLS-DA generated from GC-MS data.

The interpretation of OPLS-DA models is based on the values of the variables represented by R^2 and Q^2. As a means of providing an overview of the model's fitness, the cross-validation variance value (R^2) was used to describe the amount of explained data explained, while Q^2 (variance) measured the model's ability to predict antiplasmodial activity (Eriksson et al., 2013). The ^{1}H NMR and GC-MS metabolomics models discriminated the test fractions according to assigned parameters (Figure 4.3A and 4.3C). However, they differ in their predictive power of unknown samples. The R^2 and Q^2 values of 0.812 and 0.611, respectively, attest to the robustness of the OPLS-DA model generated from ^{1}H NMR data in predicting antiplasmodial activity (Figure 4.3B). However, the model developed from GC-MS data appears to be overfitted and cannot be relied on for predicting the antiplasmodial activity of unknown samples (Figure 4.3D).

A referencing peak (solvent peak) in ^{1}H NMR metabolomics allows aligning all spectra to a common height. This referencing affords easy data manipulation when transporting it to different statistical analytical platforms. On the other hand, GC-MS data lacks what could be equivalent to a referencing peak in the case of ^{1}H NMR - based metabolomics, which can align the data to a single common phytoconstituent present in all the samples. It is rather difficult to manipulate GC-MS data for metabolomics studies. Models are generally considered not overfitted when their R^2 and Q^2 values are ~ 0.5, while the incongruent values between R^2 and Q^2 ($R^2 > > Q^2$) describe an overfitted model (Hendriks et al., 2011). Also, the acceptable students' T-test *P*-value of a robust and non-overfitted model should be less than 0.05. Our models were further validated using CV-ANOVA and permutation score plots (Figure 4.3B & D). The generated CV-ANOVA score plots analyzed the variance in the cross-validation of the Y variable residuals, while the permutation plots assessed the degree

of risk that a model can be spurious (Eriksson et al., 2013). When applying the CV-ANOVA and permutation plots, only the OPLS-DA generated from ^{1}H NMR data was validated to run a lower risk of overfitting with a student's T-test P = 0.007 (Figure 4.3B). The OPLS-DA model generated from GC-MS ran a high risk of overfitting with R^2 and Q^2 values of 0.99 and 0.385, respectively. Its low Q^2 value handicapped its antiplasmodial bioactivity predictive capabilities (Figure 4.3C). With a students' T-test P = 0.74, the model has a high probability of overfitting. Overfitting introduces bias because the training data set is closely related to the model. It makes the model relevant only to the data set under question and not to other data sets. Cross-validation of data, data augmentation, and simplification could reduce overfitting. Regardless of the obvious clustering according to the observed bioactivity, the model's $R^2 >> Q^2$, thus completely ruled out as overfitted with a student's T-test P = 0.74.

The contribution plot generated from the ^{1}H NMR data (Figure 4.4) correlates with metabolite classes commonly found in the botanical kingdom and is tentatively identified as aliphatic, allylic, and methyl ketone-based constituents (0.9 – 1.5 ppm, 1.6 – 1.9 ppm, and 2.0 – 2.2 ppm), respectively. Constituents in the aliphatic region contribute significantly to the discrimination of the samples. Terpenoids, the most prominent aliphatic constituents, contributed the most to discriminating selective and non-selective antiplasmodial fractions. Major regions of non-selective samples contribute to the discrimination observed in the contribution plot (Figure 4.4). These have been studied, and the observed peaks have been tentatively identified to represent sugar (3.1 – 3.8 ppm), alcohol (4 – 4.8 ppm), vinylic (6.3 – 7.2 ppm), and aromatic based constituents (8.5 – 8.9 ppm).

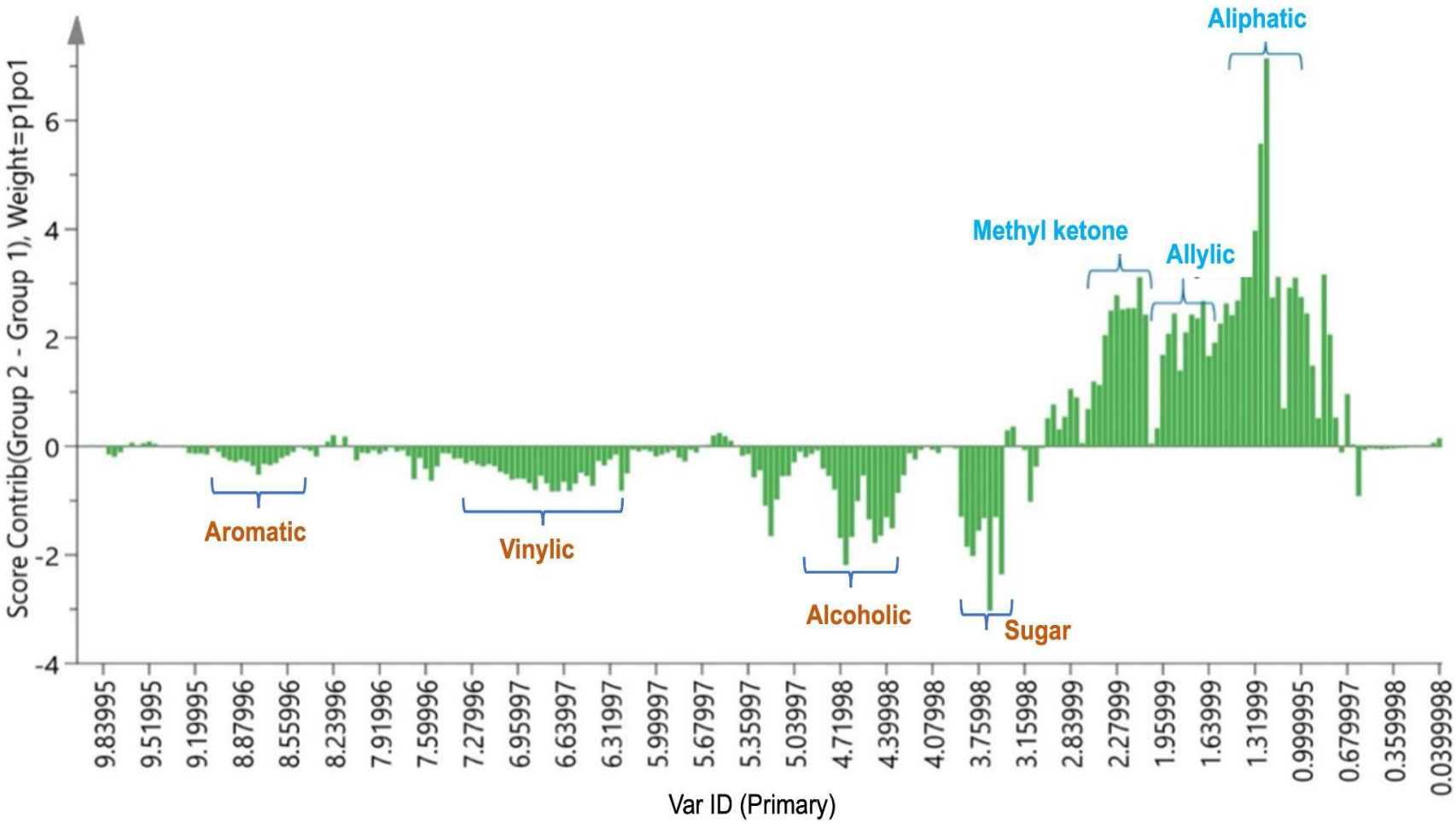

Figure 4.4. The contribution plot generated from ^{1}H NMR data of *Pappea capensis* fractions compares selective (bars projecting up) and non-selective (projecting down) clusters.

The contribution plot generated from the GC-MS data shows the different sample constituents postulated to contribute to the observed antiplasmodial activity (Figure 4.5). With GC-MS spectral libraries (NIST 11 and 14), octasiloxane, β-amyrin, pentadecanon, 3-O-methyl-d-glucose, and tetradecane were identified to have contributed significantly to the variations in the GC-MS data (Figure 4.5). Despite the poor predictability of the GC-MS-derived OPLS-DA, its analysis remains a powerful tool to identify phytoconstituents. Unknown constituents can also be easily identified and targeted using different optimized approaches for further antiplasmodial and cytotoxicity tests. All the known and unknown compounds in *P.* capensis crude extracts are documented in the appendix (Table 6.2 – 6.6). All the unknown compounds with prominent peaks can be prioritized for further extraction, isolation, and characterization to discover novel antiplasmodial compounds. The corresponding ^{1}H NMR and the GC-MS spectral data are shown in Appendix supplemental data (Figure 6.1 – 6.50).

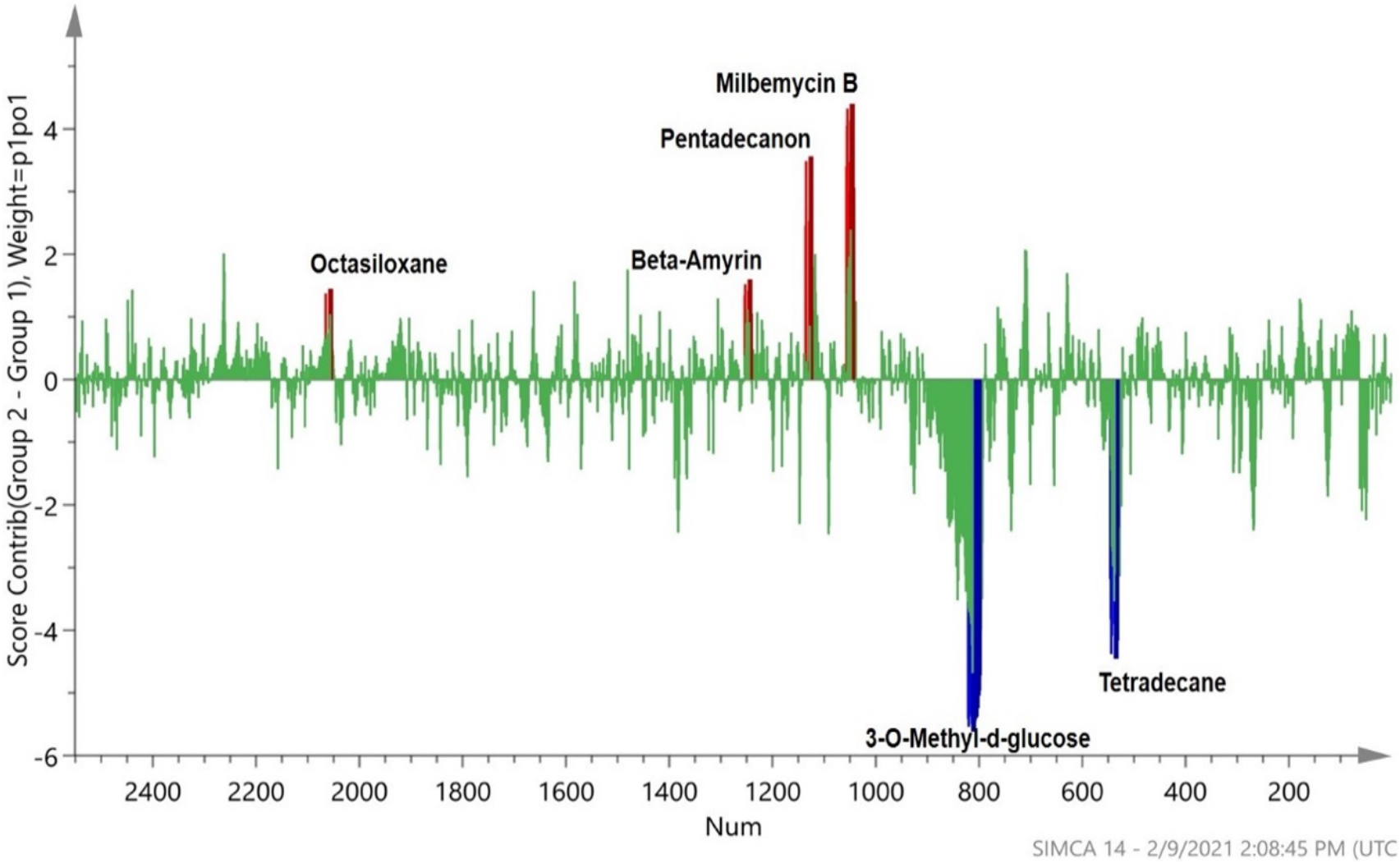

Figure 4.5. The contribution plot generated from GC-MS data of *Pappea capensis* fractions displays the comparison between the selective (bars projecting up) and non-selective (bars projecting down) constituents.

4.4. Conclusion

This study has shown the practicality of the ^{1}H NMR OPLS-DA model as a reliable and robust antiplasmodial bioactivity prediction tool over the GC-MS generated model. It can also serve as a high throughput antiplasmodial activity screening technique and can be used to identify classes of compounds. More significantly, it promises to be effective at studying antiplasmodial activity in other plant species besides *P. capensis*. The same cannot be ascertained about the GC-MS-derived model. However, GC-MS is an invaluable resource for identifying phytoconstituents in complex crude extracts. It is an effective approach to dereplicating known compounds with established antiplasmodial activity from the unknown. Metabolomics is still a growing research field and incorporating other analytical techniques like LC/MS/MS could improve the turnout in the observed results.

Crafting new approaches to how GC-MS spectra can be referenced to a common standard could also improve the model's goodness of fit, thus increasing its chances of being a reliable prediction for antiplasmodial activity. The model's predictive ability derived from 1H NMR analysis, coupled with GC-MS potential to identify constituents of interest, is reasonable in bioprospecting drug leads for antimalaria purposes. These techniques complement each other in an invaluable way that advances the study of plant metabolomics to greater heights. This study has demonstrated the possibility of using these two techniques for dereplicating known antiplasmodial compounds to focus on unknown prominent compounds. Further attempts to prioritize novel compounds it prominent peaks will need to be conducted to isolate and characterize antiplasmodial phytoconstituents.

4.5. References

Beutler, J.A., 2009. Natural products as a foundation for drug discovery. Current Protocols in Pharmacology 46, 1–21.

Demarque, D.P., Dusi, R.G., de Sousa, F.D.M., Grossi, S.M., Silvério, M.R.S., Lopes, N.P., Espindola, L.S., 2020. Mass spectrometry-based metabolomics approach in the isolation of bioactive natural products. Scientific Reports 10, 1–9.

Eilers, P.H.C., 2003. A perfect smoother. Analytical Chemistry 75, 3631–3636.

Eriksson, L., Byrne, T., Johansson, E., Trygg, J., Vikström, C., 2013. Multi-and megavariate data analysis basic principles and applications. Umetrics Academy, Sweden.

Hendriks, M.M.W.B., Eeuwijk, F.A. van, Jellema, R.H., Westerhuis, J.A., Reijmers, T.H., Hoefsloot, H.C.J., Smilde, A.K., 2011. Data-processing strategies for metabolomics studies. Trends in Analytical Chemistry 30, 1685–1698.

Heyman, H.M., Meyer, J.J.M., 2012. NMR-based metabolomics as a quality control tool for herbal products. South African Journal of Botany 82, 21–32.

Peters, K., Treutler, H., Döll, S., Kindt, A.S.D., Hankemeier, T., Neumann, S., 2019. Chemical diversity and classification of secondary metabolites in nine bryophyte species. Metabolites 9, 1–18.

Rasoanaivo, P., Wright, C.W., Willcox, M.L., Gilbert, B., 2011. Whole-plant extracts versus single compounds for the treatment of malaria: synergy and positive interactions. Malaria Journal 10, 1–12.

Sadiq, A., Hayat, M.Q., Ashraf, M., 2014. Ethnopharmacology of Artemisia annua L.: A Review, in: Aftab, T., Ferreira, J., Khan, M., Naeem, M. (Eds.), Artemisia Annua - Pharmacology and Biotechnology. Springer, Berlin, Heidelberg, Berlin, pp. 9–25.

Skwarecki, A.S., Nowak, M.G., Milewska, M.J., 2020. Synthetic strategies in the construction of organic low molecular-weight carrier-drug conjugates. Bioorganic Chemistry 104, 104311.

Uthe, H., van Dam, N.M., Hervé, M.R., Sorokina, M., Peters, K., Weinhold, A., 2020. A practical guide to implementing metabolomics in plant ecology and biodiversity research, in: Advances in Botanical Research. Academic Press Inc.

Verpoorte, R., Choi, Y.H., Kim, H.K., 2007. NMR-based metabolomics at work in phytochemistry. Phytochemistry Reviews 6, 3–14.

Wan, H., Tian, Y., Jiang, H., Zhang, X., Ju, X., 2020. An NMR-based drug screening strategy for discovering active substances from herbal medicines: using Radix polygoni multiflori as an example. Journal of Ethnopharmacology 254, 112712.

Zhang, Q.W., Lin, L.G., Ye, W.C., 2018. Techniques for extraction and isolation of natural products: A comprehensive review. Chinese Medicine 13, 20.

CHAPTER 5: GENERAL CONCLUSION

5.1. General conclusion……..101

5.2. Challenges and prospects……...……...102

5.1. General conclusion

The current research points out the significance of relying on ethnopharmacology to search for novel malaria chemotherapeutics. *Pappea capensis,* which the Vha-Venda has commonly used to treat malaria and its related symptoms, has great potential to yield different metabolites that can be taken up as new malaria drug leads. Although activity was poor in the polar extracts, which indigenous people claim to treat malaria effectively, they need not be discarded without being thoroughly studied. Often when extracts fail to yield the desired biological activity, we are quick to discredit indigenous knowledge. In the case of *P. capensis*, there is a great chance that the polar extracts may not necessarily have antiplasmodial activity but have bioactivity to its related symptoms. The alleviation of malaria-related symptoms ultimately leads to the curing of malaria. The desired antiplasmodial pharmacological response is sometimes found in an isolated constituent, not the crude extract. Finding that active metabolite becomes the key to discovering the next antimalarial effective drug. Isolation and characterization of compounds is a technical exercise requiring skill and tact. However, advances have been made to fast-track metabolite isolation, characterization, and identification.

The use of metabolomics to dereplicate known compounds with established biological activity from the unknown comes to the rescue. Coupling ^{1}H NMR and GC-MS, as has been the case in this study, has proven suitable. Extracts can be screened, and unknown compounds with prominent spectral peaks are prioritized for isolation, characterization, and antiplasmodial tests. It prevents the duplication that occurs when following activity-guided isolation of compounds, which leads to the isolation of compounds already studied. Isolating known compounds does not contribute to new

ones that can upscale the discovery of novel drug leads. This study has validated the ethnomedicinal use of jacket plum by the Vha-Venda in treating malaria. It has also shown the antiplasmodial activity of the polar methanol extract. Most of the observed activity in *P. capensis* was observed in the non-polar extracts. Having an opposite exit high antiplasmodial activity is not an observed common occurrence. It goes without saying that if malaria is to be eradicated, the discovery of novel drugs with different mechanisms of action needs to be prioritized. History has constantly supplied remedies through the heritage of medicinal plants used by indigenous people; these should be explored thoroughly. More research in medicinal plants with antimalarial properties must be prioritized and funded. Only when the antimalaria drug arsenal has a variety of the best drugs can we stand a great chance to curb the detrimental effects of the fast-evolving malaria parasite.

5.2. Challenges and prospects

Major challenges faced in completing this study include a shortage of plant material, evaporating methanol from polar crude extracts, sample contamination during GC-MS analysis and manipulating GC-MS data for metabolomics analysis. Suggested ways to avoid such challenges would be to collect more plant material. If the goal is to isolate individual constituents eventually, starting with a sizable amount of plant material is important. During extraction, column chromatography, antiplasmodial and cytotoxicity screening, some plant material is lost in the process of which compound isolations are to be conducted; there remains a small amount of it. Evaporating methanol from water can be challenging; incorporating other methods like blowing nitrogen gas or drying in a vacuum will ensure no traces of methanol remain. Removing all methanol is important, especially when the polar extracts are freeze-dried. Even a

small amount of methanol can cause the freeze-drying machine to malfunction. During GC-MS analysis, samples are prone to contamination by traces of pieces that remain in the device from the previous user. It results in incorrect spectral information that contains data of the prior user. It is therefore imperative to clean the machine thoroughly before analyzing samples. Manipulating GC-MS spectral data can be limiting, especially when using one analytical platform. It is best to use two or more platforms to overcome these. Examples of analytical platforms that work best when coupled are Shimadzu and MesteRNova. These platforms work complementary and make up for each other's shortcomings.

Prospects should prioritize the isolation, characterization, and identification of unknown secondary metabolites from extracts and fractions that showed antiplasmodial bioactivity. It is the best way to target constituents that have not been studied before. It increases the chances of discovering new compounds with novel mechanisms of action that can be used as lead antimalarial drugs. This dereplication approach to antiplasmodial constituent isolation allows novel lead compounds to be discovered without wasting time, money, and resources studying what has already been explored.

CHAPTER 6: APPENDIX

Tables:

Table 6.1. Metabolite composition of Extract I……107

Table 6.2. Metabolite composition of extract II……119

Table 6.3. Metabolite composition of Extract III……112

Table 6.4. Metabolite composition of Extract IV……114

Table 6.5. Metabolite composition of Extract V……117

Figures:

Figure 6.1. ^{1}H NMR spectrum of A……119

Figure 6.2. ^{1}H NMR spectrum of B……120

Figure 6.3. ^{1}H NMR spectrum of C……121

Figure 6.4. ^{1}H NMR spectrum of D……122

Figure 6.5. ^{1}H NMR spectrum of E……123

Figure 6.6. ^{1}H NMR spectrum of F……124

Figure 6.7. ^{1}H NMR spectrum of G……125

Figure 6.8. ^{1}H NMR spectrum of H……126

Figure 6.9. ^{1}H NMR spectrum of I……127

Figure 6.10. ^{1}H NMR spectrum of J……128

Figure 6.11. ^{1}H NMR spectrum of K. ……129

Figure 6.12. ^{1}H NMR spectrum of L……130

Figure 6.13. ^{1}H NMR spectrum of M.....131

Figure 6.14. ^{1}H NMR spectrum of N.....132

Figure 6.15. ^{1}H NMR spectrum of O. 133

Figure 6.16. ^{1}H NMR spectrum of P.....134

Figure 6.17. ^{1}H NMR spectrum of Q.....135

Figure 6.18. ^{1}H NMR spectrum of R.....136

Figure 6.19. ^{1}H NMR spectrum of S.....137

Figure 6.20. ^{1}H NMR spectrum of T.....138

Figure 6.21. ^{1}H NMR spectrum of U.....139

Figure 6.22. ^{1}H NMR spectrum of V.....140

Figure 6.23. ^{1}H NMR spectrum of W.....141

Figure 6.24. ^{1}H NMR spectrum of X.....142

Figure 6.25. ^{1}H NMR spectrum of Y.....143

Figure 6.26. GC-MS spectrum of A.....144

Figure 6.27. GC-MS spectrum of B.....145

Figure 6.28. GC-MS spectrum of C.....146

Figure 6.29. GC-MS spectrum of D.....147

Figure 6.30. GC-MS spectrum of E.....148

Figure 6.31. GC-MS spectrum of F.....149

Figure 6.32. GC-MS spectrum of G.....150

Figure 6.33. GC-MS spectrum of H.....151

Figure 6.34. GC-MS spectrum of I.....152

Figure 6.35. GC-MS spectrum of J.....153

Figure 6.36. GC-MS spectrum of K.....154

Figure 6.37. GC-MS spectrum of L.....155

Figure 6.38. GC-MS spectrum of M.....156

Figure 6.39. GC-MS spectrum of N.....157

Figure 6.40. GC-MS spectrum of O.....158

Figure 6.41. GC-MS spectrum of P.....159

Figure 6.42. GC-MS spectrum of Q.....160

Figure 6.43. GC-MS spectrum of R.....161

Figure 6.44. GC-MS spectrum of S.....162

Figure 6.45. GC-MS spectrum of T.....163

Figure 6.46. GC-MS spectrum of U.....164

Figure 6.47. GC-MS spectrum of V.....165

Figure 6.48. GC-MS spectrum of W.....166

Figure 6.49. GC-MS spectrum of X.....167

Figure 6.50. GC-MS spectrum of Y.....168

Table 6.1. Metabolite composition of Extract I

Ret.Time	Proc.From	Proc. To	Mass	Area	Height	A/H	Conc.	Name

11.556	11.535	11.595	TIC	32663	20372	1.6	0.33	2(4H)-Benzofuranone, 5,6,7,7a-tetrahydro-4,4,7a-trimethyl-, (R)-
12.21	12.19	12.23	TIC	30669	23583	1.3	0.31	Caryophyllene oxide
14.229	14.2	14.25	TIC	14635	13397	1.09	0.15	5-Isopropyl-6-methyl-hepta-3,5-dien-2-ol
14.47	14.445	14.505	TIC	30394	17522	1.73	0.3	Nonadecane, 9-methyl-
14.95	14.91	14.99	TIC	151951	82827	1.83	1.52	2-Pentadecanone, 6,10,14-trimethyl-
15.005	14.99	15.045	TIC	31660	18879	1.68	0.32	Tetradecanoic acid, trimethylsilyl ester
15.761	15.735	15.805	TIC	68201	42747	1.6	0.68	Myristic acid
16.934	16.895	16.99	TIC	215399	121098	1.78	2.15	Palmitic acid
23.7	23.66	23.77	TIC	184075	81581	2.26	1.84	2-methylhexacosane
25.023	24.97	25.19	TIC	2525473	525923	4.8	25.25	Tetratetracontane
25.195	25.19	25.22	TIC	82102	53731	1.53	0.82	**Unknown**
25.245	25.22	25.255	TIC	70481	35638	1.98	0.7	**Unknown**
25.293	25.255	25.33	TIC	130139	39468	3.3	1.3	Silane, trimethyl(octacosyloxy)-
25.354	25.33	25.415	TIC	84922	27973	3.04	0.85	Octacosyl heptafluorobutyrate
26.257	26.21	26.29	TIC	876608	337387	2.6	8.77	Tetratetracontane
26.312	26.29	26.46	TIC	1038757	211125	4.92	10.39	1-Heptacosanol

26.505	26.46	26.53	TIC	62253	13804	4.51	0.62	**Unknown**
26.851	26.815	26.95	TIC	916341	363110	2.52	9.16	.alpha.-Amyrin
26.983	26.95	27.03	TIC	123071	48283	2.55	1.23	Lup-20(29)-en-3-one
27.125	27.03	27.28	TIC	3331011	1482396	2.25	33.31	Lup-20(29)-en-3-ol, acetate, (3.beta.)-

Table 6.2. Metabolite composition of extract II.

Ret.Time	Proc.From	Proc.To	Mass	Area	Height	A/H	Conc.	Name
5.075	5.01	5.185	TIC	147886	23815	6.21	7.43	6,6,8,8,10,10-Hexamethyl-2,5,7,9,11,14-hexaoxa-6,8,10-trisilapentadecane
5.734	5.67	5.83	TIC	251630	50381	4.99	12.63	Undecane
7.134	7.095	7.205	TIC	103194	34458	2.99	5.18	Dodecane
7.428	7.395	7.465	TIC	42944	19201	2.24	2.16	Cyclotetrasiloxane, octamethyl-
7.557	7.515	7.6	TIC	67620	27405	2.47	3.4	2,2'-Bis-trimethylsilylbenzhydryl methyl ether
8.828	8.8	8.85	TIC	35867	16771	2.14	1.8	2',6'-Dihydroxyacetophenone, bis(trimethylsilyl) ether
9.772	9.75	9.795	TIC	47497	26170	1.81	2.38	Cyclopentasiloxane, decamethyl-
9.821	9.795	9.845	TIC	155236	85754	1.81	7.79	Pentadecane
9.858	9.845	9.89	TIC	81993	51423	1.59	4.12	Trimethylsilyl 3-methyl-4-[(trimethylsilyl)oxy]benzoate
9.9	9.89	9.905	TIC	8929	12161	0.73	0.45	**Unknown**
9.921	9.905	9.93	TIC	19381	15139	1.28	0.97	**Unknown**
9.96	9.93	9.965	TIC	22297	13398	1.66	1.12	**Unknown**

10.981	10.97	11.015	TIC	18629	14000	1.33	0.94	Hexasiloxane, tetradecamethyl-
11.056	11.015	11.085	TIC	29623	13319	2.22	1.49	Cycloheptasiloxane,tetradecamety-
11.862	11.84	11.885	TIC	29036	18059	1.61	1.46	Cyclohexasiloxane, dodecamethyl-
11.914	11.885	11.965	TIC	68658	40787	1.68	3.45	1,1,1,5,7,7,7-Heptamethyl-3,3-bis(trimethylsiloxy)tetrasiloxane
12.269	12.245	12.31	TIC	65152	34965	1.86	3.27	Hexadecane
12.904	12.855	12.92	TIC	29870	13152	2.27	1.5	Heptasiloxane, hexadecamethyl-
13.753	13.7	13.78	TIC	92473	42724	2.16	4.64	Cycloheptasiloxane,tetradecamety-
14.478	14.445	14.535	TIC	77330	30991	2.5	3.88	Heptadecane
14.631	14.535	14.665	TIC	47548	15356	3.1	2.39	Trimethylsilyl 3-methyl-4-[(trimethylsilyl)oxy]benzoate
15.414	15.355	15.45	TIC	86034	41361	2.08	4.32	Cyclooctasiloxane,hexadecamethy-
15.966	15.95	16	TIC	21121	14554	1.45	1.06	Benzenepropanoic acid, 3,5-bis(1,1-dimethylethyl)-4-hydroxy-, methyl ester
16.202	16.175	16.23	TIC	22520	12886	1.75	1.13	Hexasiloxane, tetradecamethyl-
16.482	16.445	16.52	TIC	65383	27382	2.39	3.28	Heptadecane
16.925	16.895	16.955	TIC	58995	35357	1.67	2.96	Cyclononasiloxane,octadecamethyl

17.642	17.625	17.685	TIC	24005	12158	1.97	1.21	Heptasiloxane, hexadecamethyl
18.31	18.28	18.36	TIC	56585	26651	2.12	2.84	Trimethylsilyl 3-methyl-4-[(trimethylsilyl)oxy]benzoate
19.592	19.55	19.625	TIC	34615	15883	2.18	1.74	Cyclononasiloxane,octadecamethyl
20.794	20.75	20.81	TIC	21205	11097	1.91	1.06	Cyclononasiloxane,octadecamethyl
22.756	22.7	22.83	TIC	34645	10017	3.46	1.74	**Unknown**
26.235	26.225	26.375	TIC	47190	9857	4.79	2.37	**Unknown**
28.293	28.135	28.305	TIC	47526	11147	4.26	2.39	**Unknown**
28.43	28.42	28.445	TIC	8280	10427	0.79	0.42	**Unknown**
28.654	28.63	28.68	TIC	20674	10459	1.98	1.04	**Unknown**

Table 6.3. Metabolite composition of Extract III.

Ret.Time	Proc.From	Proc.To	Mass	Area	Height	A/H	Conc.	Name
11.563	11.535	11.61	TIC	49168	25063	1.96	0.46	2(4H)-Benzofuranone, 5,6,7,7a-tetrahydro-4,4,7a-trimethyl-, (R)-
12.209	12.19	12.235	TIC	24943	18511	1.35	0.24	Caryophyllene oxide
14.949	14.915	14.98	TIC	130963	81728	1.6	1.24	2-Pentadecanone, 6,10,14 trimethyl-
14.999	14.98	15.04	TIC	32427	18691	1.73	0.31	Myristic acid
16.932	16.895	16.98	TIC	266674	154968	1.72	2.51	Palmitic acid
22.292	22.265	22.335	TIC	60953	29103	2.09	0.57	Tetratetracontane
23.701	23.66	23.78	TIC	269047	104854	2.57	2.54	2-methylhexacosane
25.022	24.97	25.44	TIC	3054741	603089	5.07	28.81	Tetratetracontane
25.355	25.34	25.43	TIC	61922	23837	2.6	0.58	**Unknown**
26.255	26.2	26.285	TIC	673488	273696	2.46	6.35	Tetratetracontane
26.311	26.285	26.47	TIC	900091	198993	4.52	8.49	1-Heptacosanol
26.852	26.805	26.95	TIC	981983	382169	2.57	9.26	.beta.-Amyrin
26.985	26.95	27.045	TIC	143161	57119	2.51	1.35	Lup-20(29)-en-3-one
27.125	27.075	27.3	TIC	3825650	1672040	2.29	36.08	Lup-20(29)-en-3-ol, acetate, (3.beta.)-

27.563	27.53	27.62	TIC	128883	47293	2.73	1.22	Lup-20(29)-en-3-ol, acetate, (3.beta.)-

Table 6.4. Metabolite composition of Extract IV.

Ret.Time	Proc.From	Proc.To	Mass	Area	Height	A/H	Conc.	Name
5.713	5.66	5.835	TIC	305057	58432	5.22	4.43	Undecane
7.13	7.09	7.19	TIC	131306	45972	2.86	1.91	Dodecane
7.564	7.535	7.59	TIC	33780	17904	1.89	0.49	2,2'-Bis-trimethylsilylbenzhydryl methyl ether
9.817	9.745	9.845	TIC	202966	125403	1.62	2.95	Pentadecane
9.865	9.845	9.895	TIC	29893	19085	1.57	0.43	(3-Hydroxy-4-methoxyphenyl)ethylene glycol tris(trimethylsilyl) ether
11.565	11.535	11.595	TIC	34356	21911	1.57	0.5	2(4H)-Benzofuranone, 5,6,7,7a-tetrahydro-4,4,7a-trimethyl-
11.919	11.89	11.95	TIC	29503	22420	1.32	0.43	1,2-Epoxy-3,4-dihydroxycyclohexano[a]pyrene,
12.258	12.235	12.3	TIC	118716	73347	1.62	1.72	Hexadecane
13.752	13.72	13.785	TIC	31985	17759	1.8	0.46	Tetradecamethyl-
14.466	14.44	14.5	TIC	69139	44136	1.57	1.00	Heptadecane
14.947	14.905	14.995	TIC	304445	182291	1.67	4.42	2-Pentadecanone
15.418	15.385	15.45	TIC	34189	20972	1.63	0.5	Hexadecamethyl-
15.757	15.685	15.805	TIC	377238	184737	2.04	5.48	Palmitic acid

15.963	15.94	16.015	TIC	57097	30702	1.86	0.83	Benzenepropanoic acid
16.13	16.105	16.19	TIC	51706	19635	2.63	0.75	Octane, 1,1'-oxybis-
16.471	16.445	16.495	TIC	30164	19355	1.56	0.44	Hexadecane
16.931	16.9	16.96	TIC	37781	21715	1.74	0.55	Octadecamethyl-
17.464	17.425	17.5	TIC	54269	26023	2.09	0.79	Cyclopentanol, 2,4,4-trimethyl-
17.837	17.81	17.855	TIC	32897	20762	1.58	0.48	Palmitoyl chloride
18.314	18.28	18.365	TIC	49248	19774	2.49	0.72	Palmitic acid
19.669	19.64	19.715	TIC	63347	29211	2.17	0.92	4,8,12,16-Tetramethylheptadecan-4-olide
23.631	23.59	23.65	TIC	54662	22067	2.48	0.79	1,5,9,9-Tetramethyl-2-oxatricyclo[6.4.0.0(4,8)]dodecane
23.71	23.66	23.79	TIC	173575	62875	2.76	2.52	Hexacosyl heptafluorobutyrate
25.058	25.01	25.095	TIC	74814	31805	2.35	1.09	17-Pentatriacontene
26.314	26.28	26.355	TIC	71394	29376	2.43	1.04	1-Heptacosanol
26.848	26.78	26.94	TIC	1134902	491176	2.31	16.49	.alpha.-Amyrin
26.983	26.94	27.035	TIC	118316	46787	2.53	1.72	Lup-20(29)-en-3-one
27.121	27.07	27.185	TIC	2976885	1423712	2.09	43.25	Lupeol

27.2	27.185	27.265	TIC	153221	70695	2.17	2.23	D:B-Friedo-B':A'-neogammacer-5-en-3-ol, (3.beta.)-
27.567	27.535	27.615	TIC	46742	17517	2.67	0.68	Lupeol

Table 6.5. Metabolite composition of Extract V.

Ret.Time	Proc.From	Proc.To	Mass	Area	Height	A/H	Conc.	Name
5.713	5.66	5.81	TIC	294354	57601	5.11	5.48	Undecane
7.126	7.08	7.20	TIC	125261	46538	2.69	2.33	Dodecane
7.405	7.39	7.53	TIC	34816	10915	3.19	0.65	Cyclotetrasiloxane, octamethyl-
7.563	7.53	7.595	TIC	33266	17151	1.94	0.62	**Unknown**
9.72	9.705	9.79	TIC	30994	10056	3.08	0.58	1-Tetradecene
9.818	9.79	9.845	TIC	179065	110400	1.62	3.34	Pentadecane
9.86	9.845	9.875	TIC	44084	30091	1.47	0.82	**Unknown**
9.91	9.875	9.935	TIC	44308	15734	2.82	0.83	1,5,9-Decatriene, 2,3,5,8-tetramethyl-
11.065	11.035	11.09	TIC	17974	10410	1.73	0.33	Cycloheptasiloxane, tetradecamethyl-
11.305	11.29	11.33	TIC	35292	18919	1.87	0.66	**Unknown**
11.914	11.89	11.935	TIC	32148	23262	1.38	0.6	**Unknown**
12.185	12.155	12.21	TIC	19357	11806	1.64	0.36	Dichloroacetic acid, heptadecyl ester
12.258	12.21	12.295	TIC	105953	64480	1.64	1.97	Hexadecane
12.602	12.405	12.655	TIC	1750438	241361	7.25	32.61	1-Methyl-1-n-pentyloxy-1-silacyclobutane
12.765	12.655	12.88	TIC	2068215	219316	9.43	38.52	.alpha.-d-Mannofuranoside, methyl

12.905	12.88	12.965	TIC	123050	41717	2.95	2.29	**Unknown**
13.301	13.275	13.335	TIC	18137	12266	1.48	0.34	**Unknown**
13.75	13.69	13.78	TIC	68727	30049	2.29	1.28	**Unknown**
13.807	13.78	13.85	TIC	32372	18963	1.71	0.6	**Unknown**
14.469	14.435	14.51	TIC	48240	27671	1.74	0.9	Hexadecane
14.638	14.61	14.67	TIC	20368	12192	1.67	0.38	**Unknown**
15.411	15.37	15.46	TIC	48959	22685	2.16	0.91	**Unknown**
15.96	15.91	16.015	TIC	58861	32964	1.79	1.1	Benzenepropanoic acid
16.925	16.885	16.975	TIC	51975	25239	2.06	0.97	**Unknown**
27.12	27.085	27.17	TIC	82396	38449	2.14	1.53	Lupeol

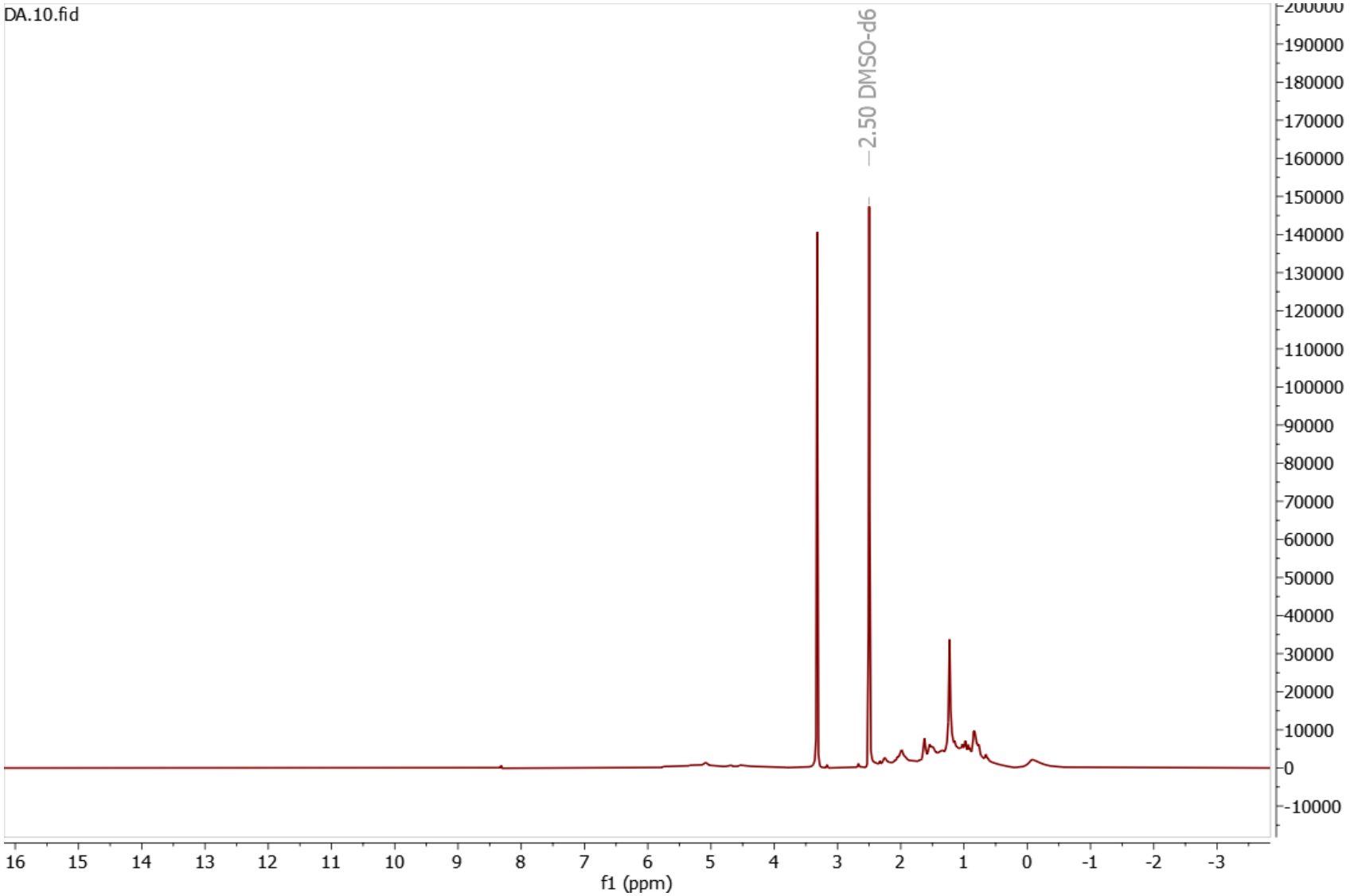

Figure 6.1. 1H NMR spectrum of A.

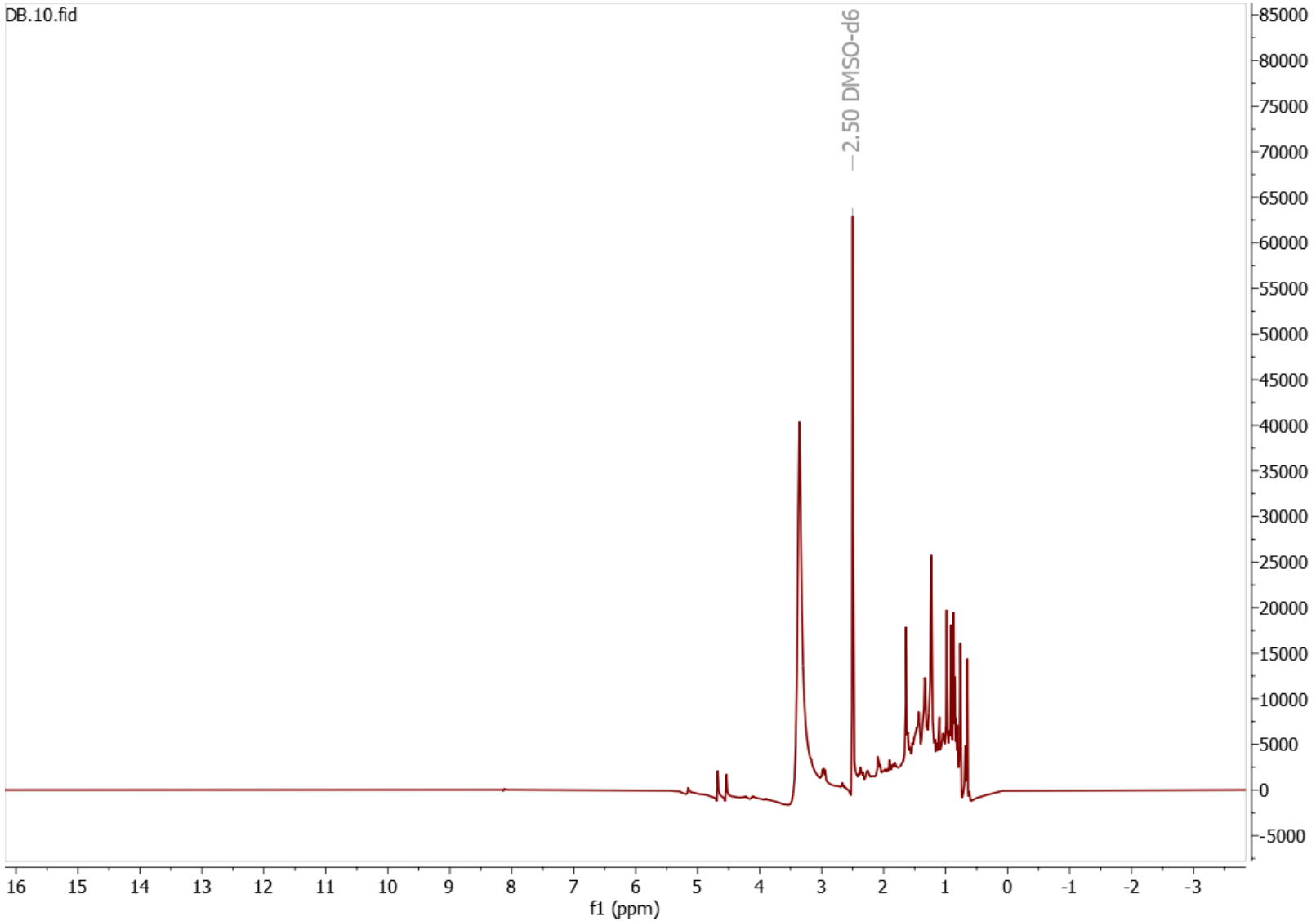

Figure 6.2. ^{1}H NMR spectrum of B.

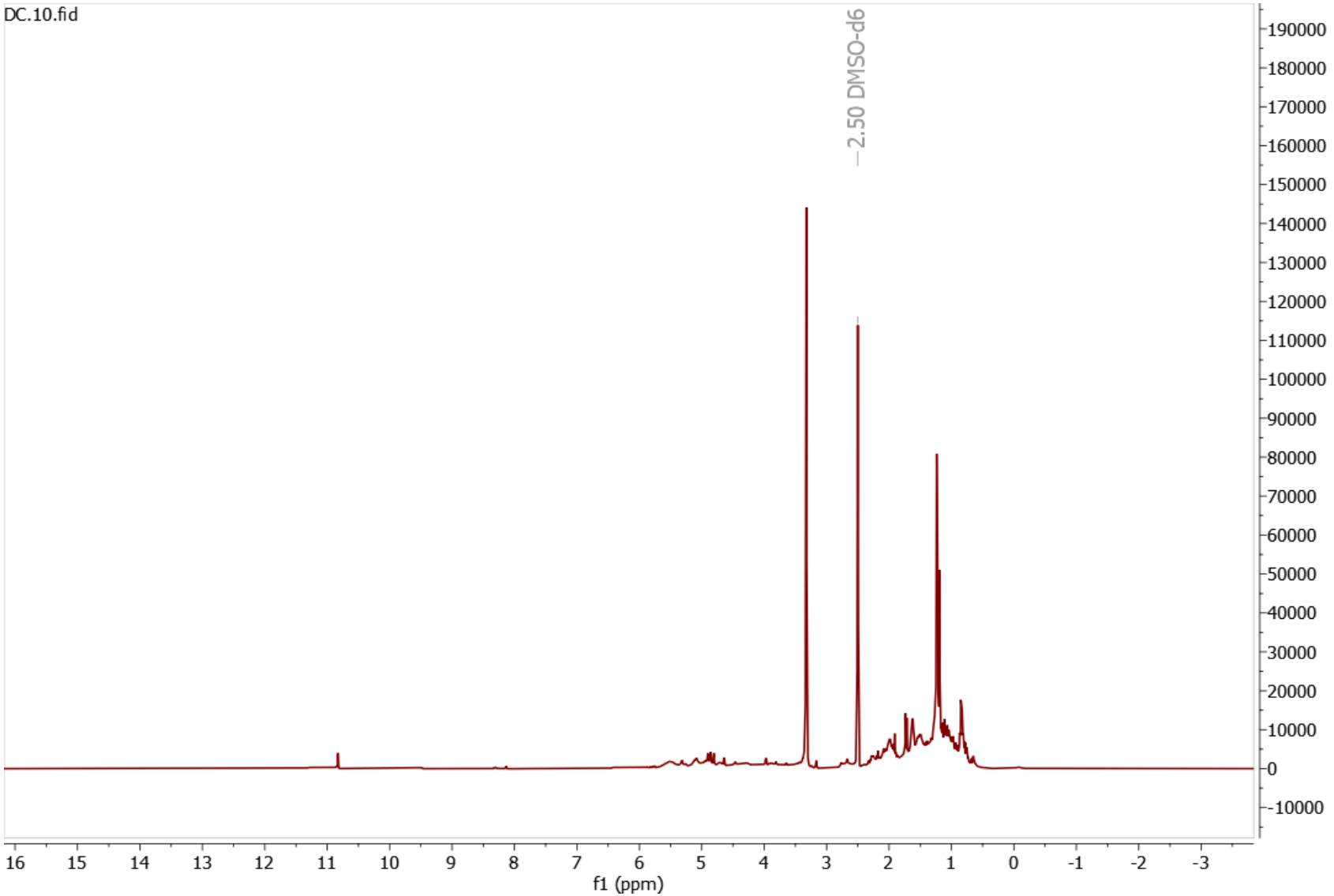

Figure 6.3. ^{1}H NMR spectrum of C.

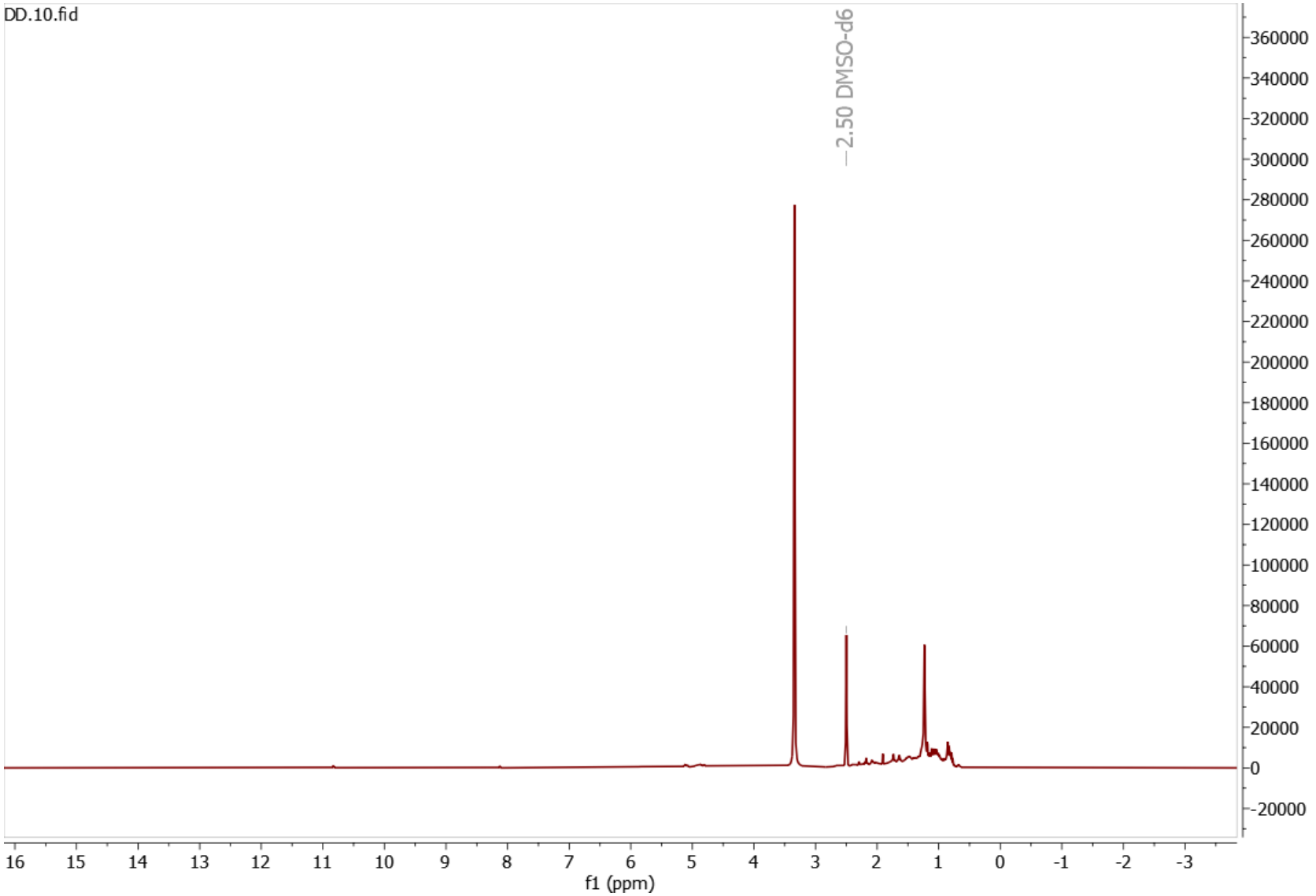

Figure 6.4. ^{1}H NMR spectrum of D.

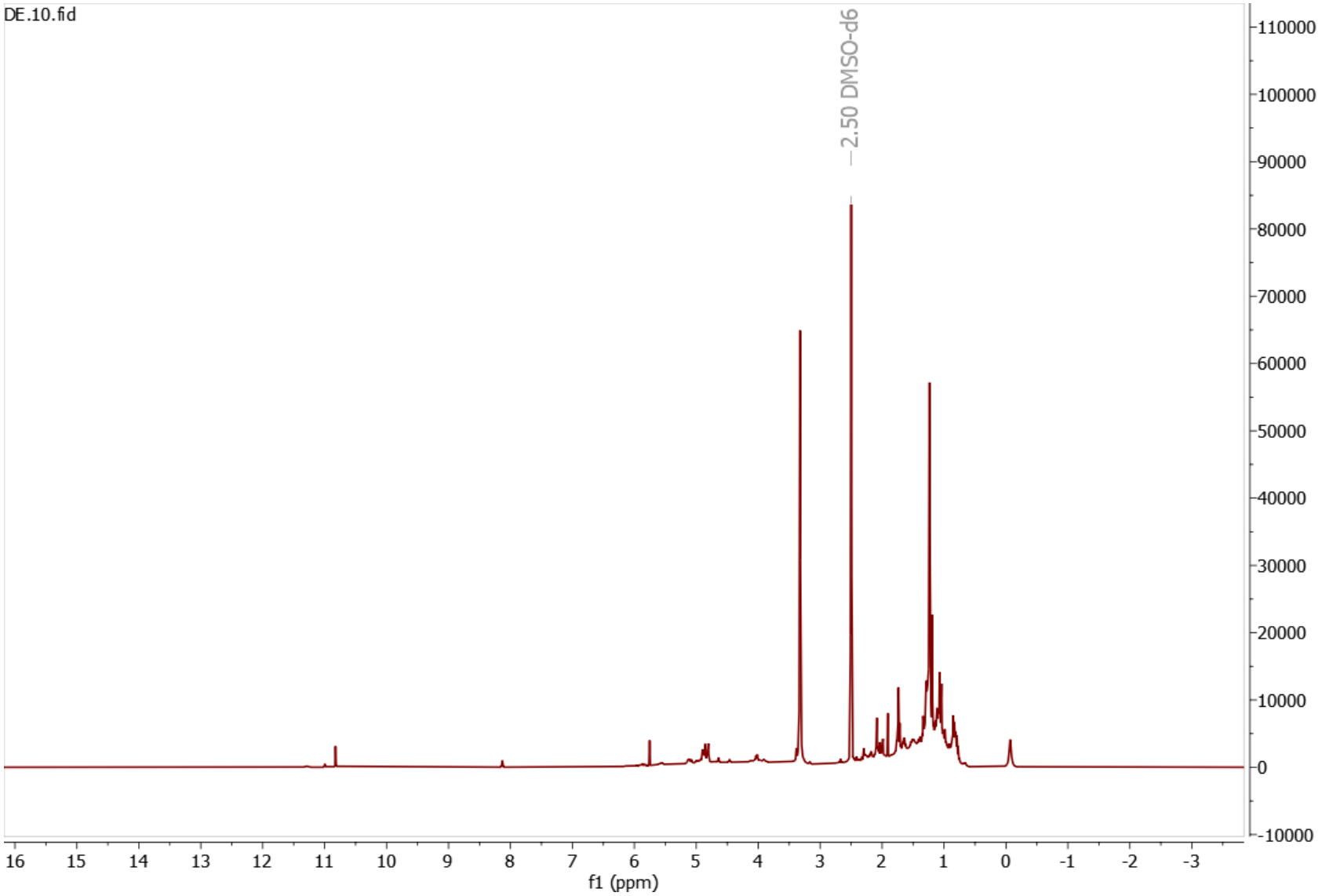

Figure 6.5. ^{1}H NMR spectrum of E.

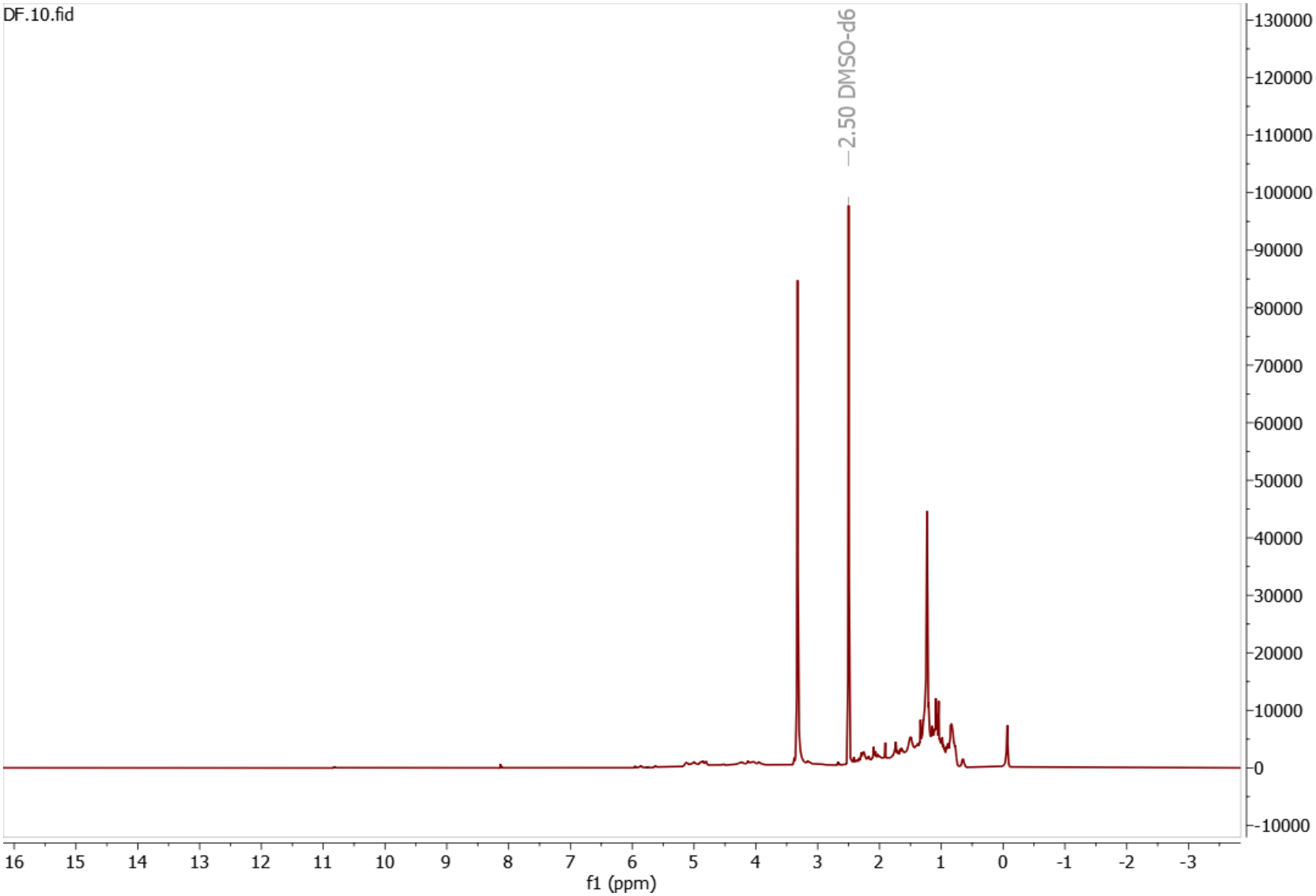

Figure 6.6. ^{1}H NMR spectrum of F.

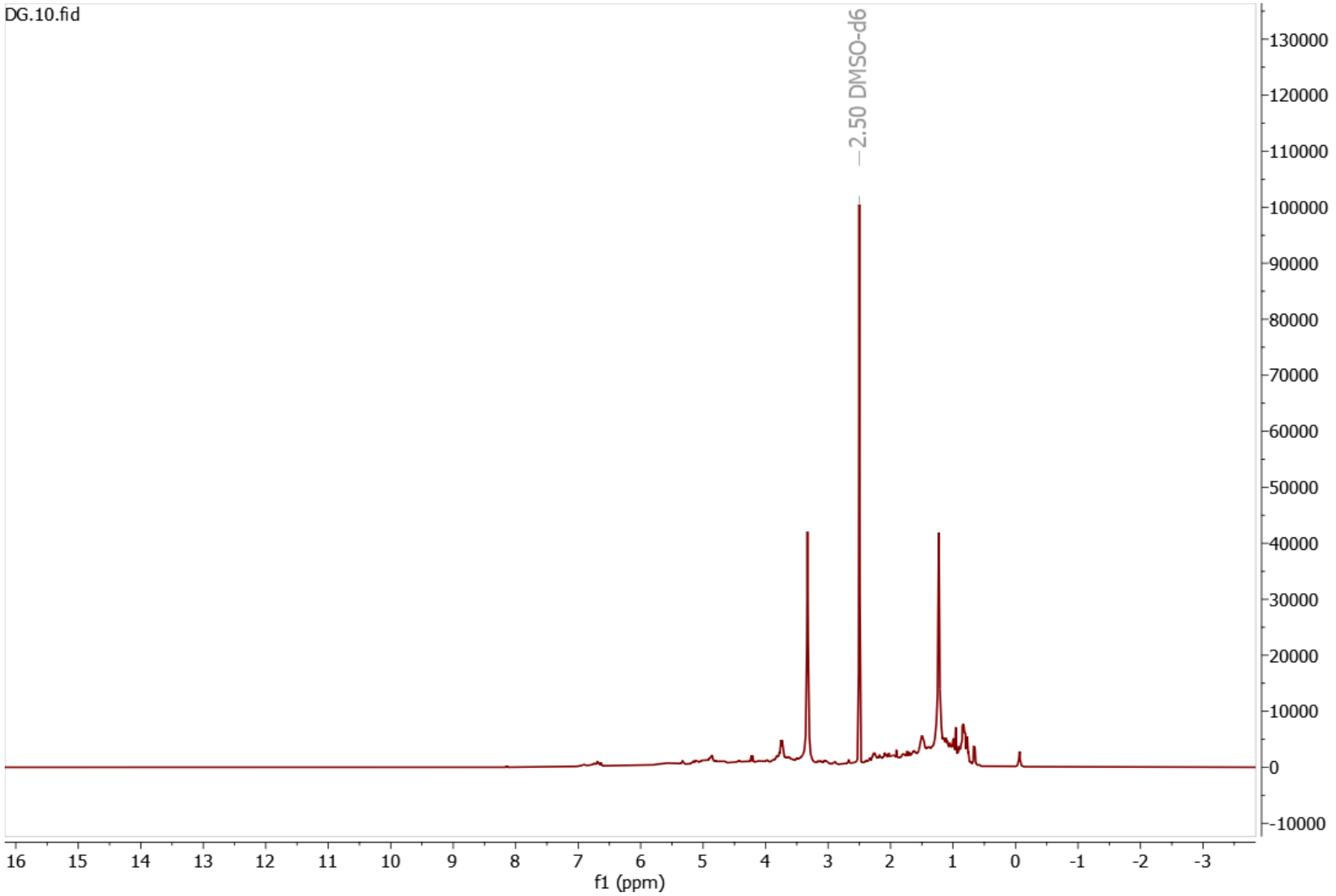

Figure 6.7. ^{1}H NMR spectrum of G.

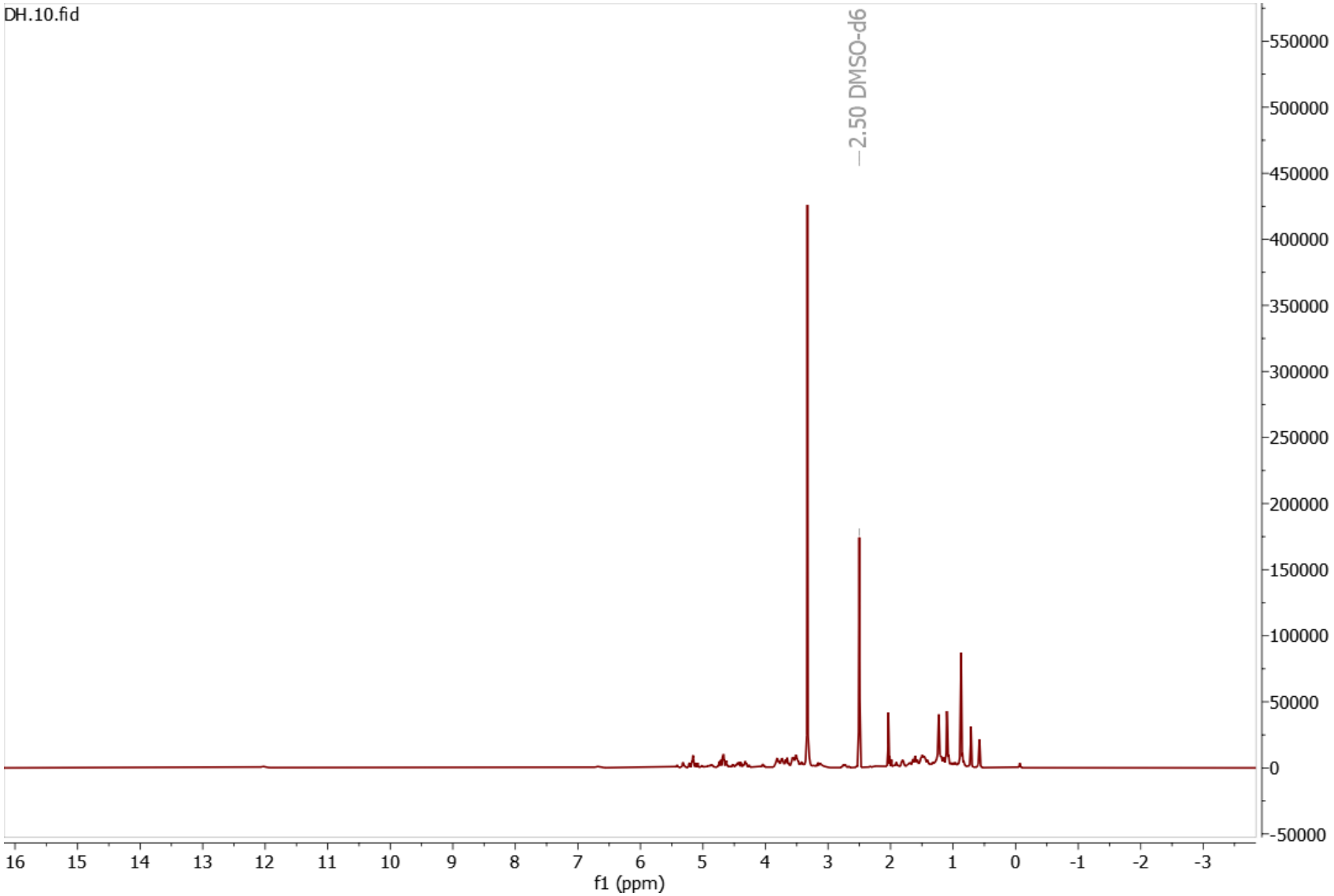

Figure 6.8. ^{1}H NMR spectrum of H.

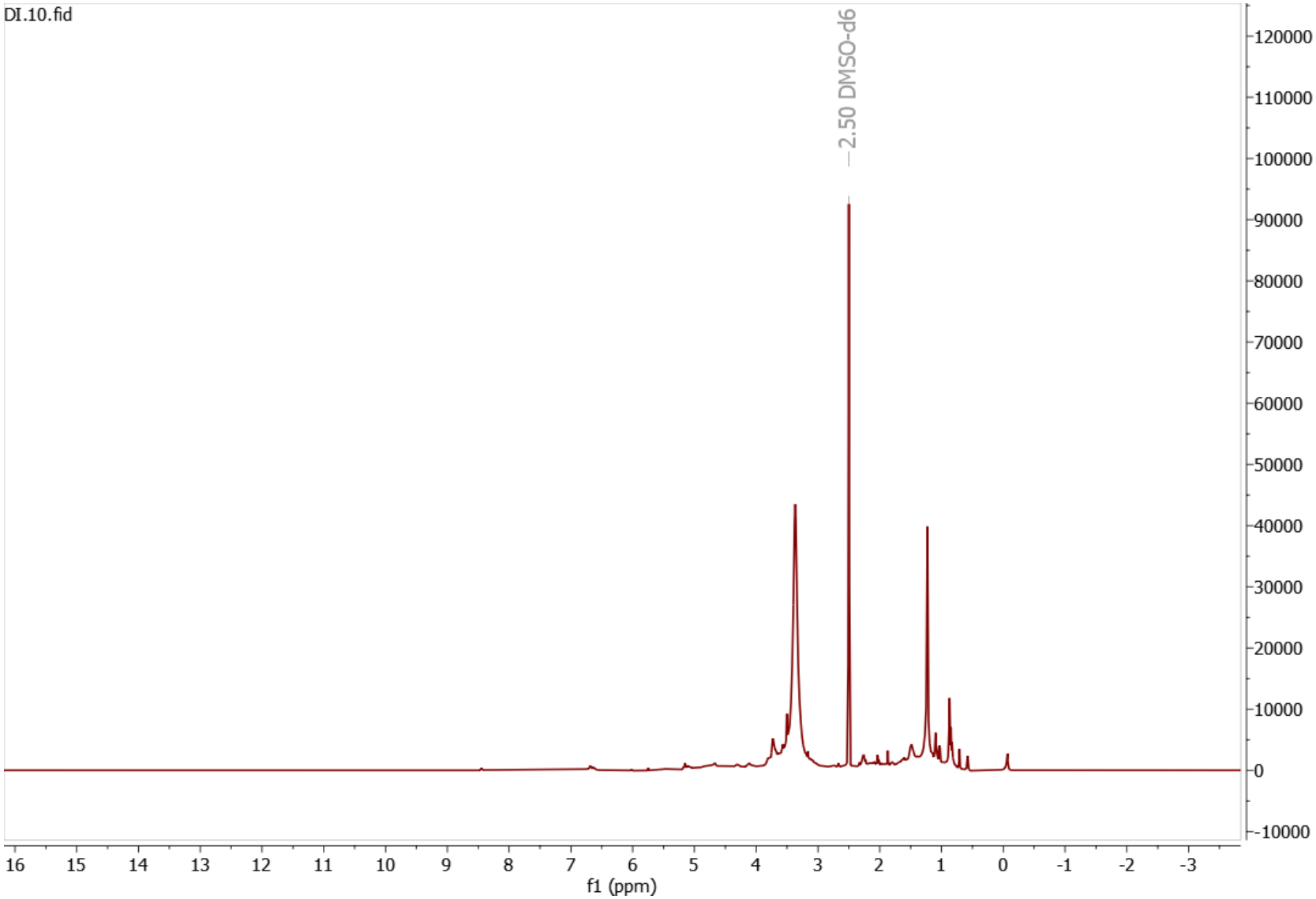

Figure 6.9. ^{1}H NMR spectrum of I.

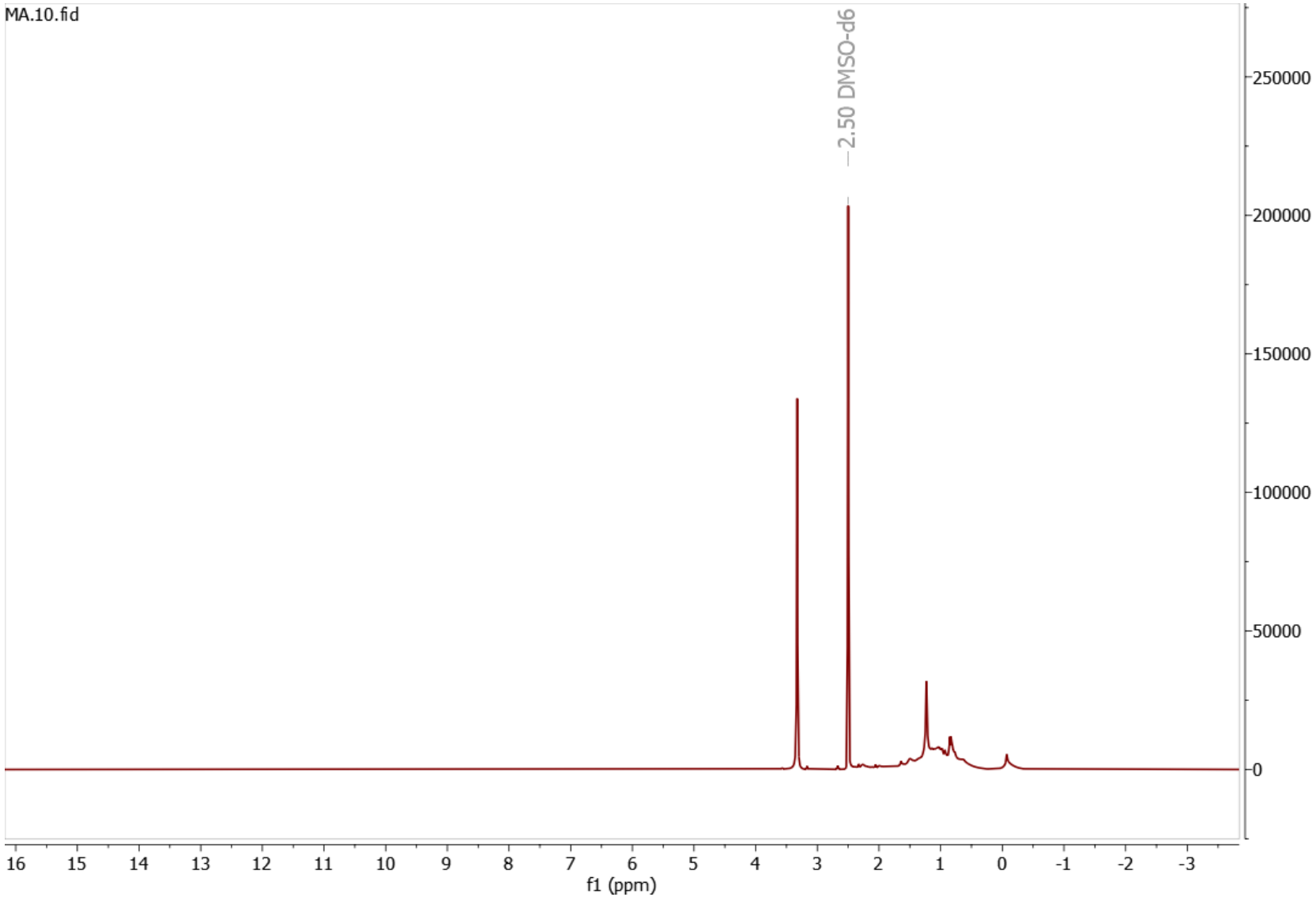

Figure 6.10. ^{1}H NMR spectrum of J.

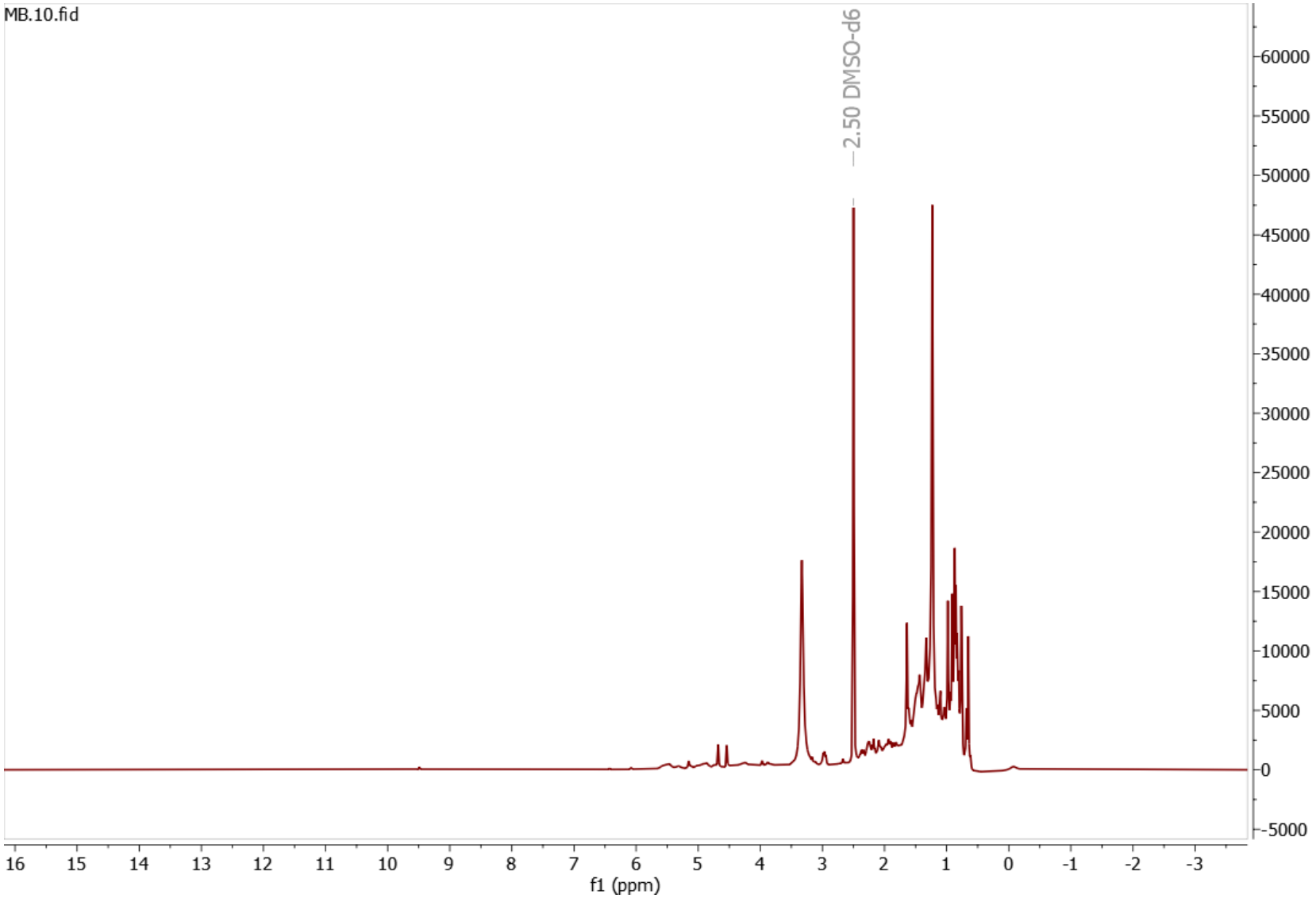

Figure 6.11. ^{1}H NMR spectrum of K.

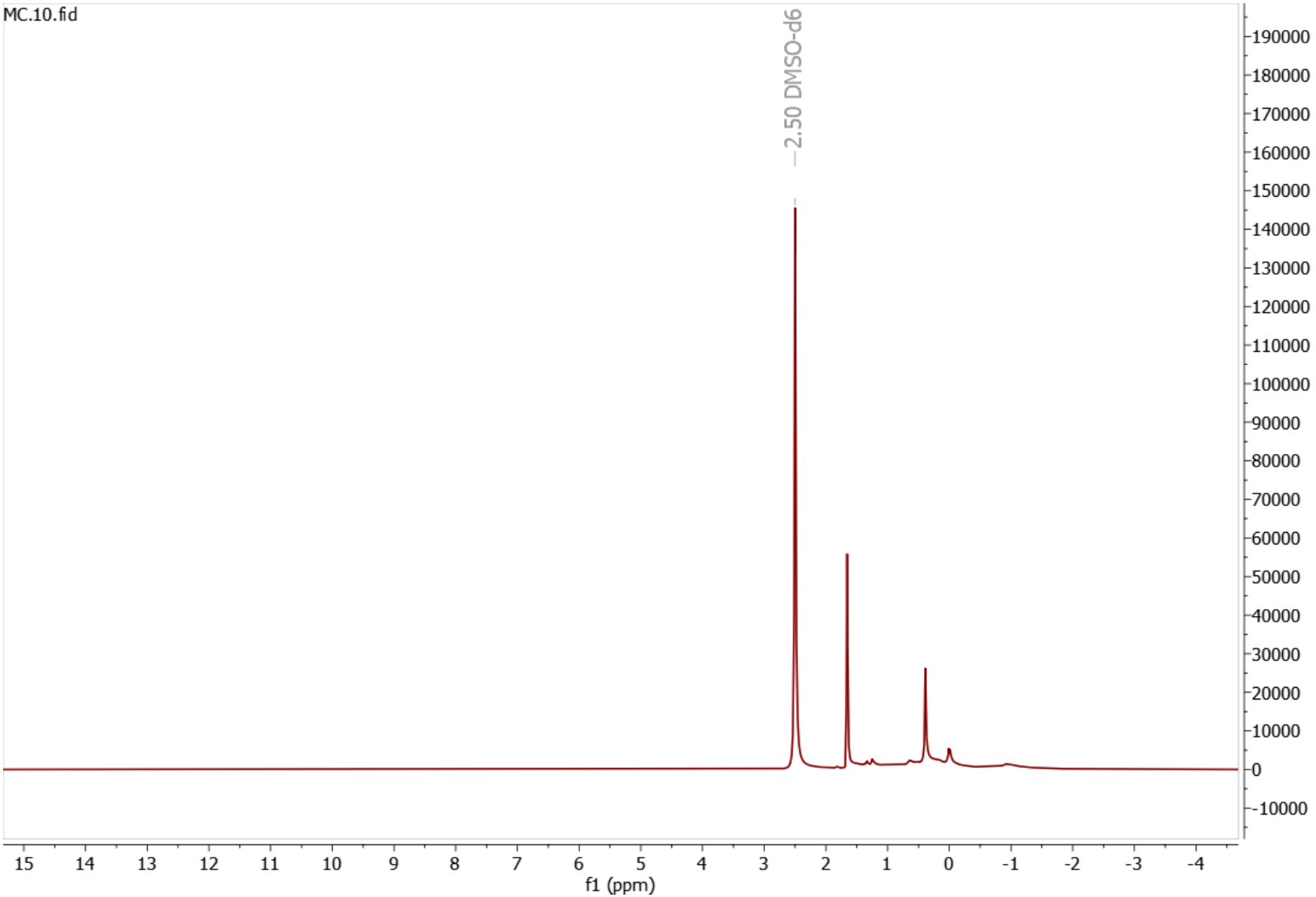

Figure 6.12. ^{1}H NMR spectrum of L.

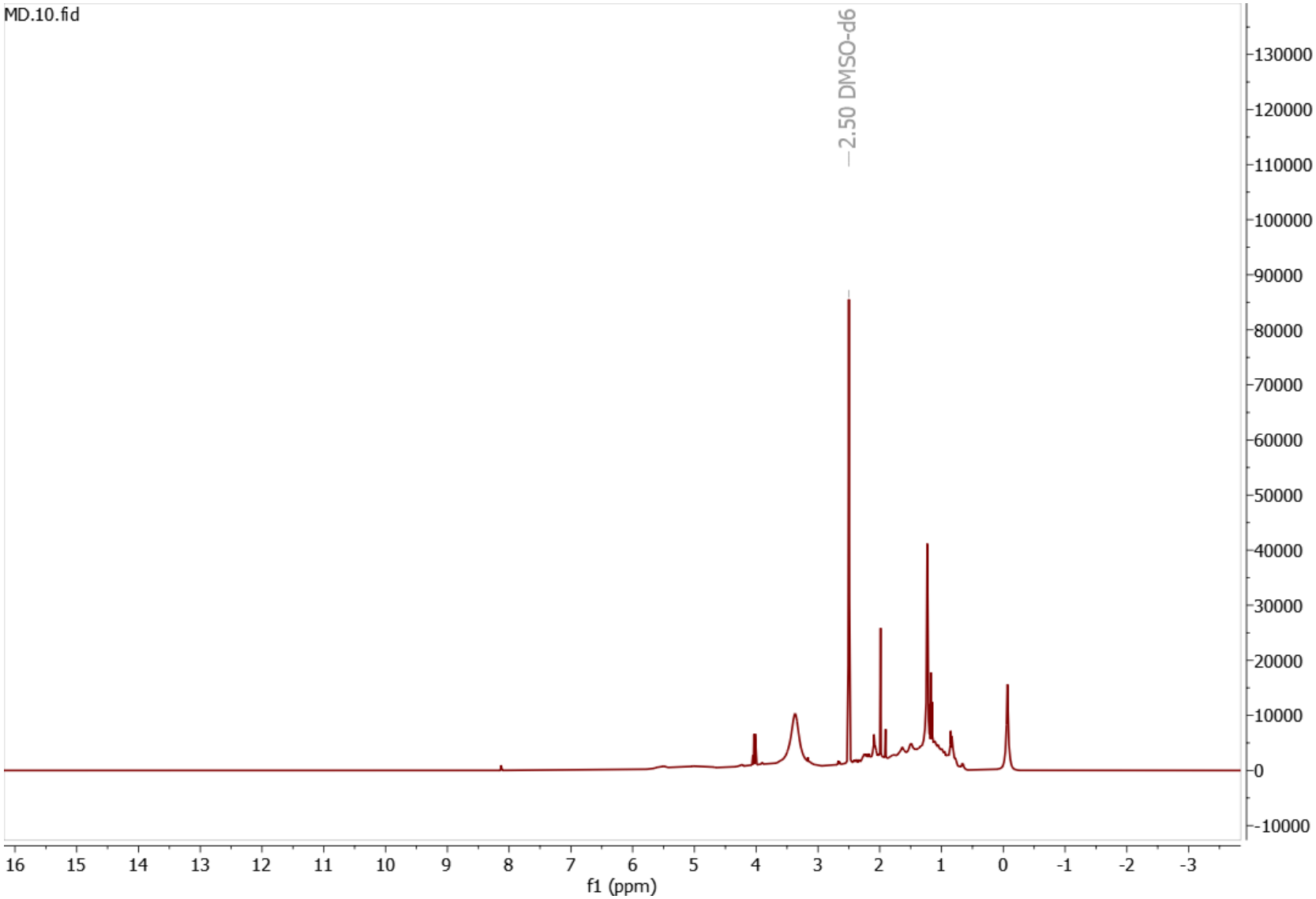

Figure 6.13. ^{1}H NMR spectrum of M.

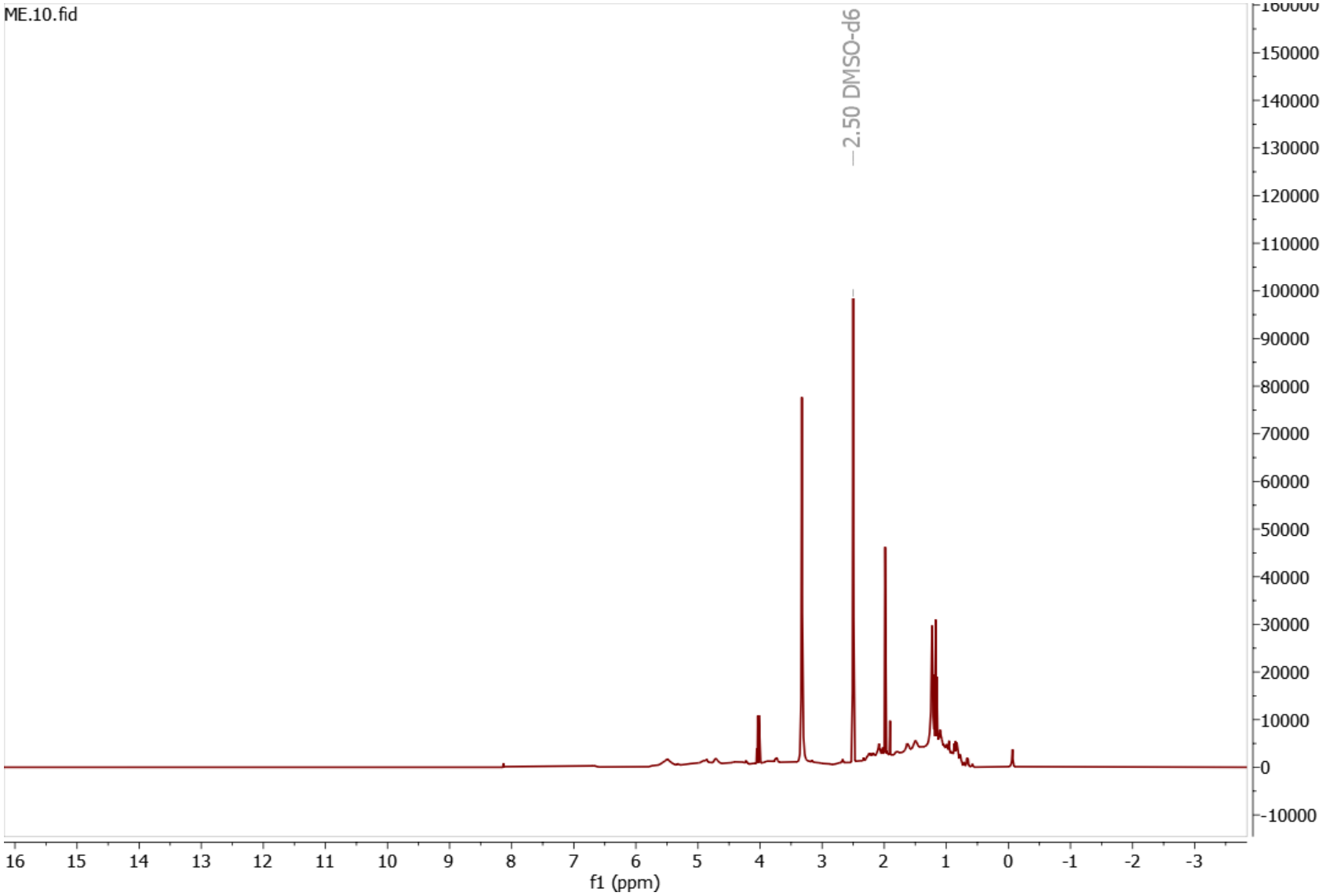

Figure 6.14. ^{1}H NMR spectrum of N.

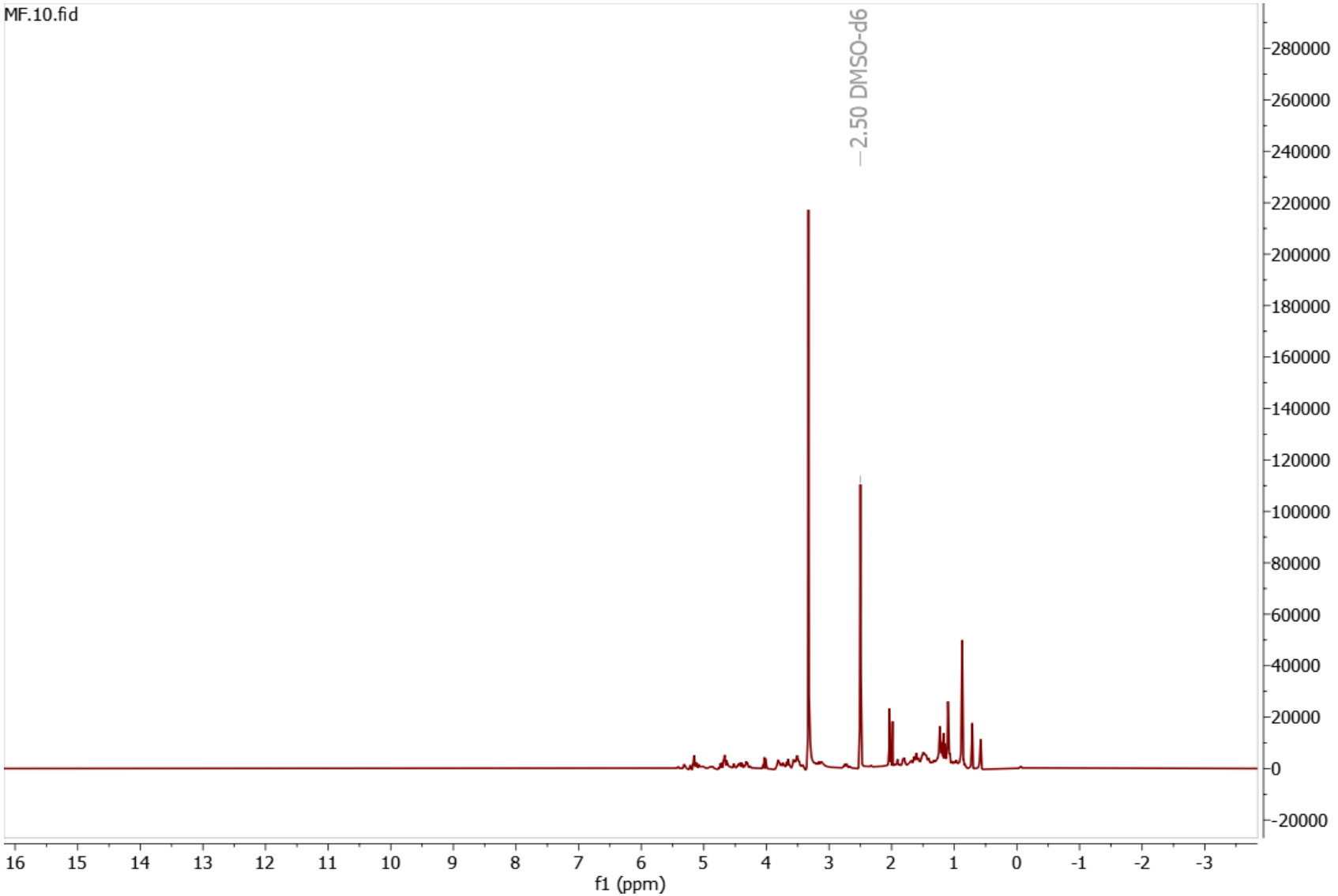

Figure 6.15. ^{1}H NMR spectrum of O.

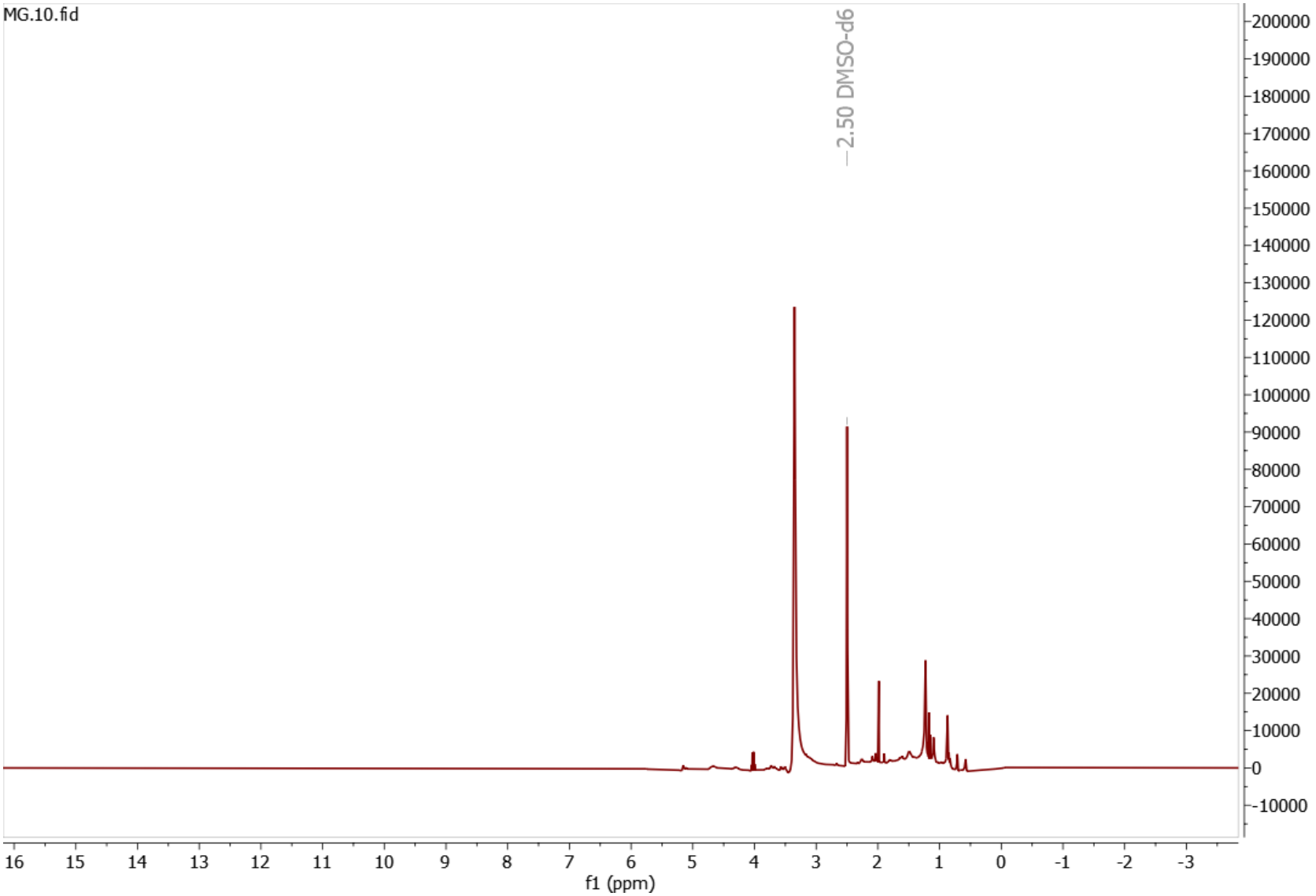

Figure 6.16. ^{1}H NMR spectrum of P.

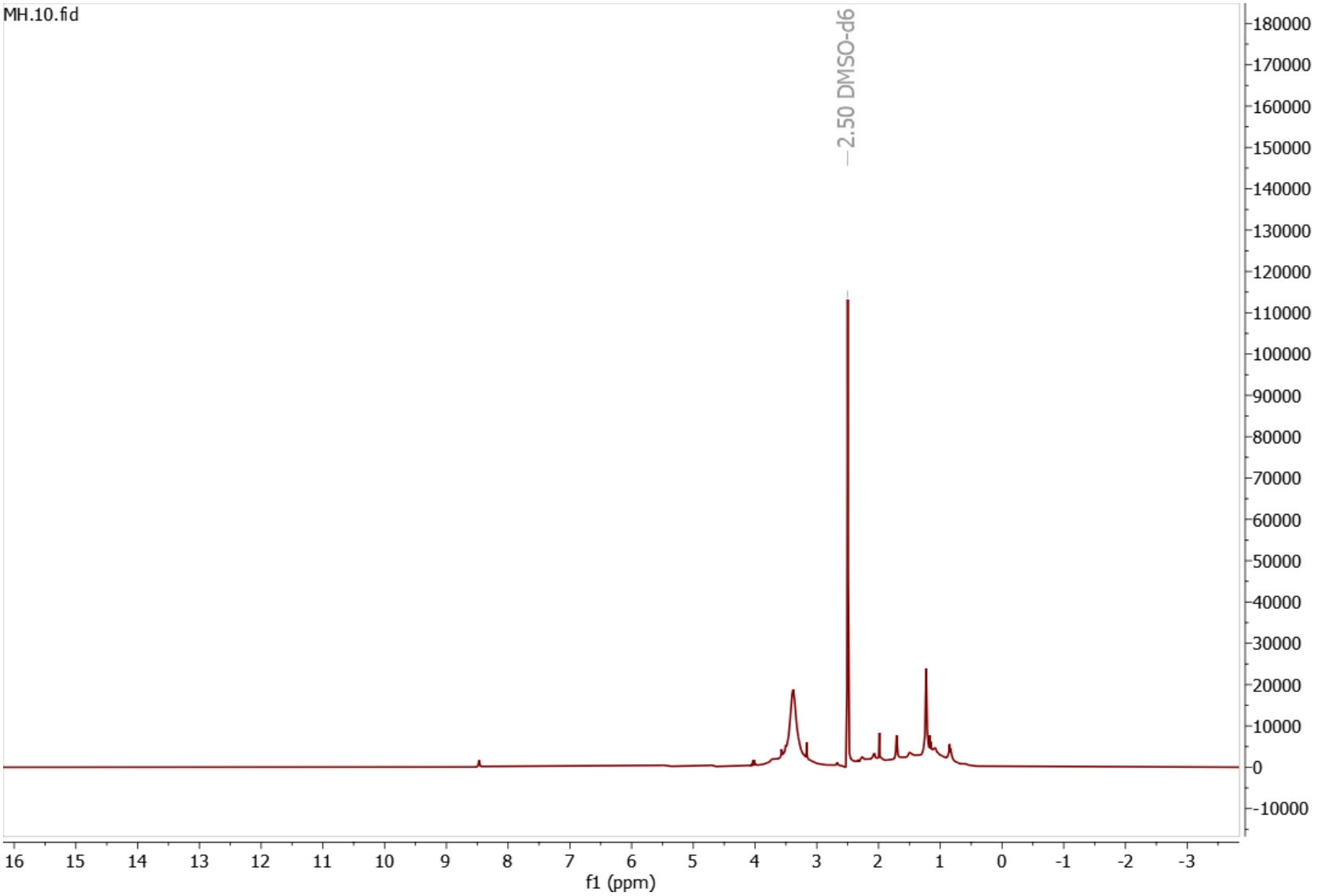

Figure 0.1. ^{1}H NMR spectrum of Q.

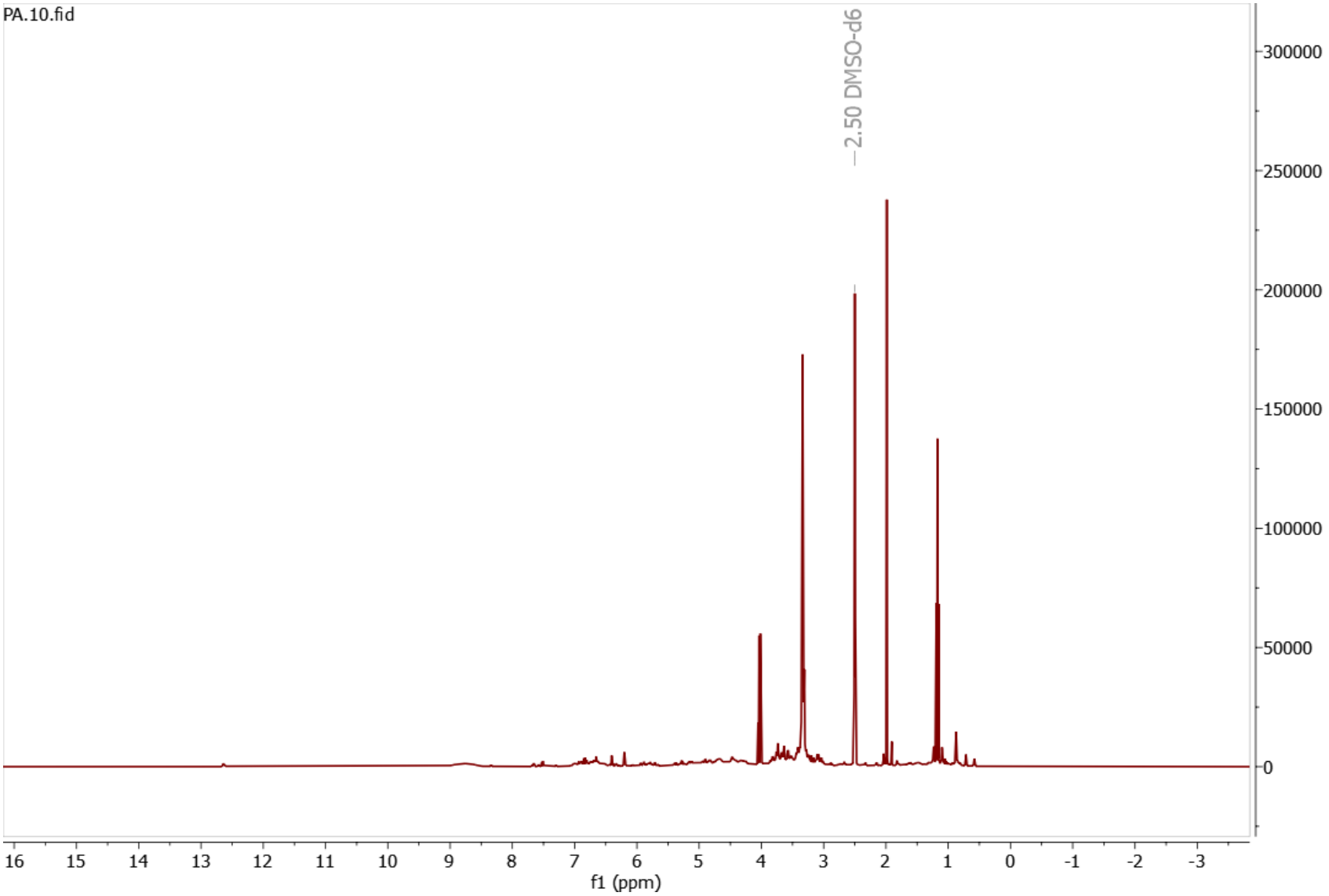

Figure 6.18. ^{1}H NMR spectrum of R.

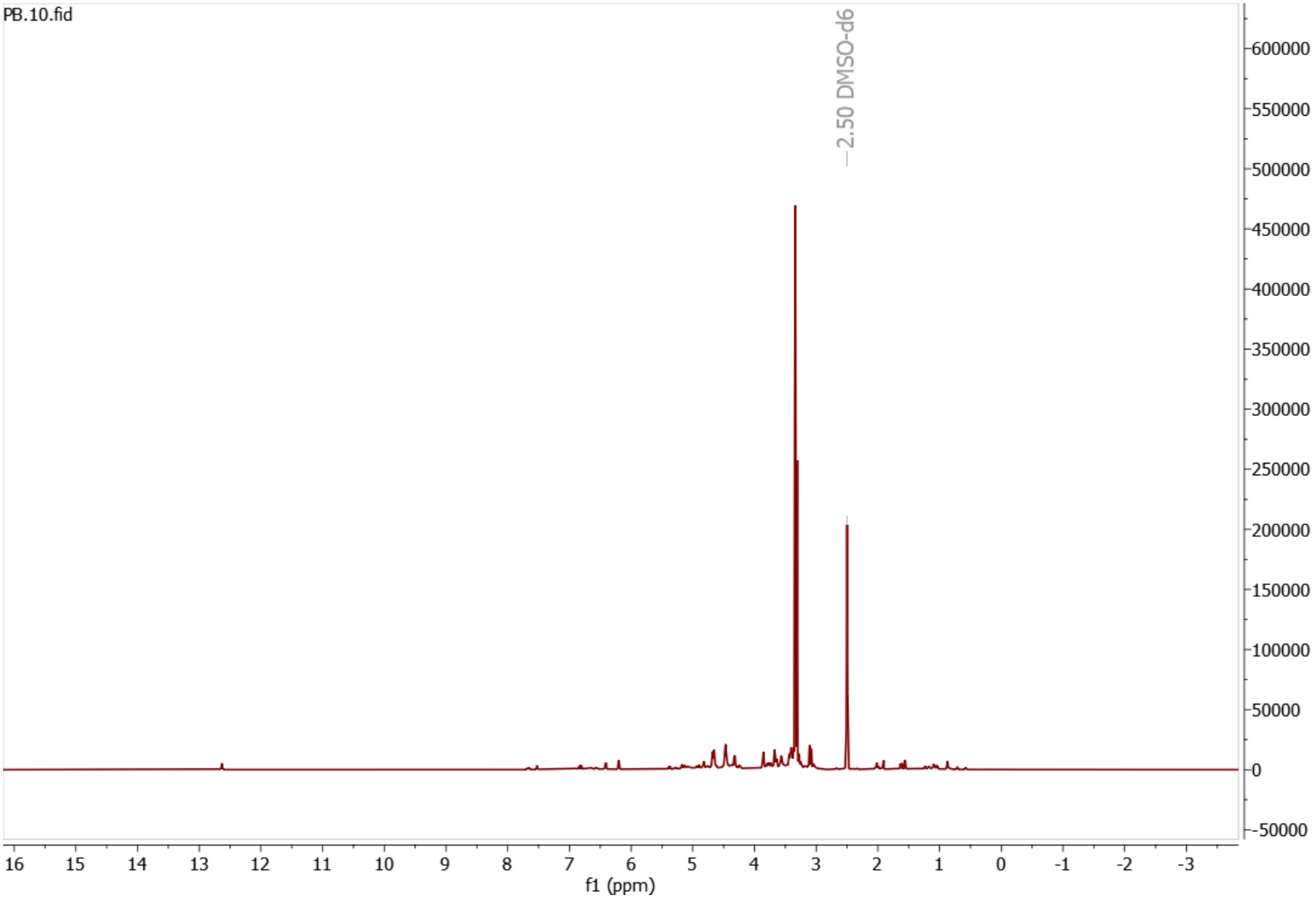

Figure 6.19. ^{1}H NMR spectrum of S.

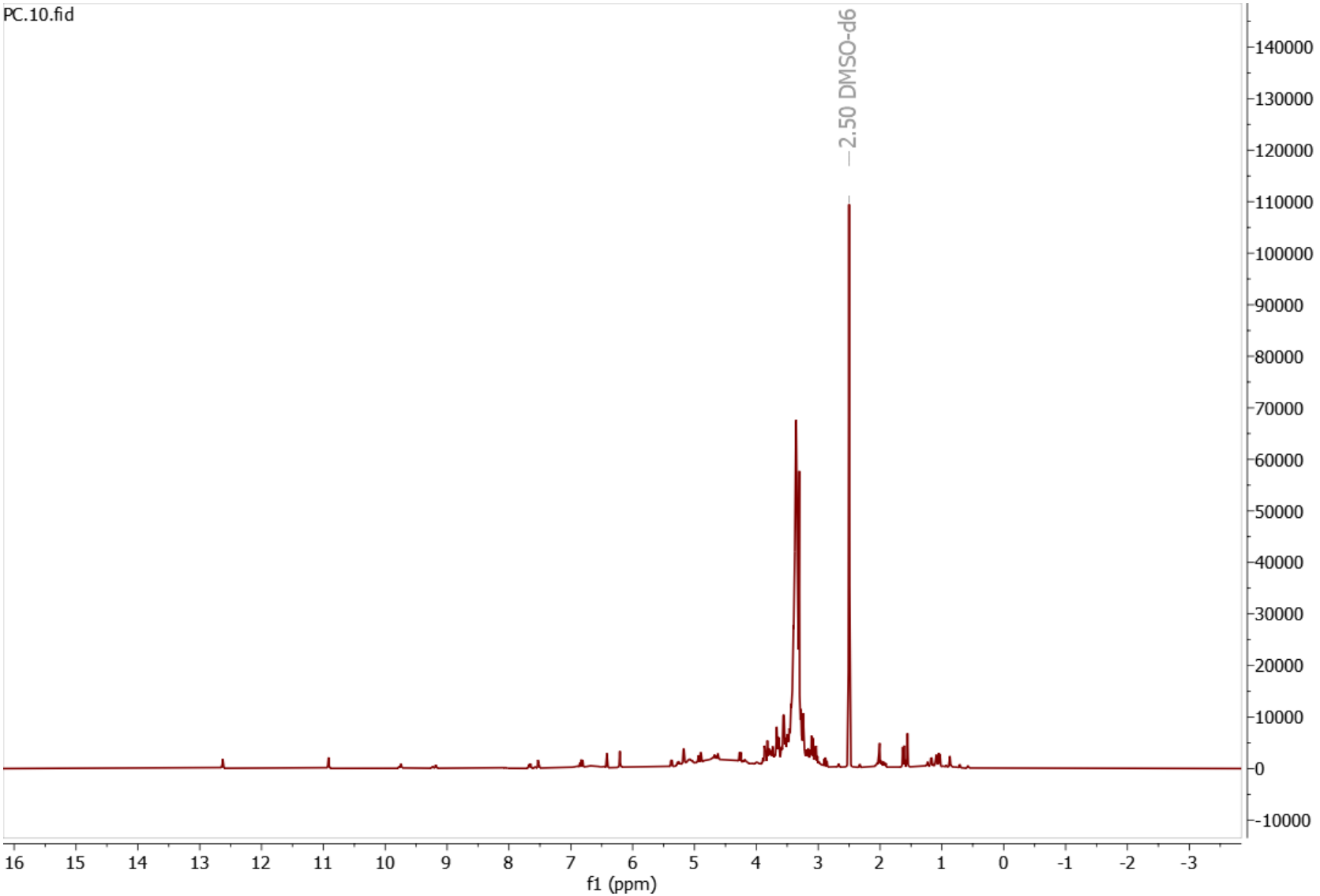

Figure 6.20. ^{1}H NMR spectrum of T.

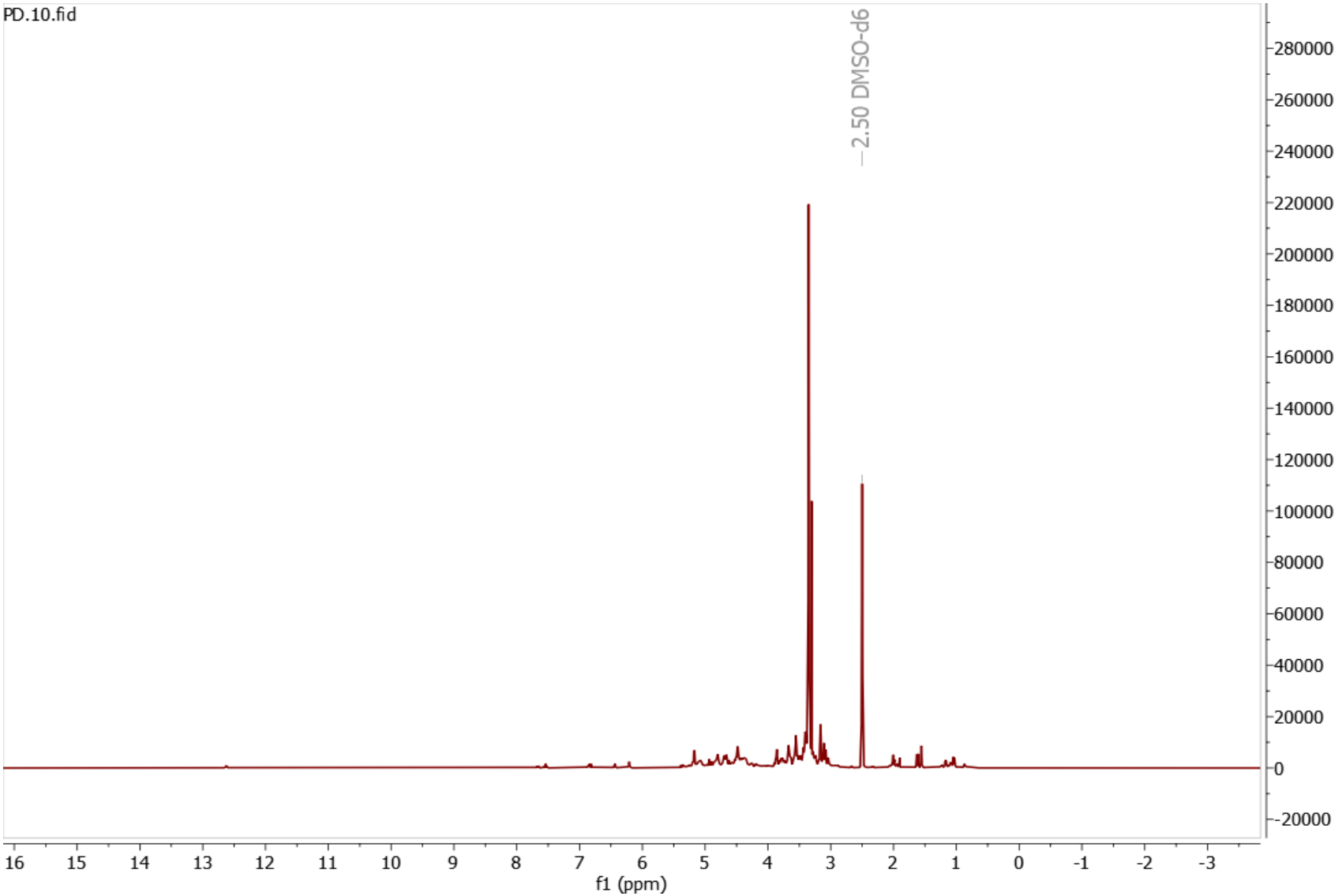

Figure 6.21. ^{1}H NMR spectrum of U.

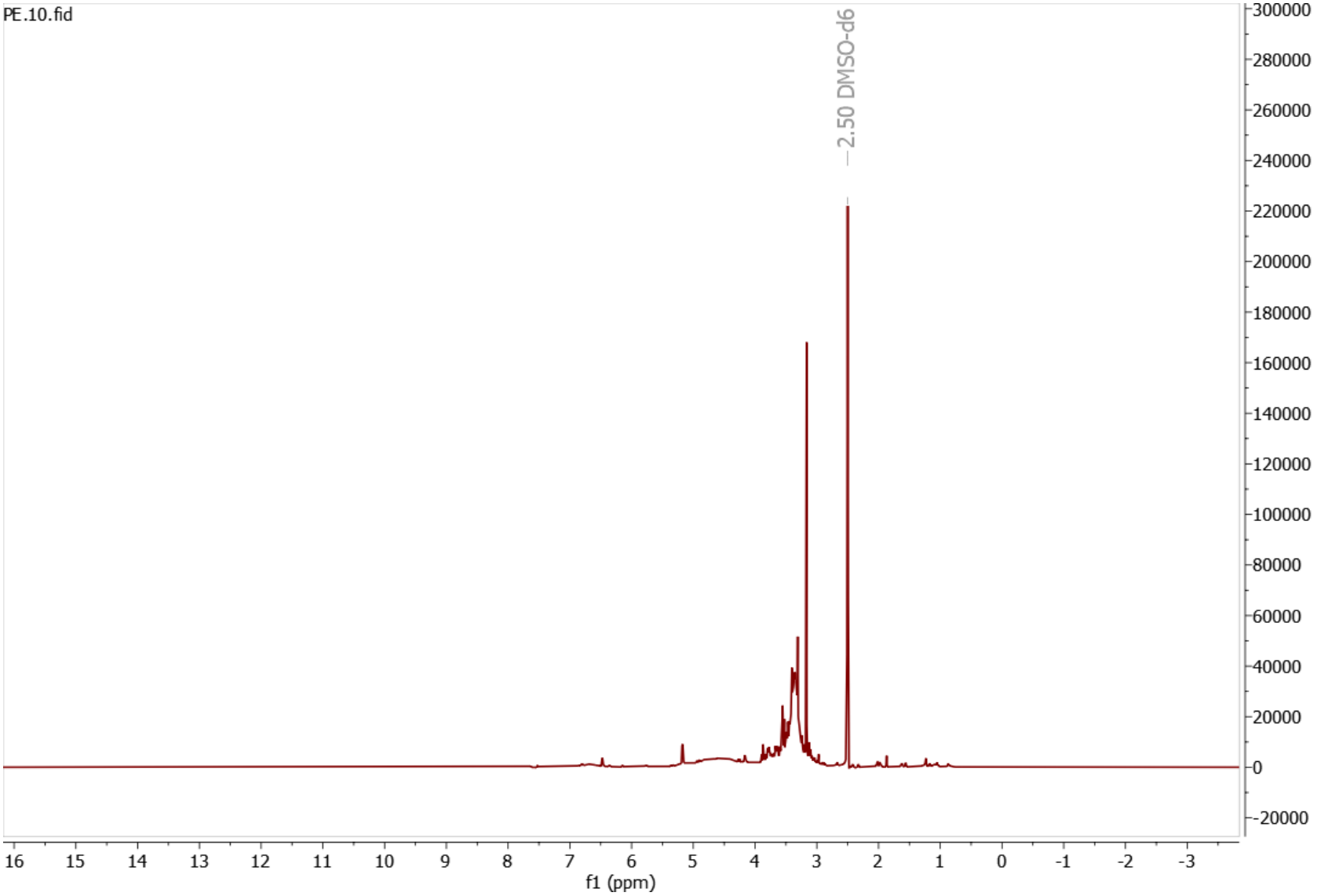

Figure 6.22. ^{1}H NMR spectrum of V.

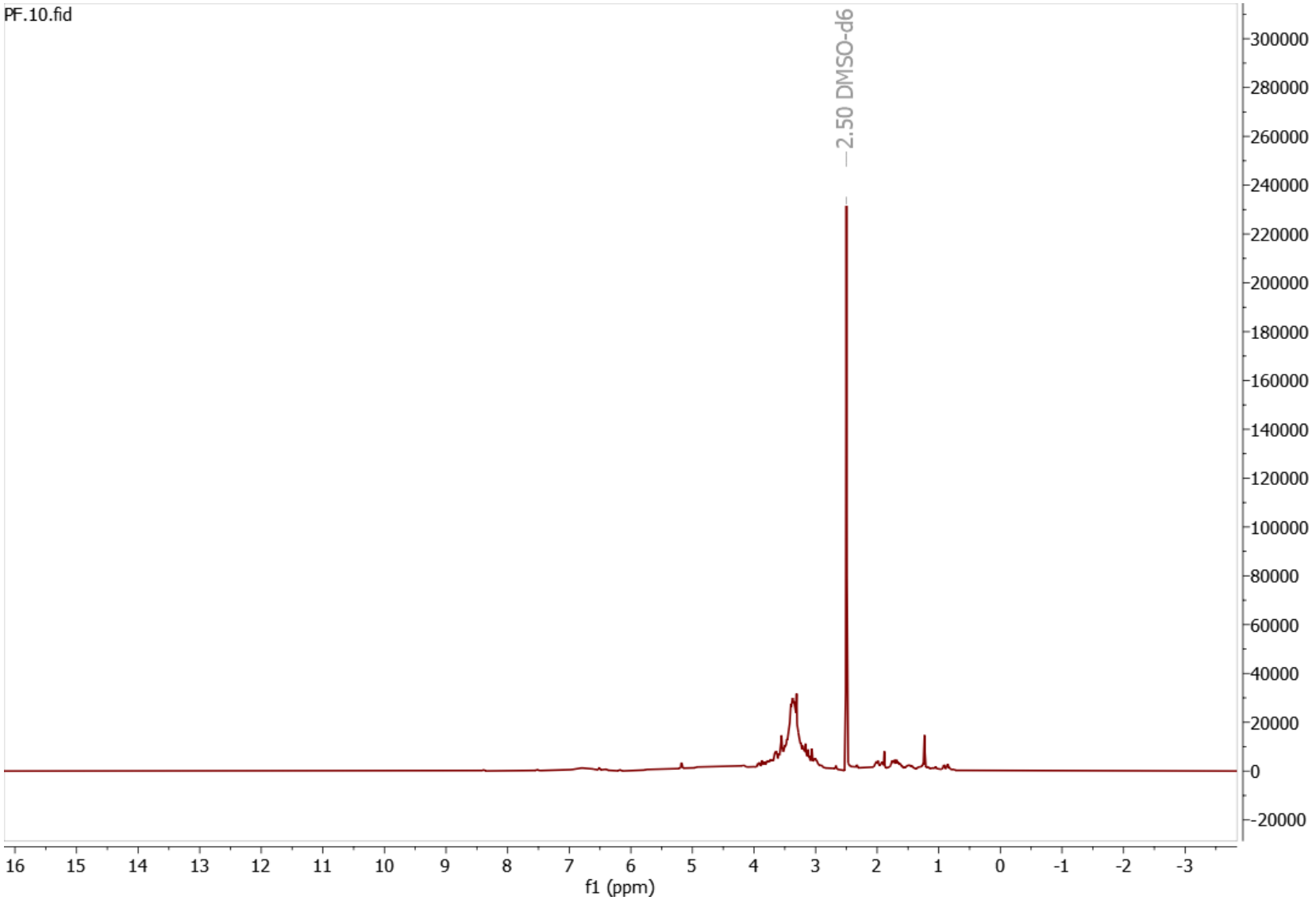

Figure 6.23. ^{1}H NMR spectrum of W.

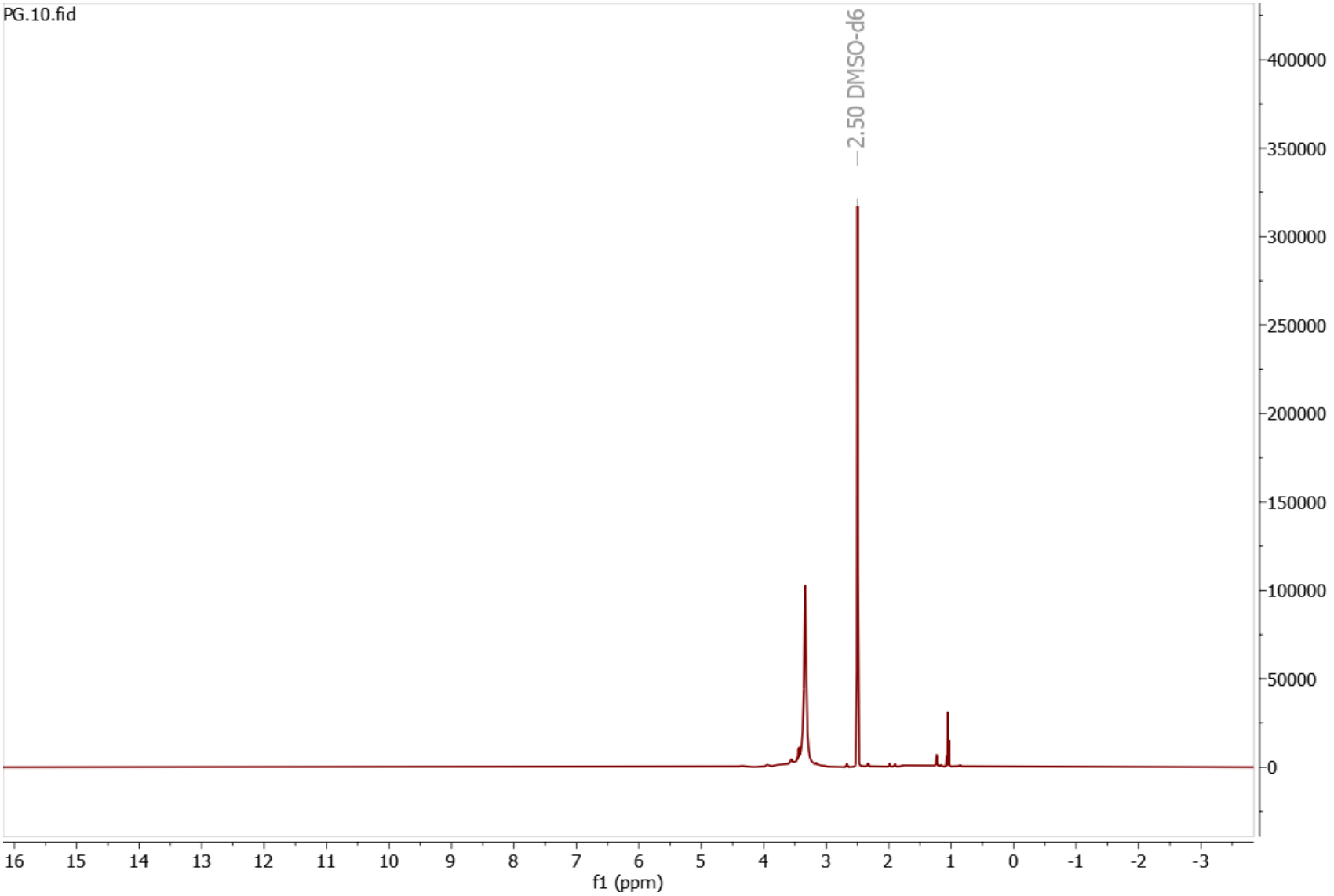

Figure 6.24. ^{1}H NMR spectrum of X.

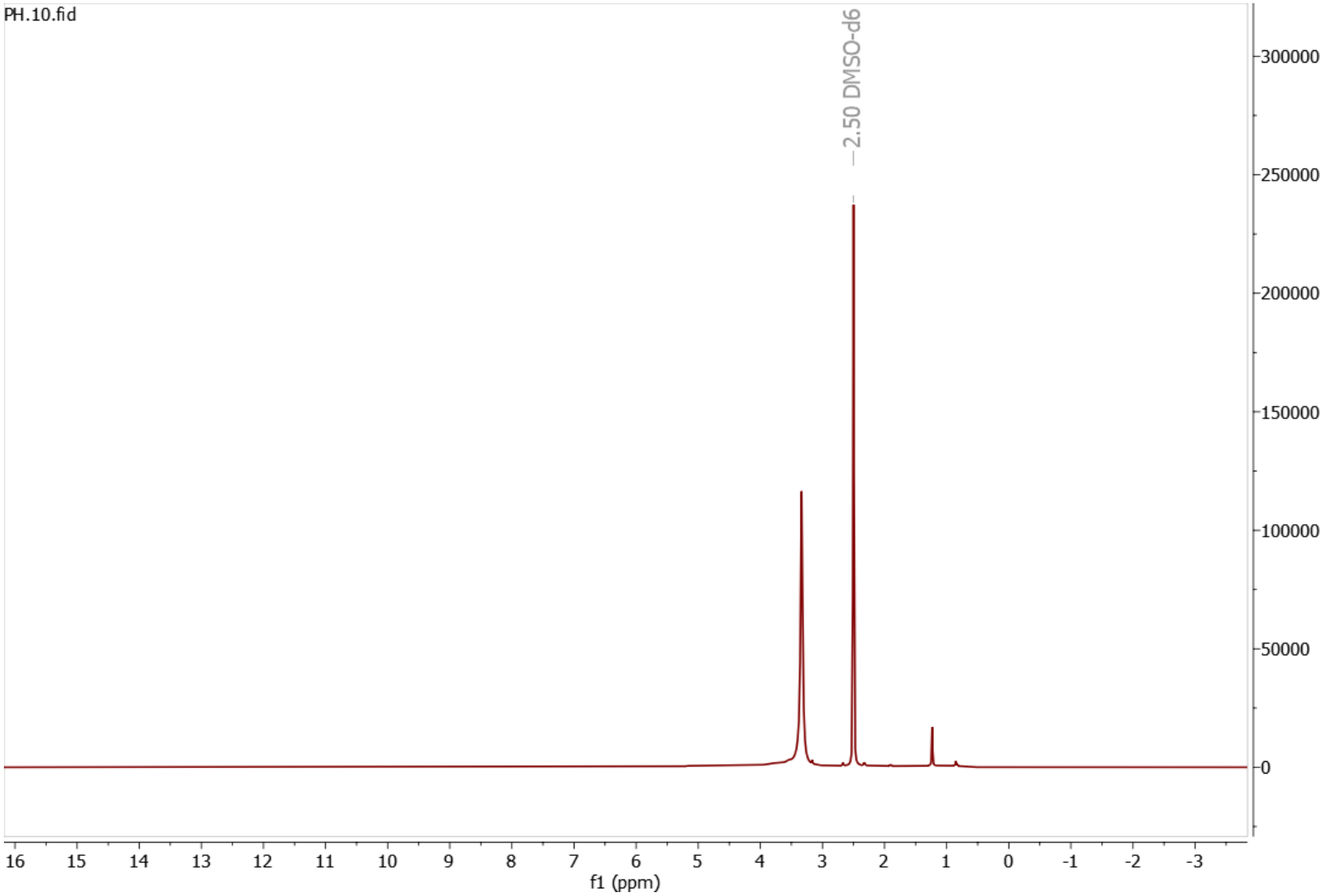

Figure 6.25. ^{1}H NMR spectrum of Y.

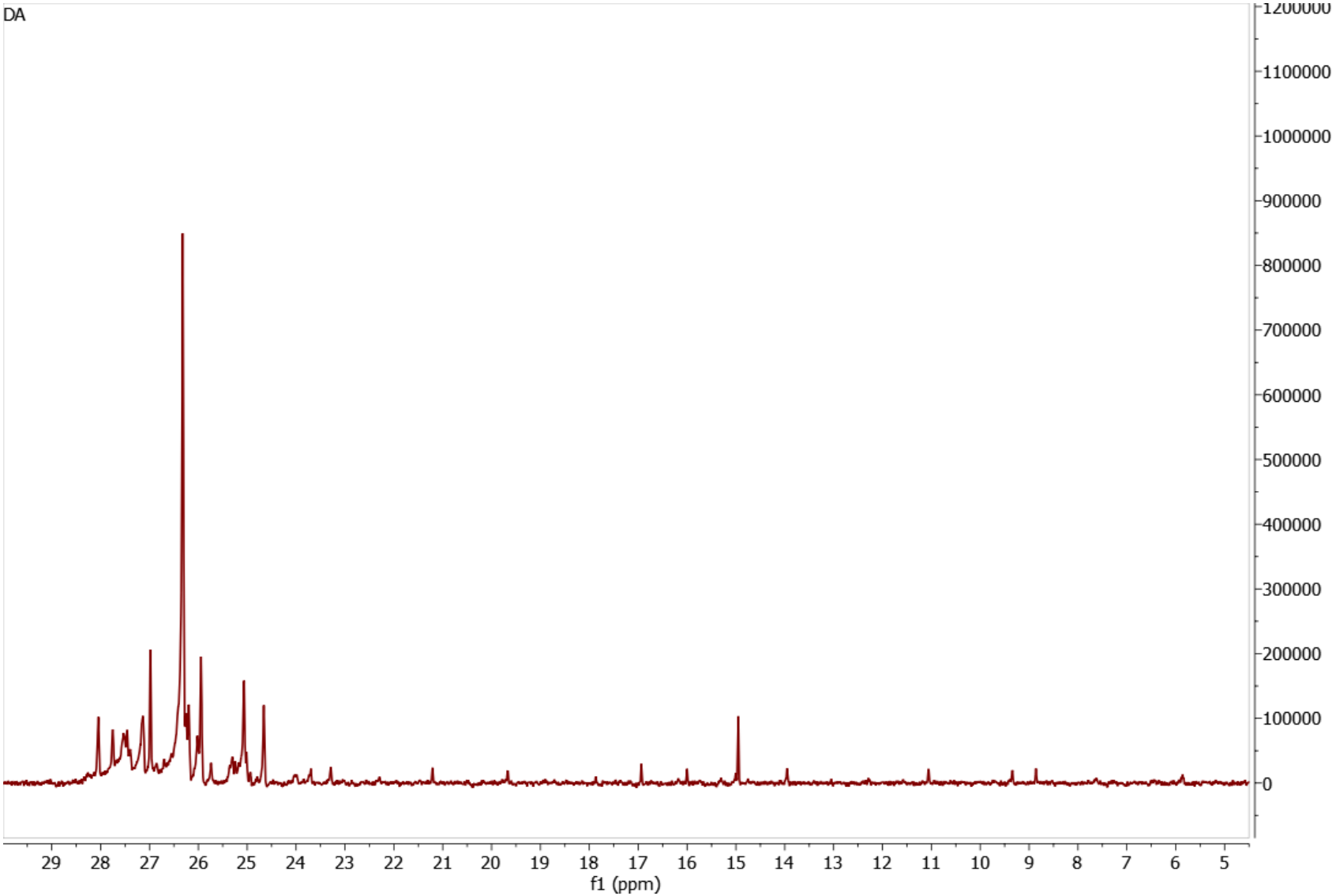

Figure 0.2. GC-MS spectrum of A.

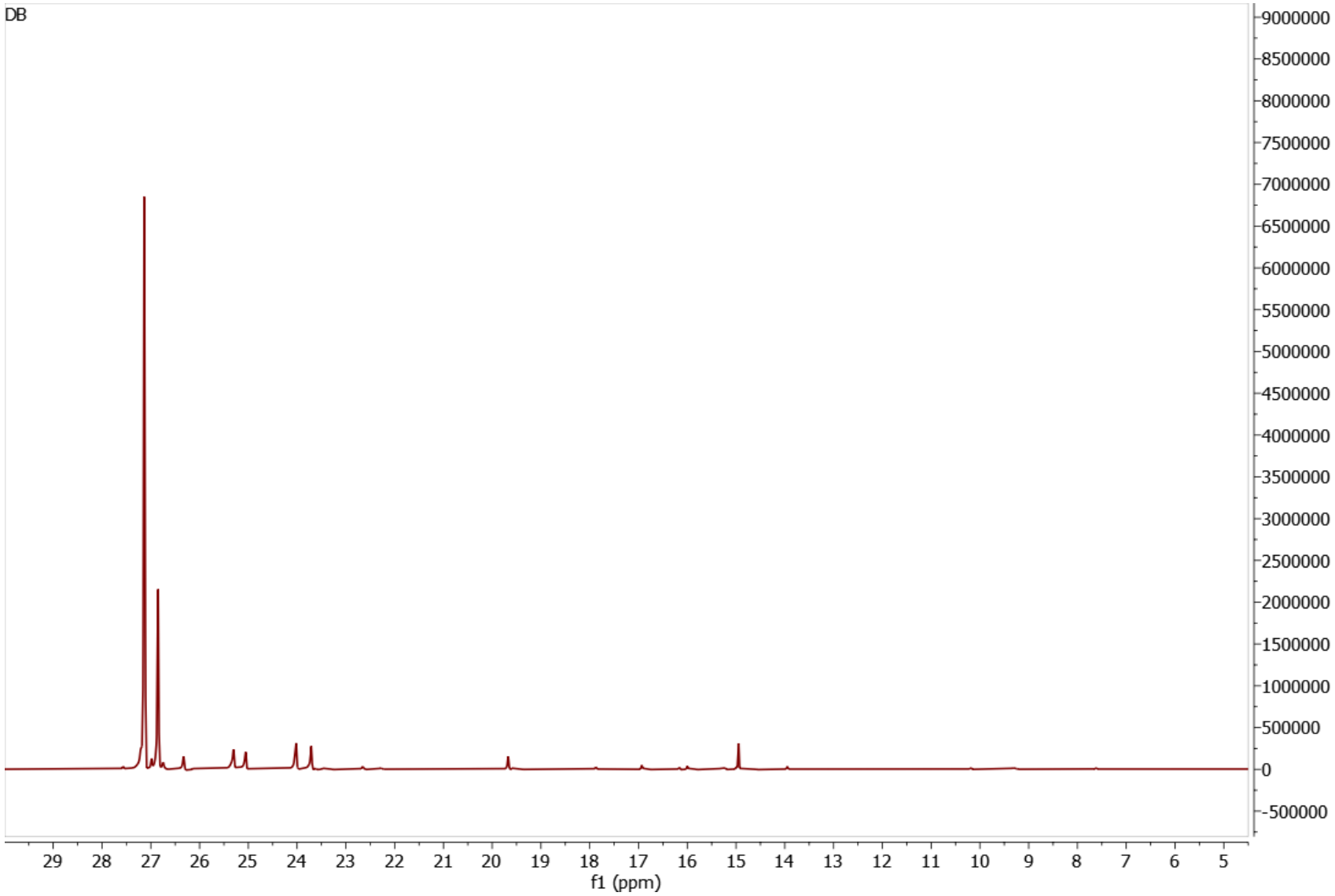

Figure 6.27. GC-MS spectrum of B.

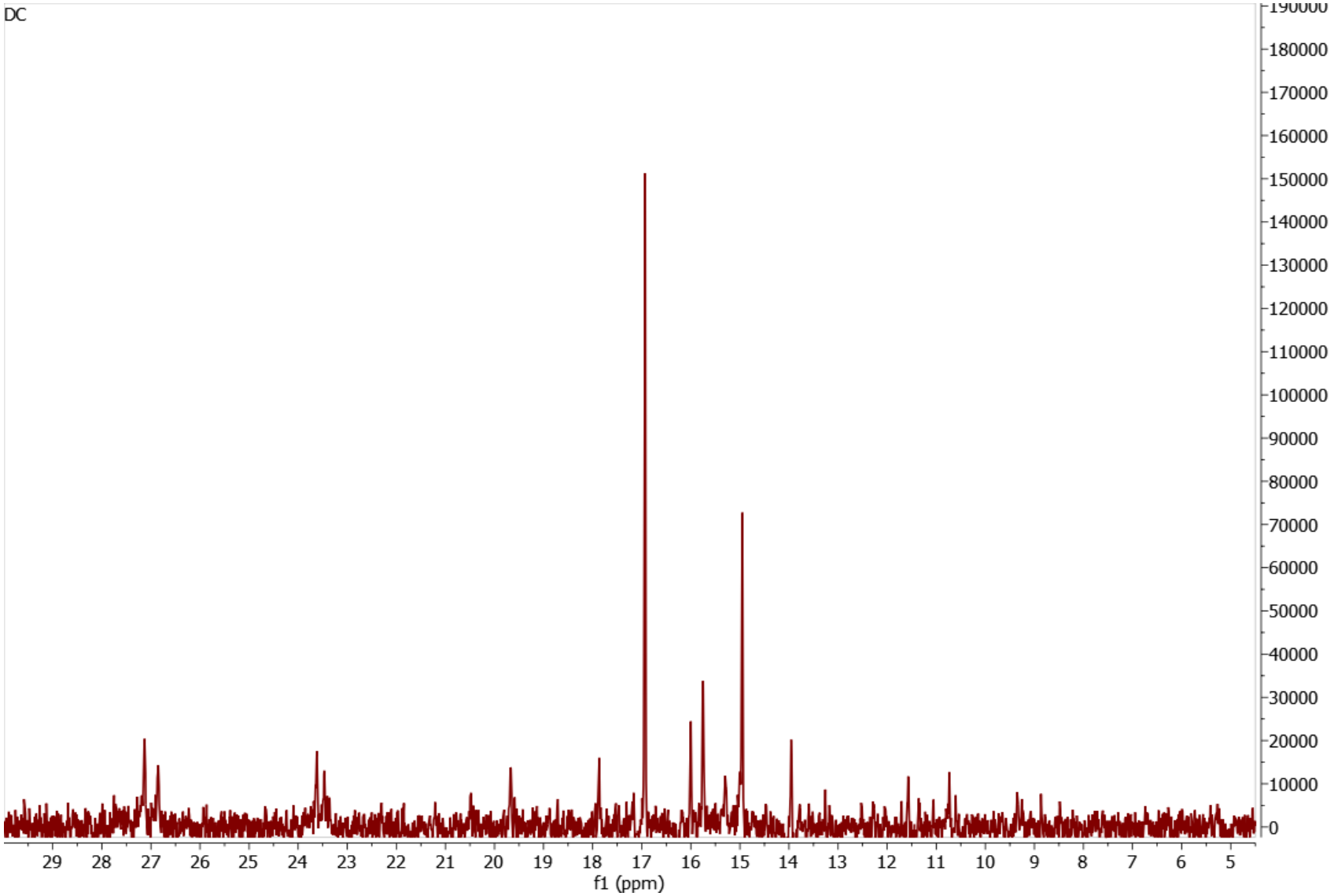

Figure 6.28. GC-MS spectrum of C.

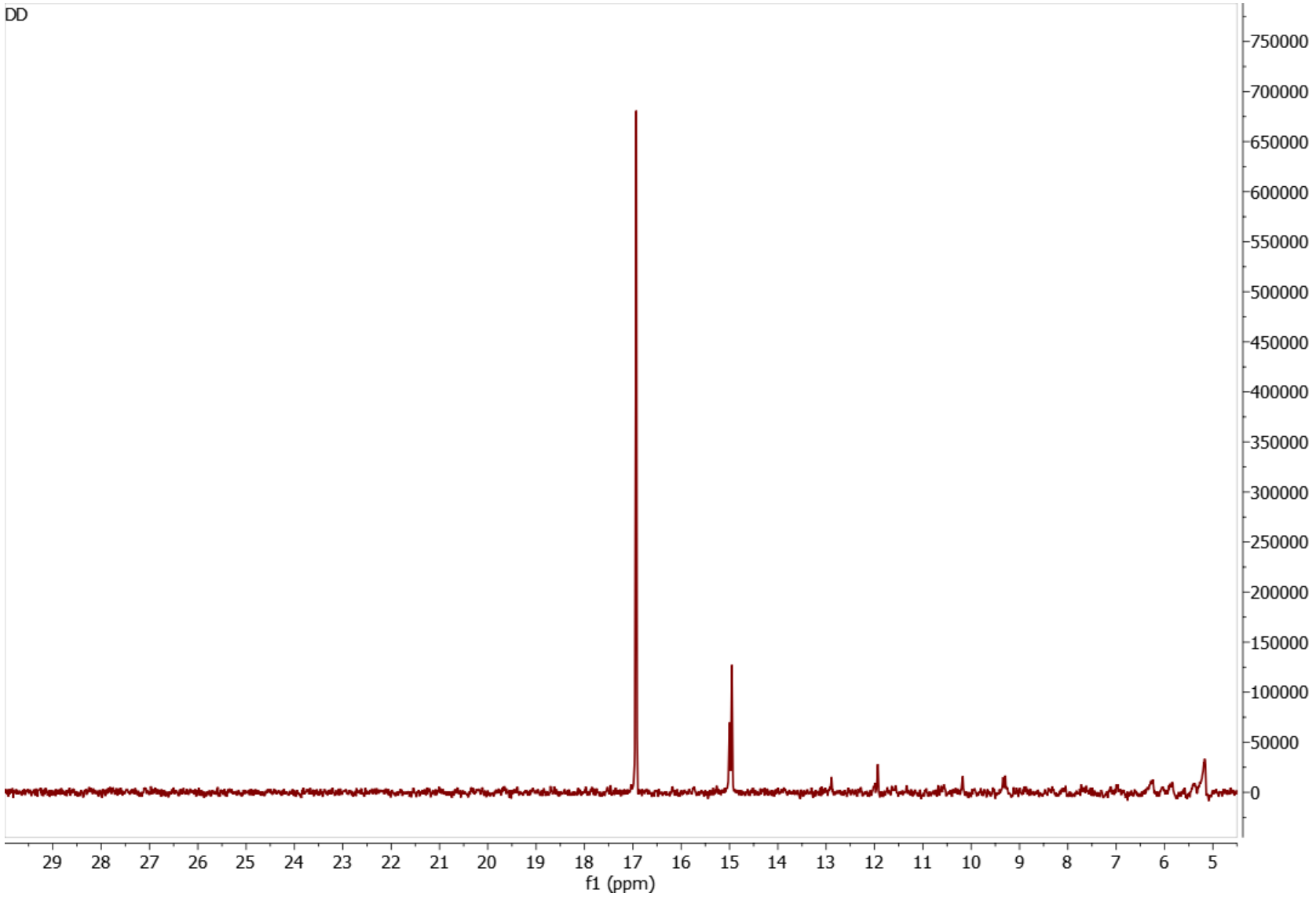

Figure 6.29. GC-MS spectrum of D.

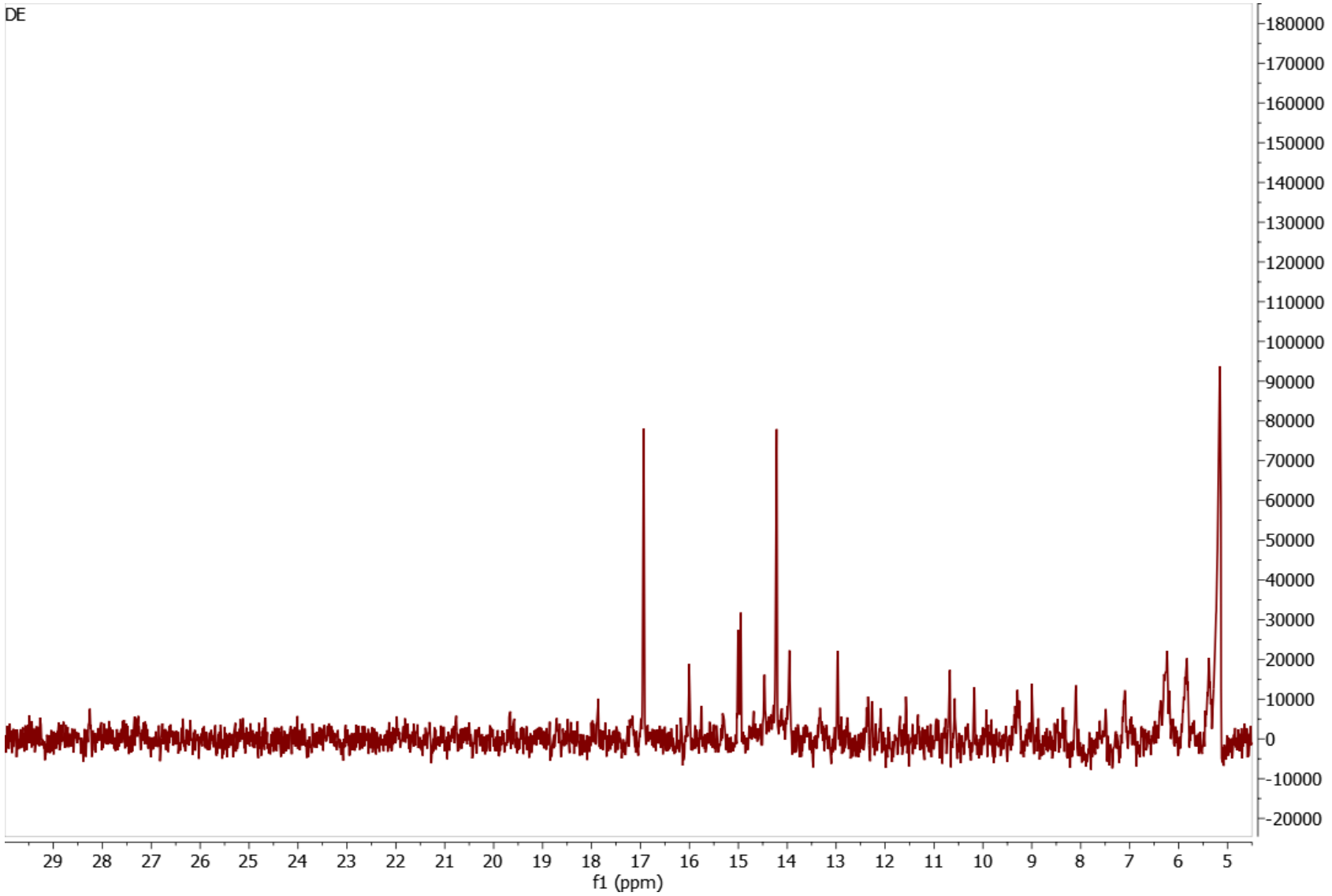

Figure 6.30. GC-MS spectrum of E.

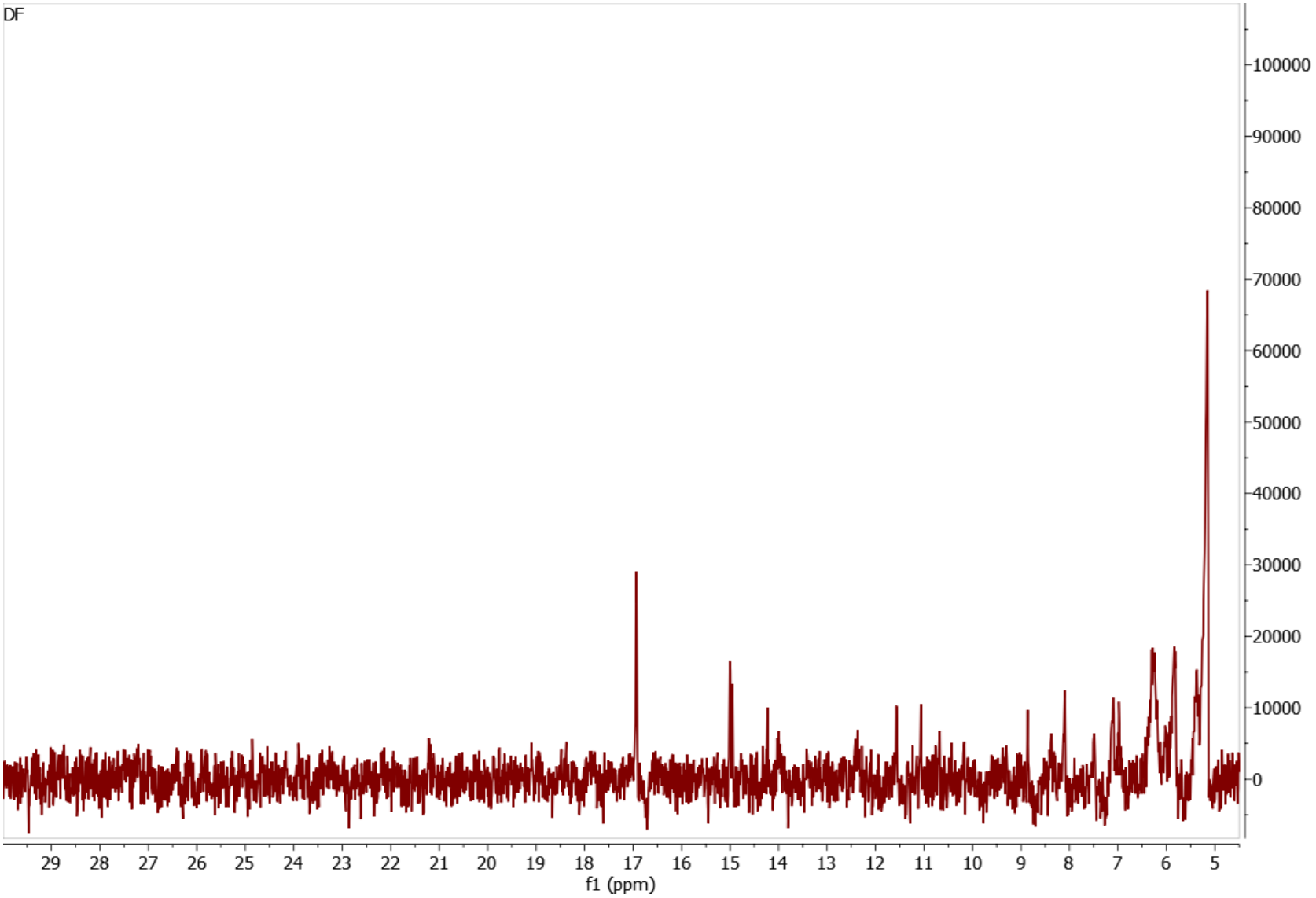

Figure 6.31. GC-MS spectrum of F.

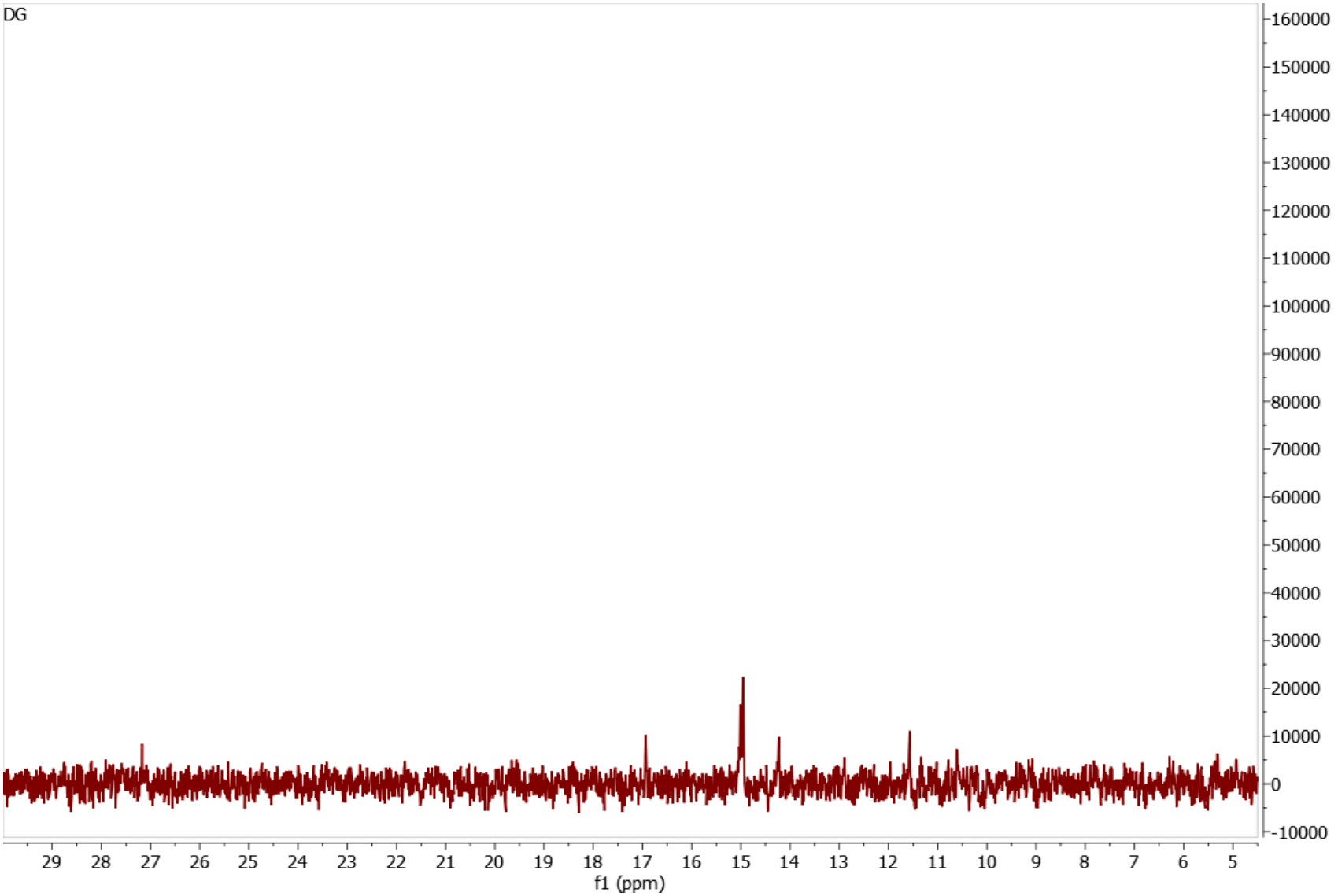

Figure 6.32. GC-MS spectrum of G.

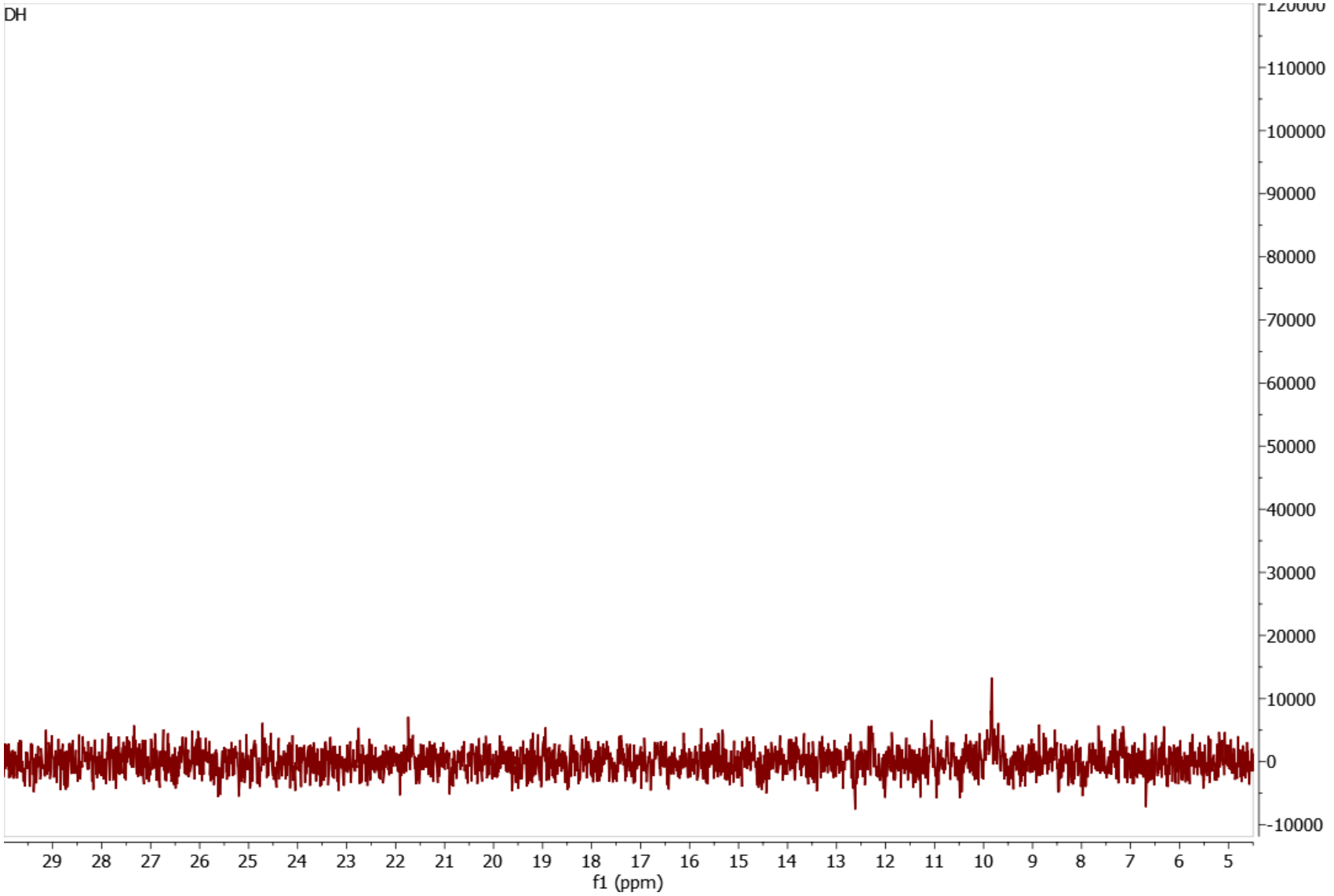

Figure 6.33. GC-MS spectrum of H.

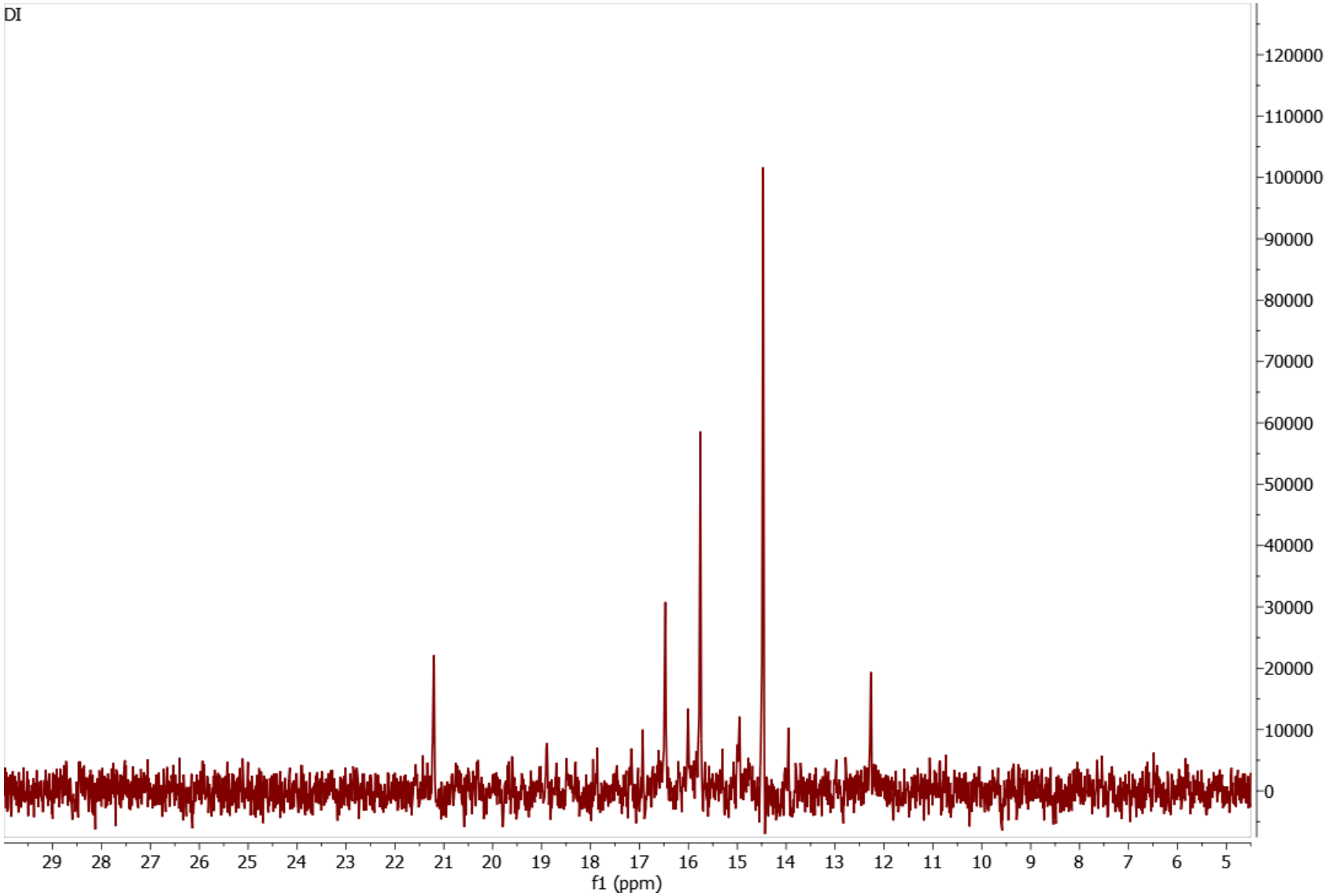

Figure 6.34. GC-MS spectrum of I.

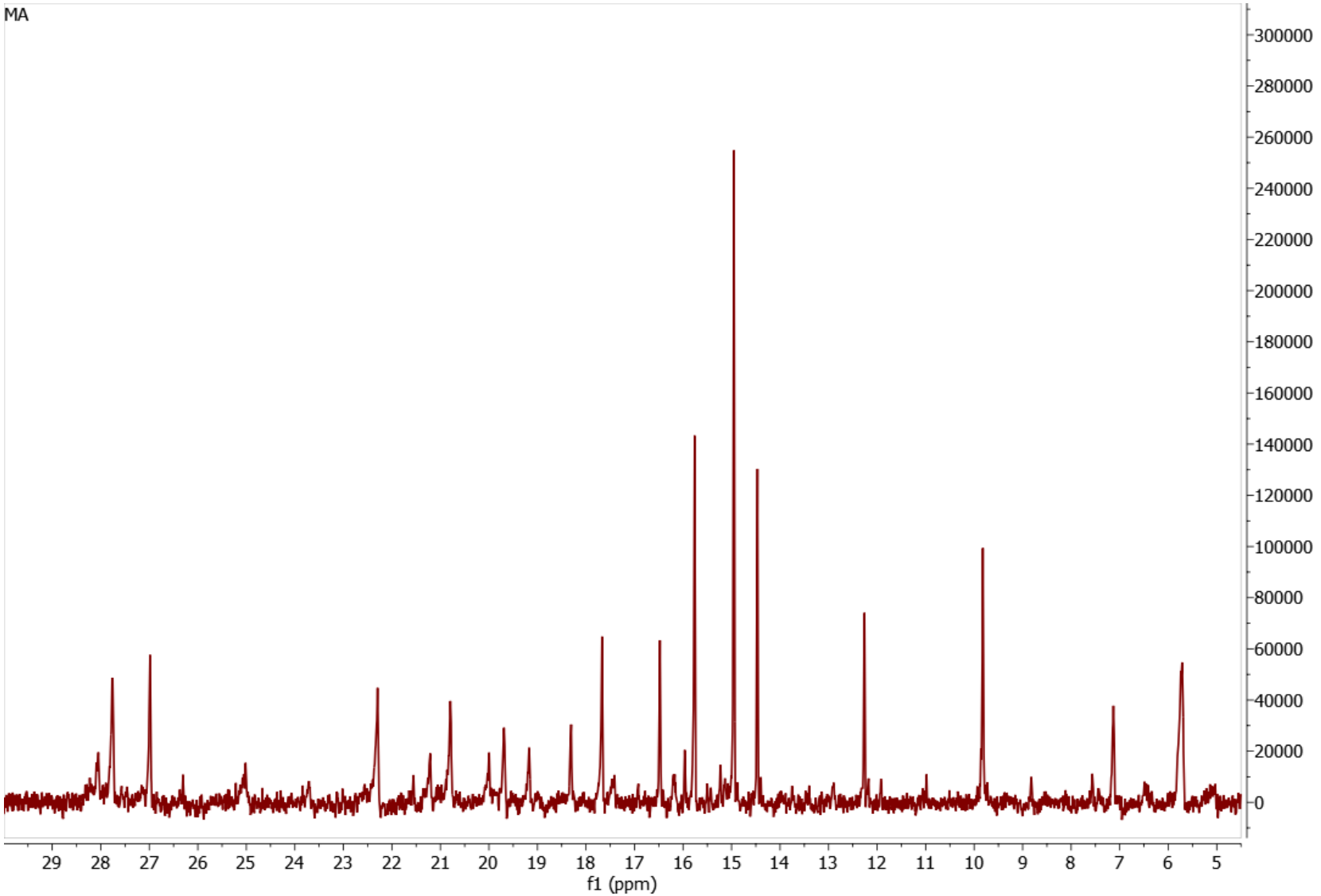

Figure 6.35. GC-MS spectrum of J.

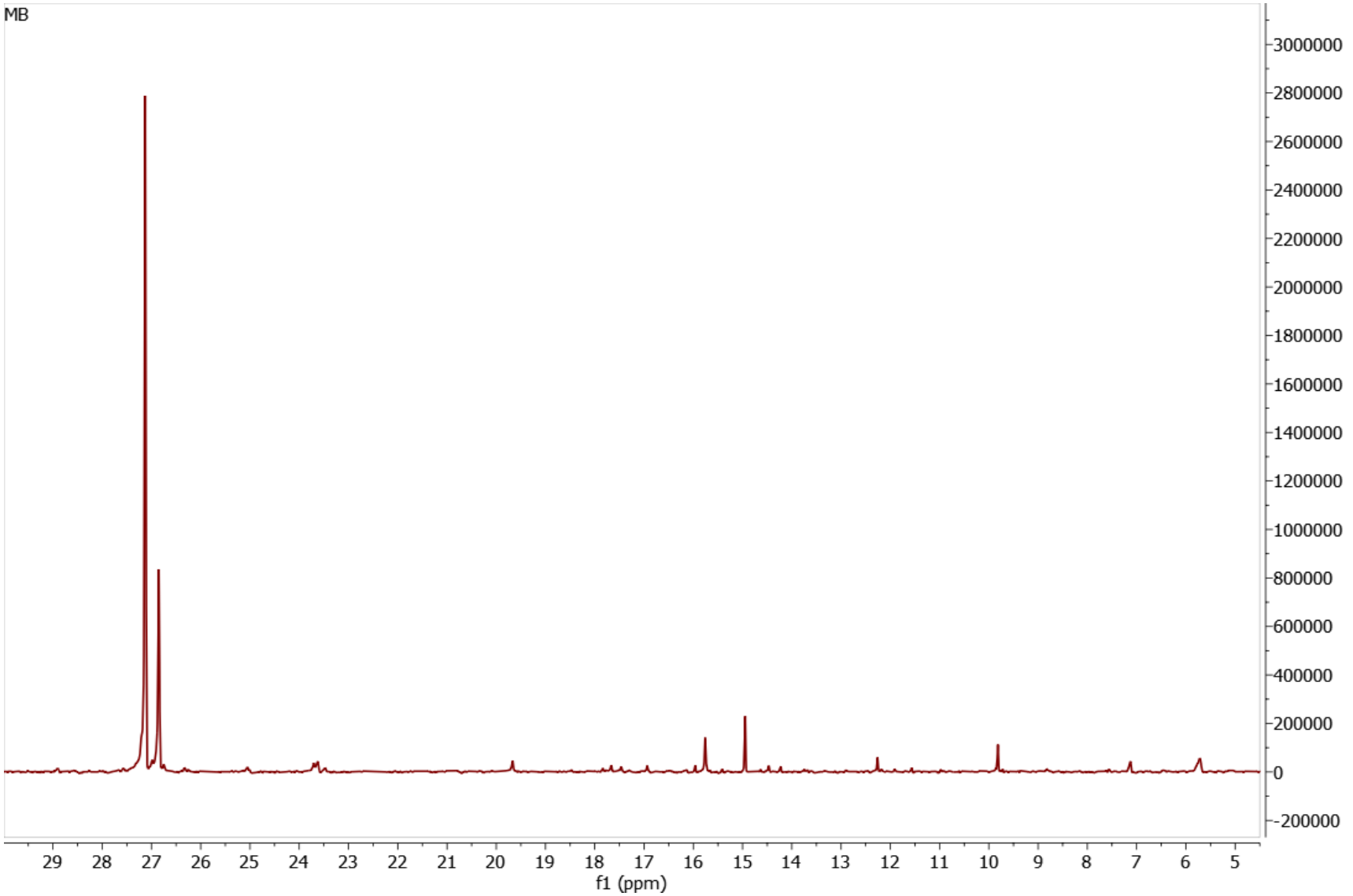

Figure 6.36. GC-MS spectrum of K.

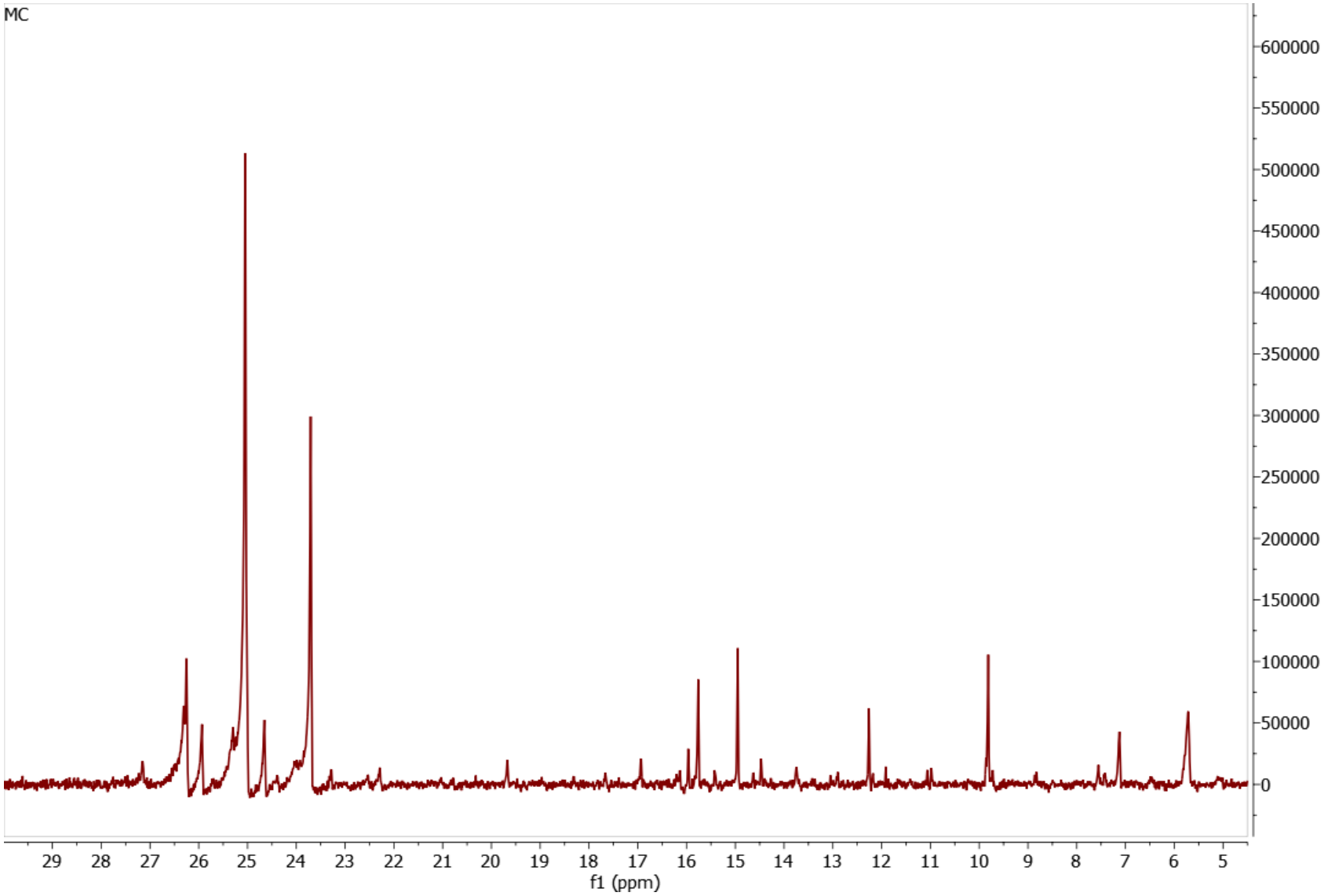

Figure 6.37. GC-MS spectrum of L.

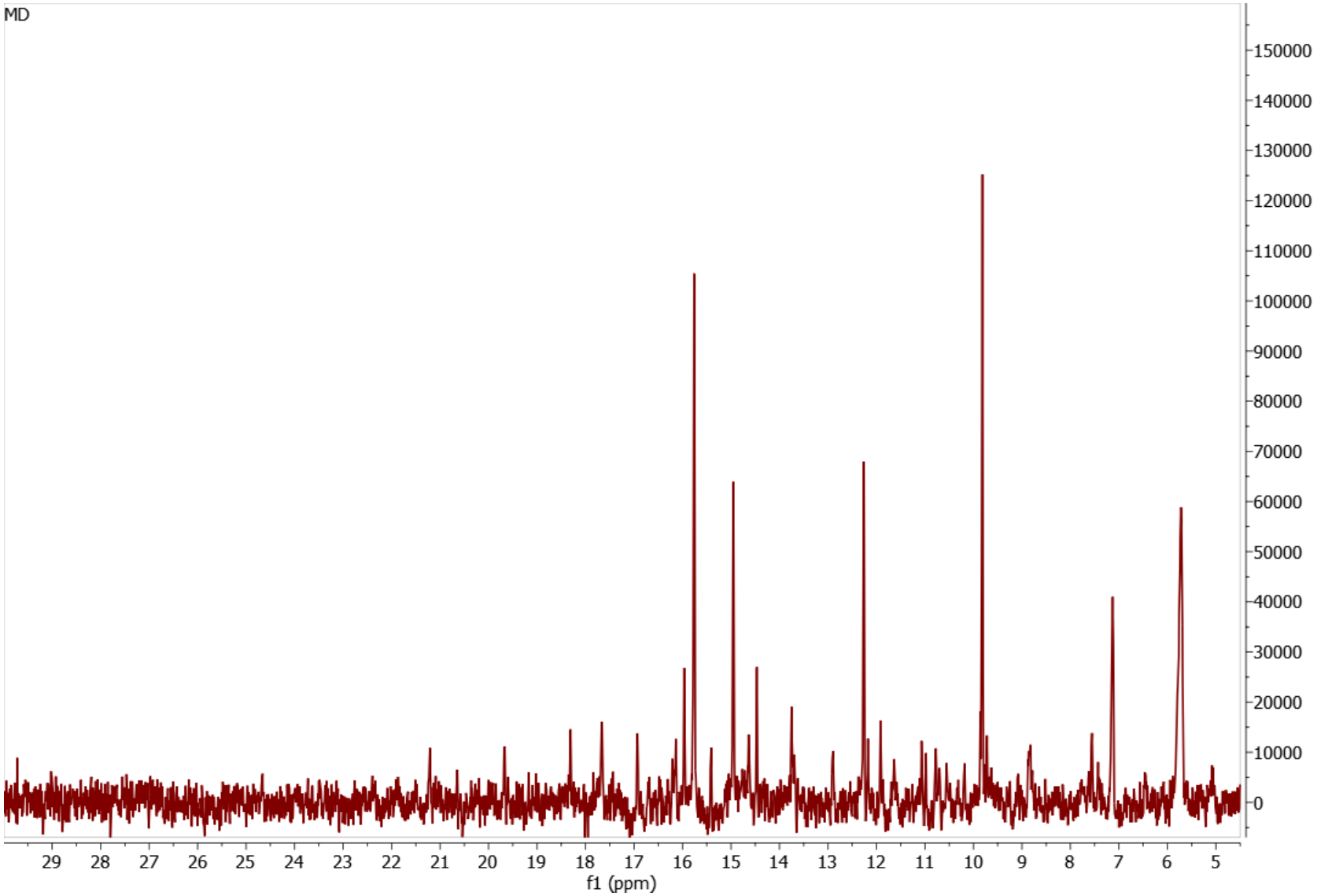

Figure 6.38. GC-MS spectrum of M.

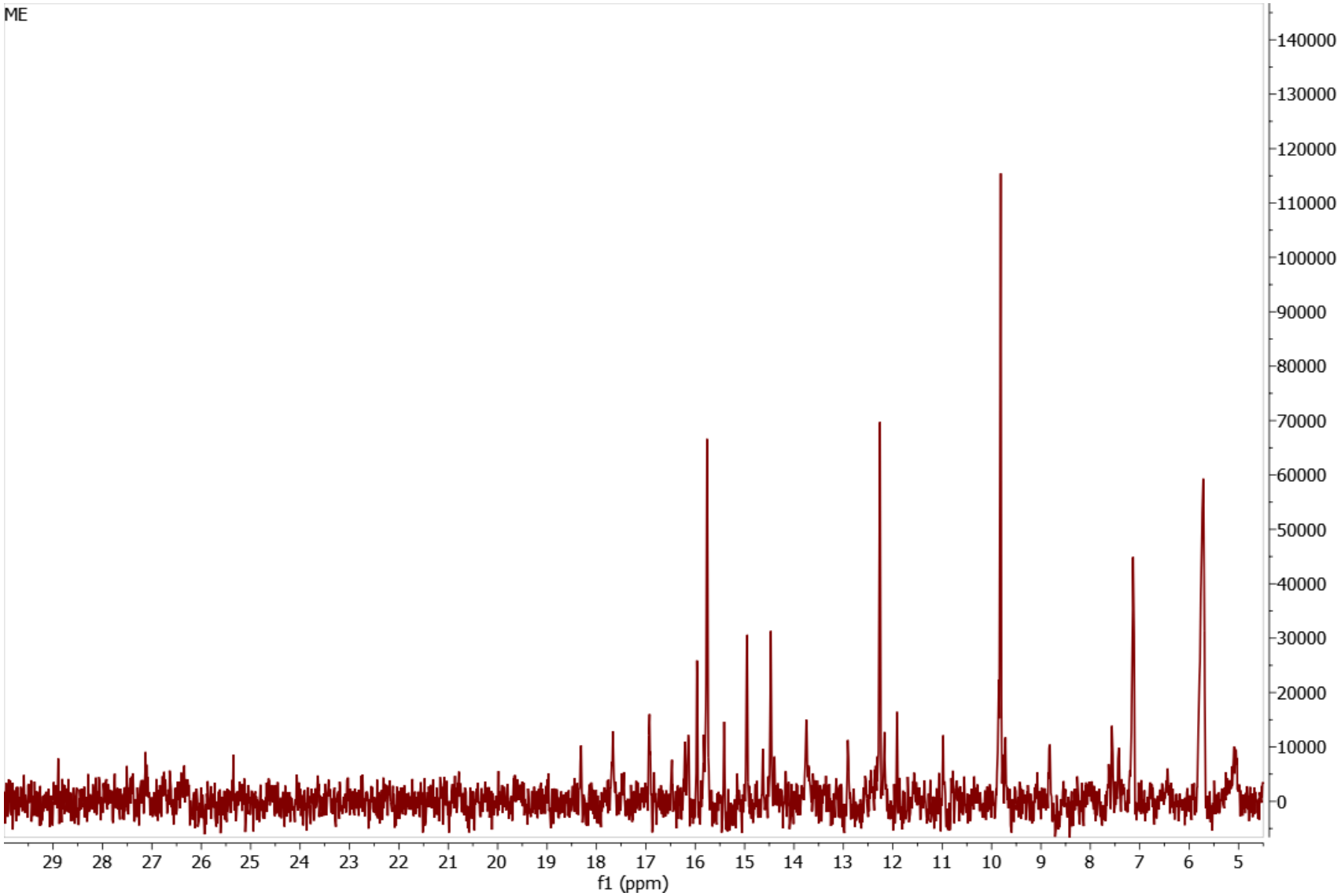

Figure 6.39. GC-MS spectrum of N.

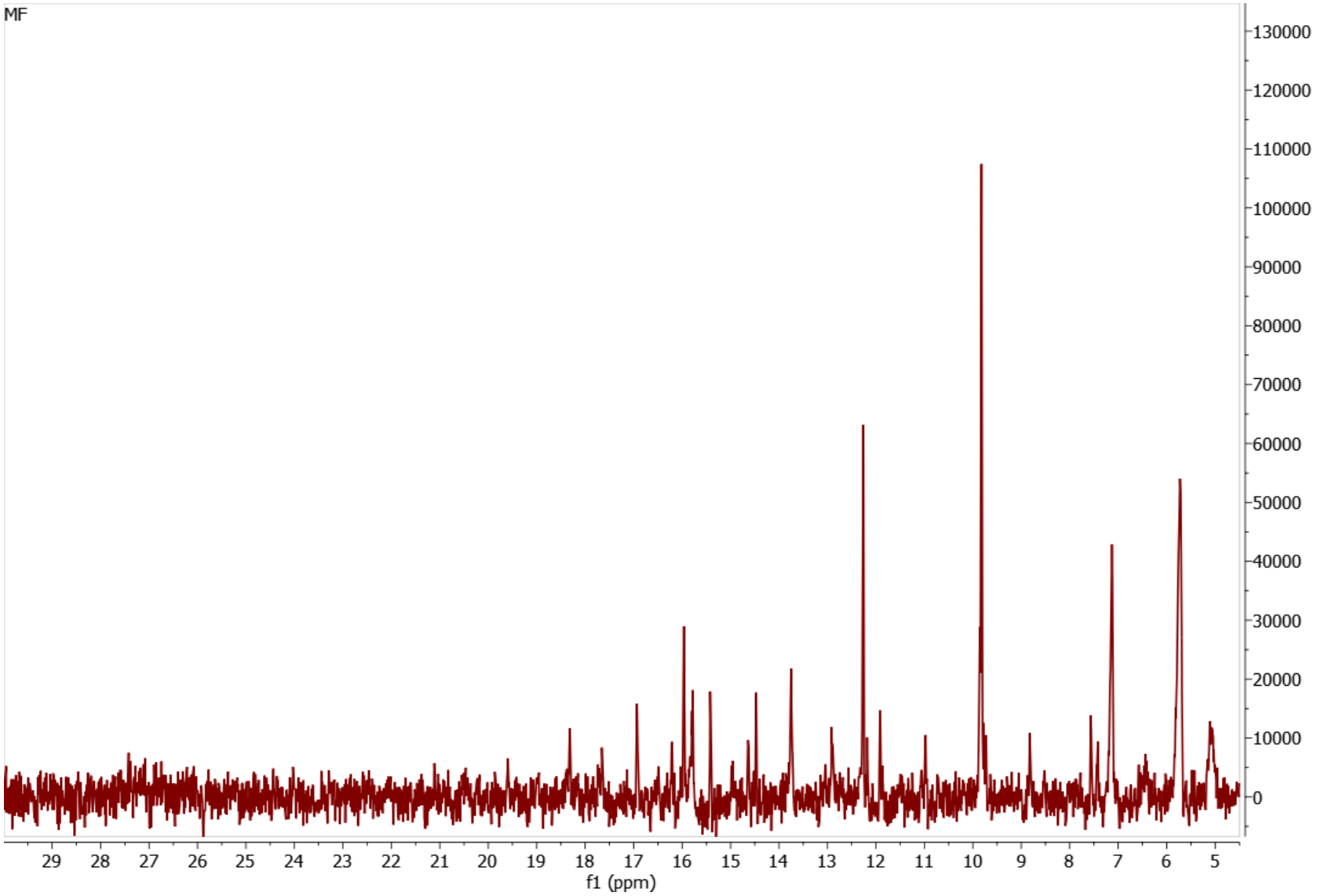

Figure 6.40. GC-MS spectrum of O.

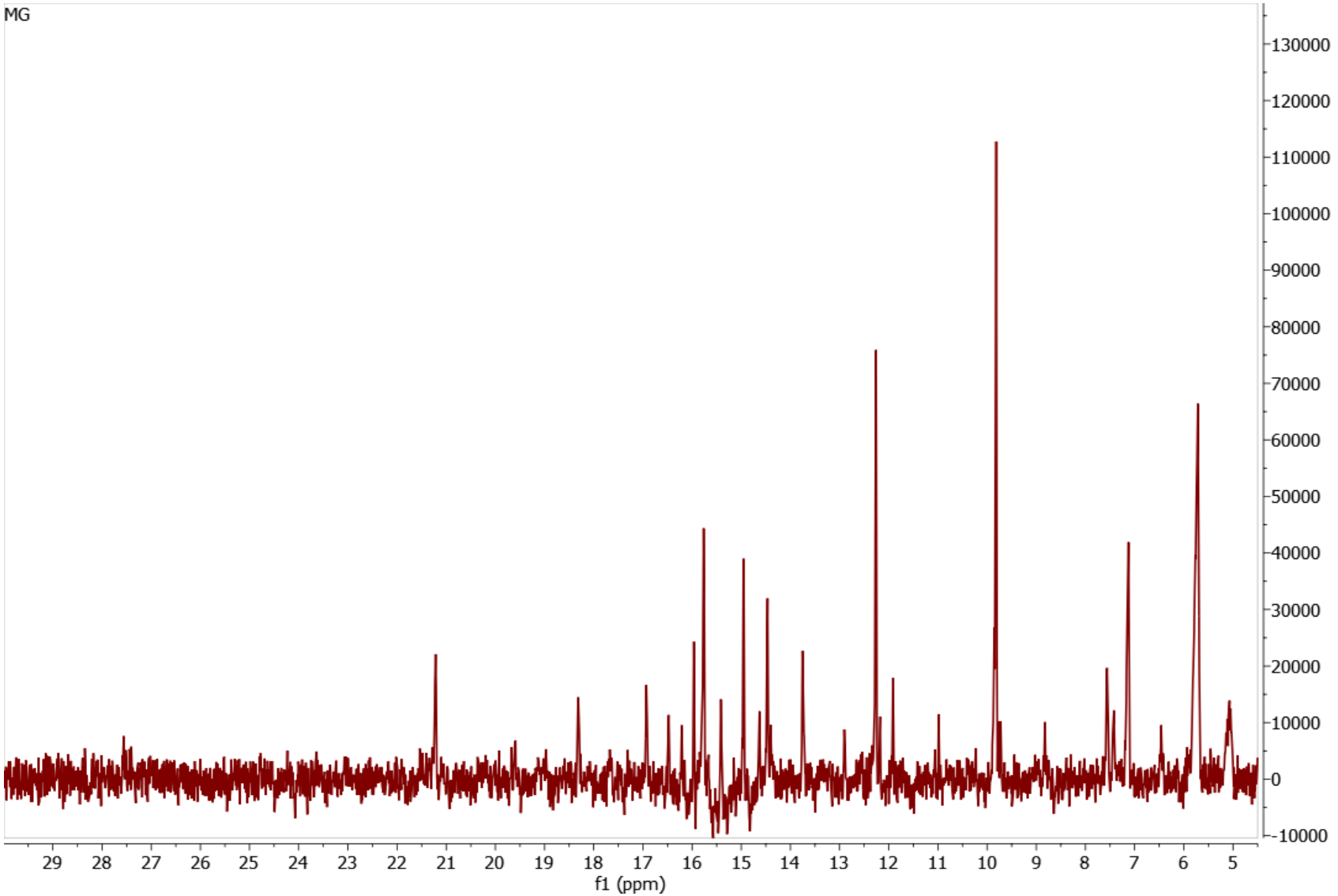

Figure 6.41. GC-MS spectrum of P.

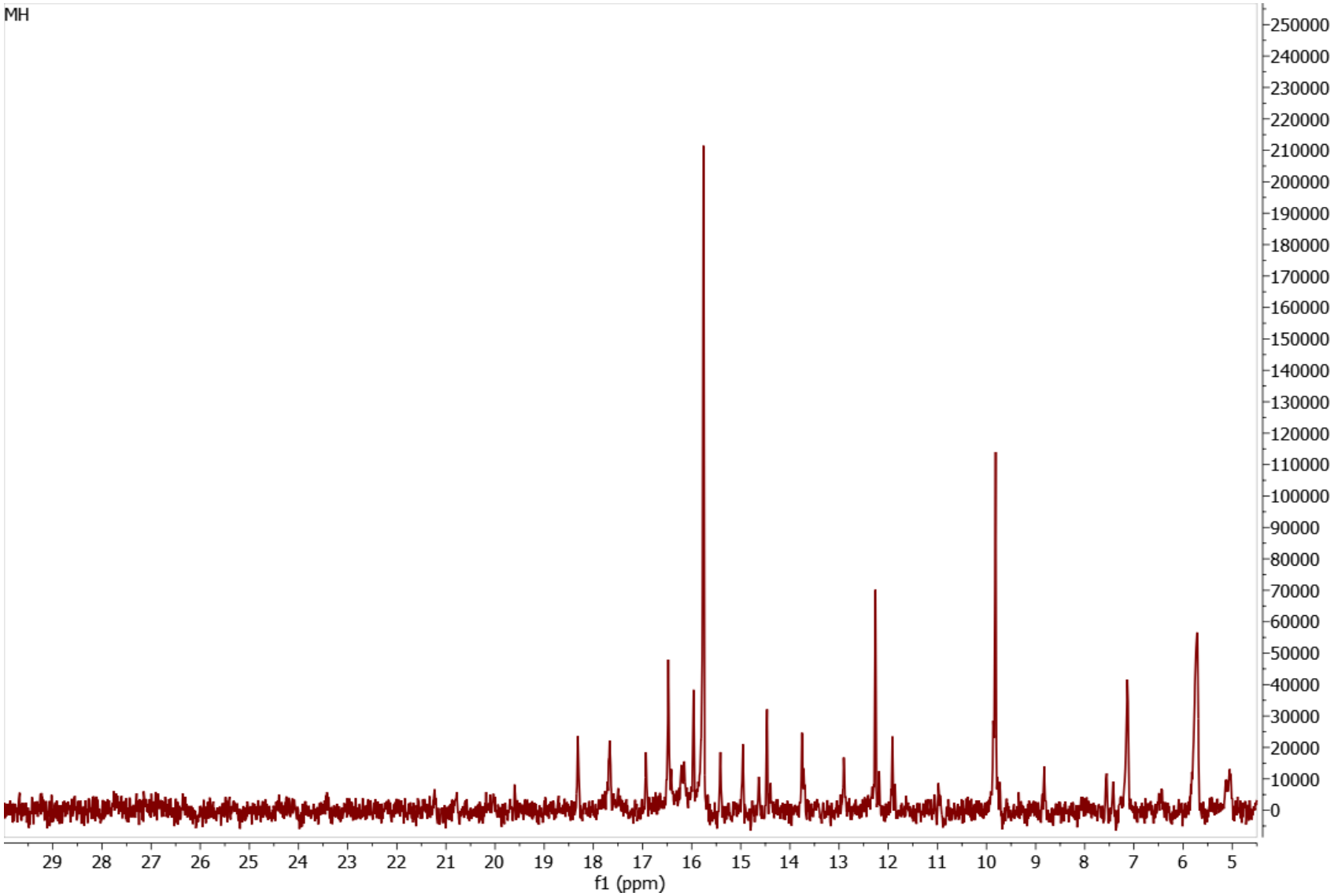

Figure 6.42. GC-MS spectrum of Q.

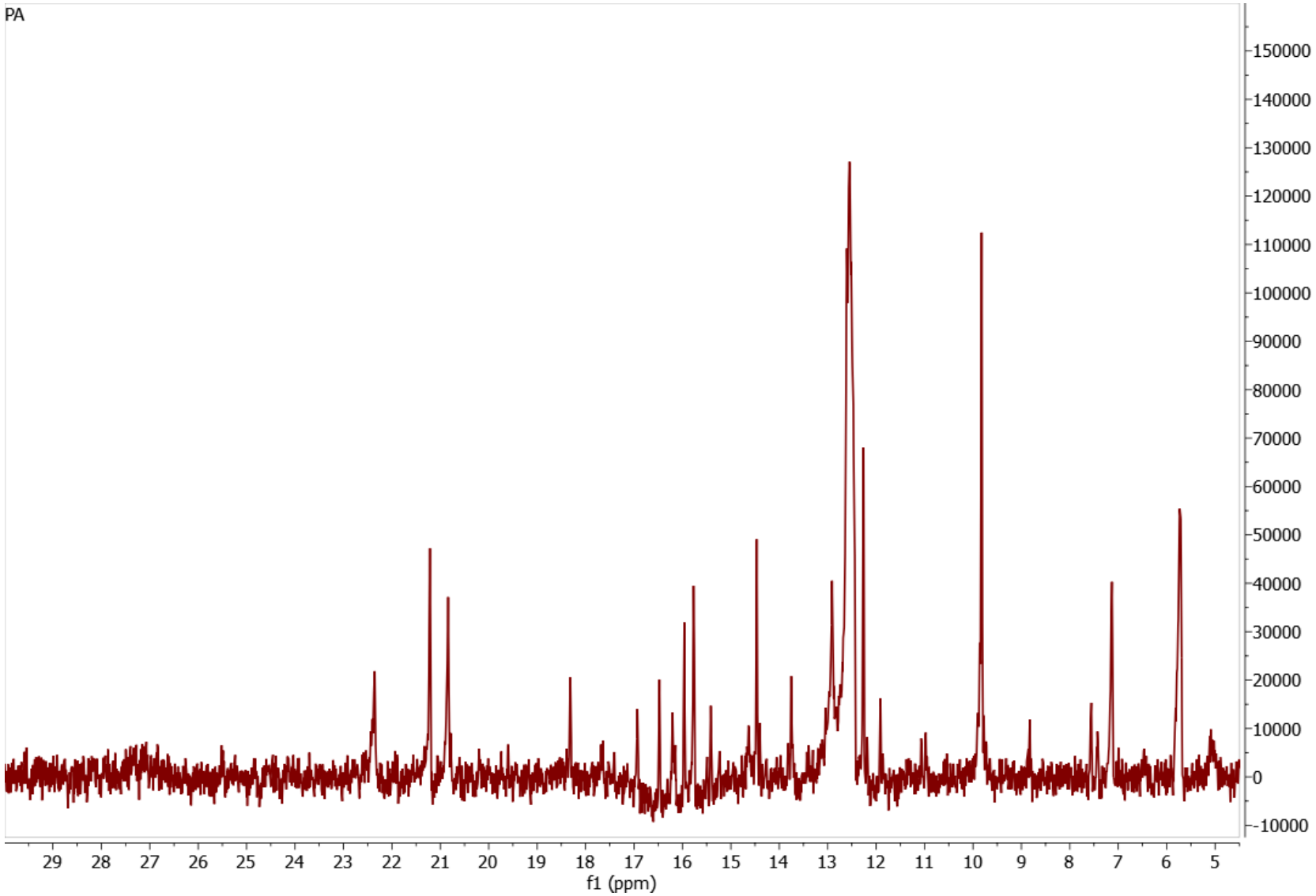

Figure 6.43. GC-MS spectrum of R.

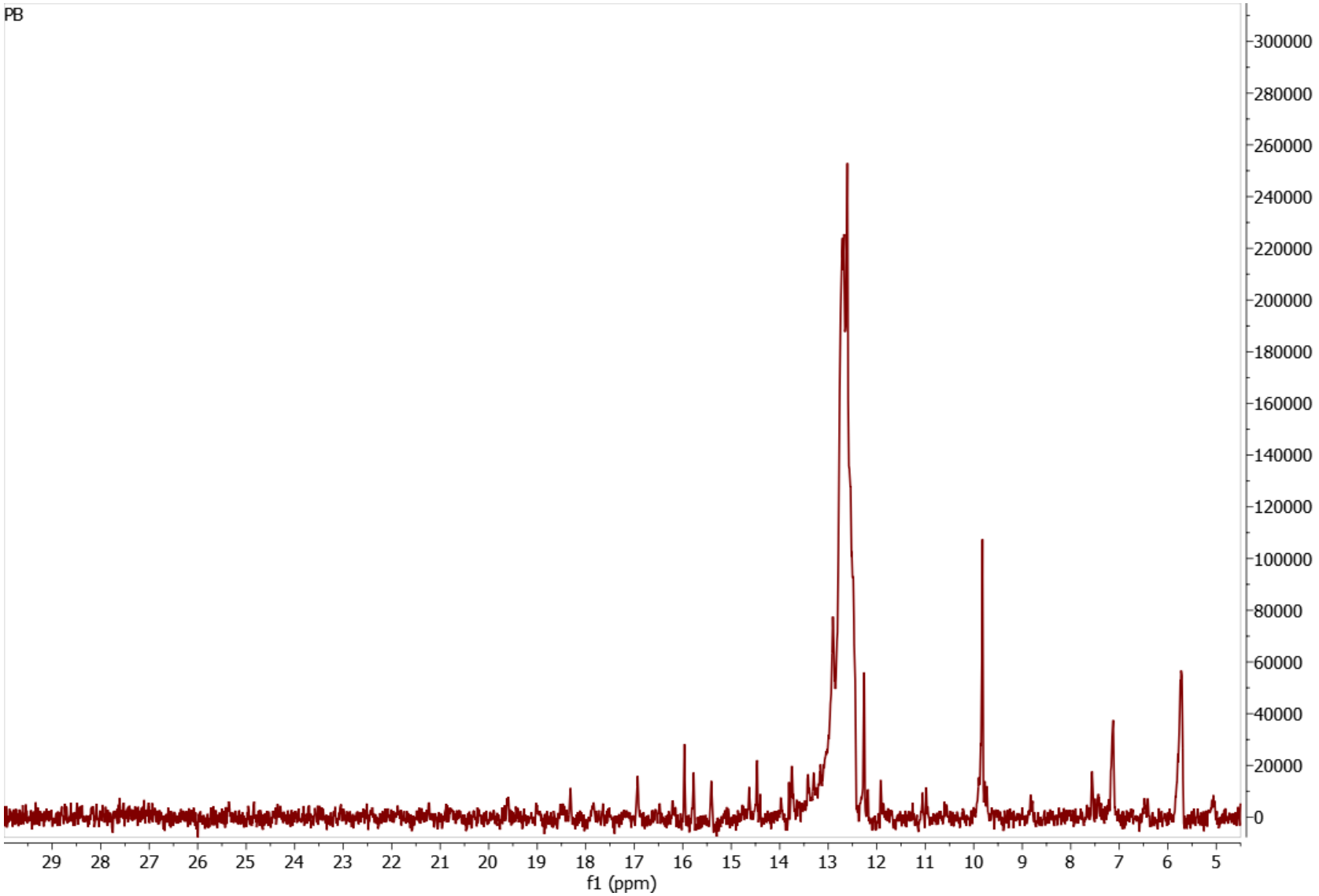

Figure 6.44. GC-MS spectrum of S.

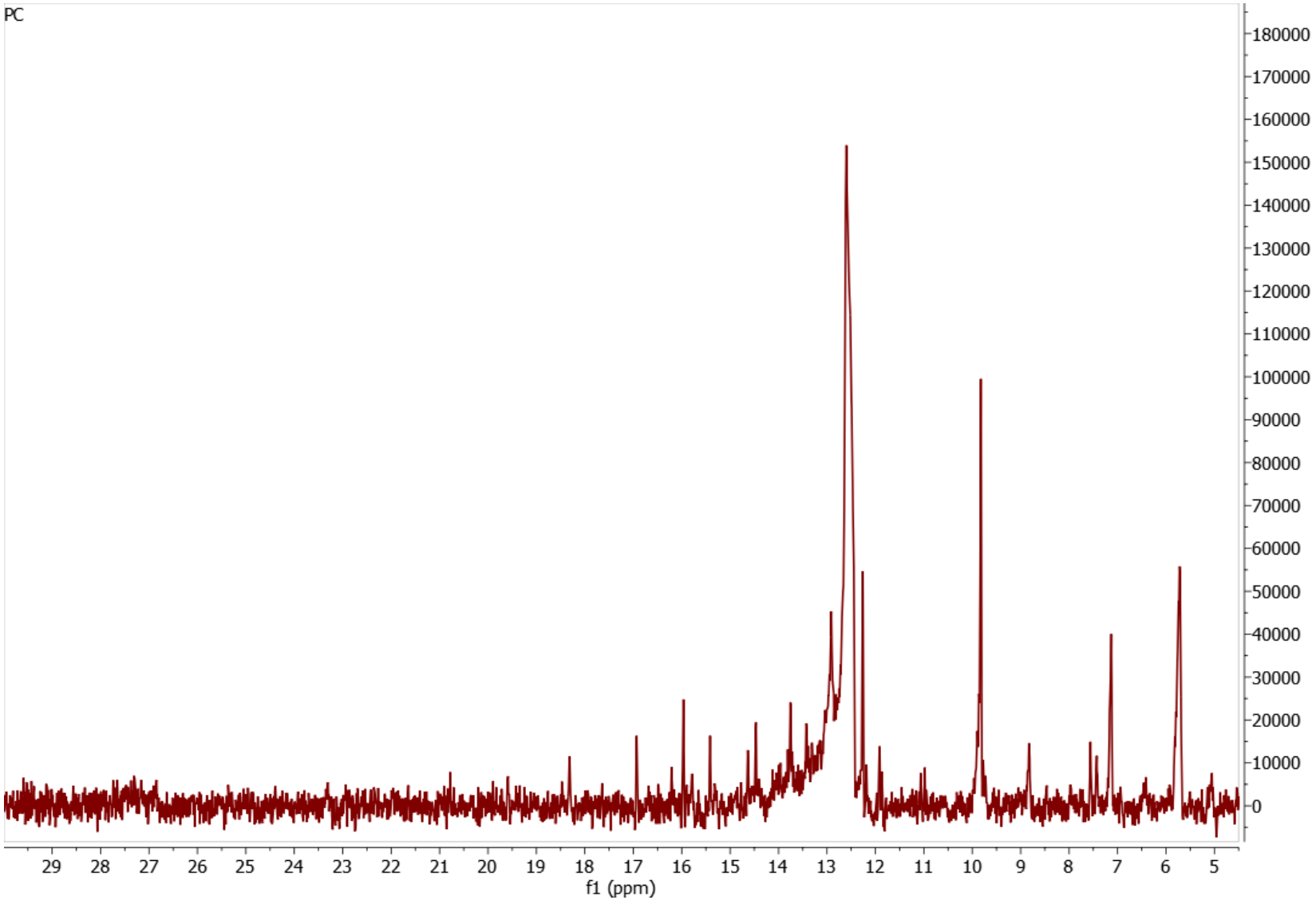

Figure 6.45. GC-MS spectrum of T.

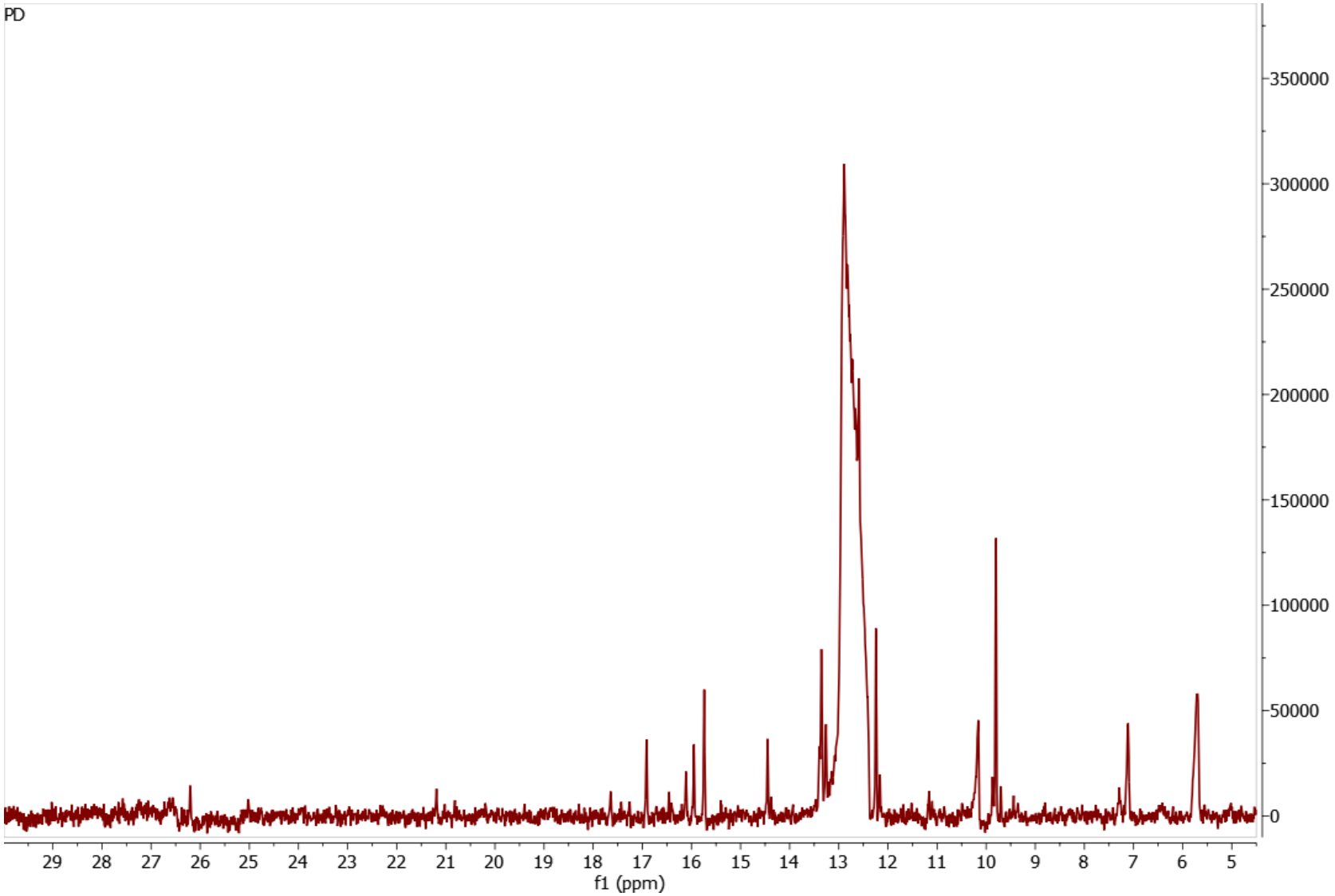

Figure 0.3. GC-MS spectrum of U.

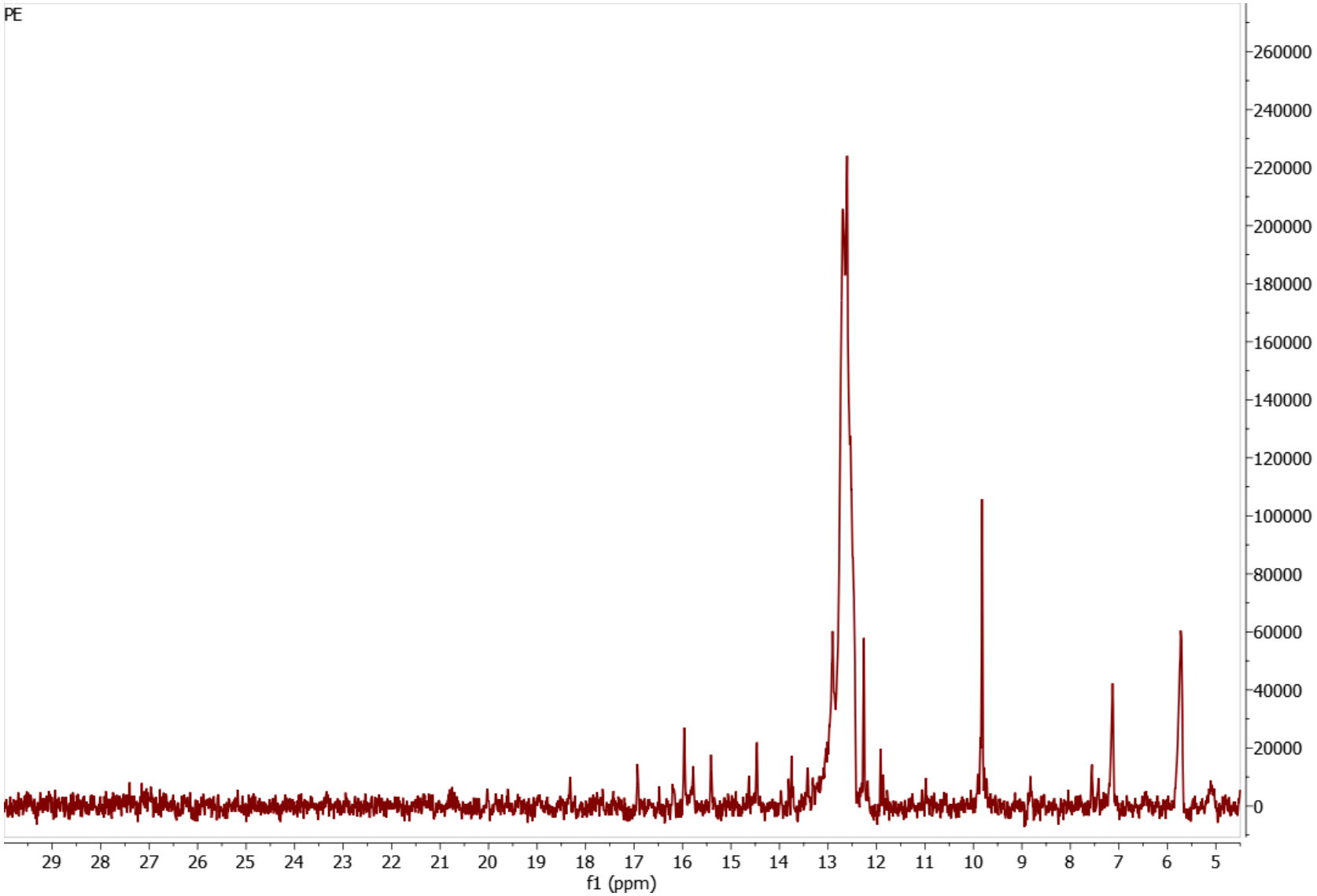

Figure 6.47. GC-MS spectrum of V.

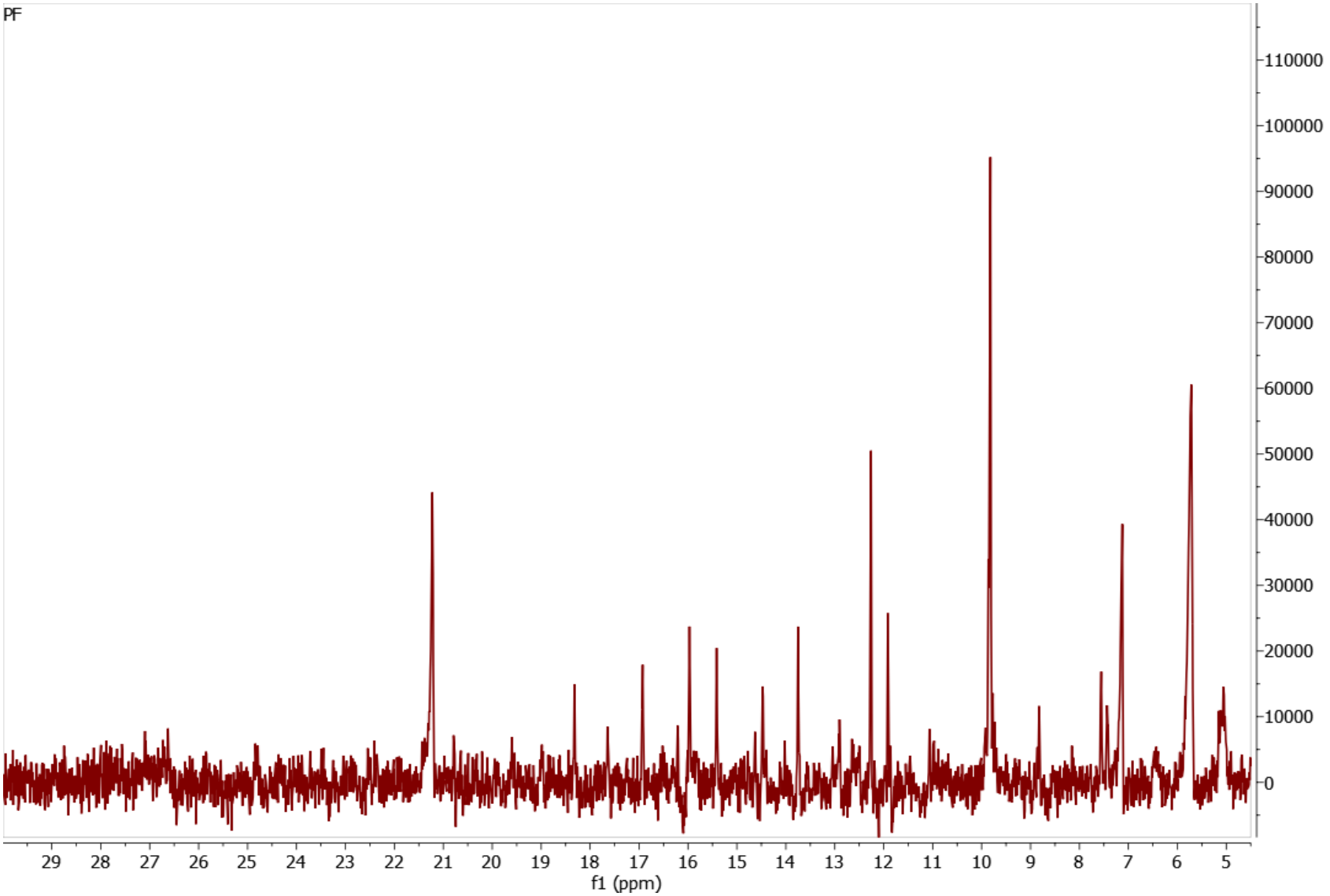

Figure 6.48. GC-MS spectrum of W.

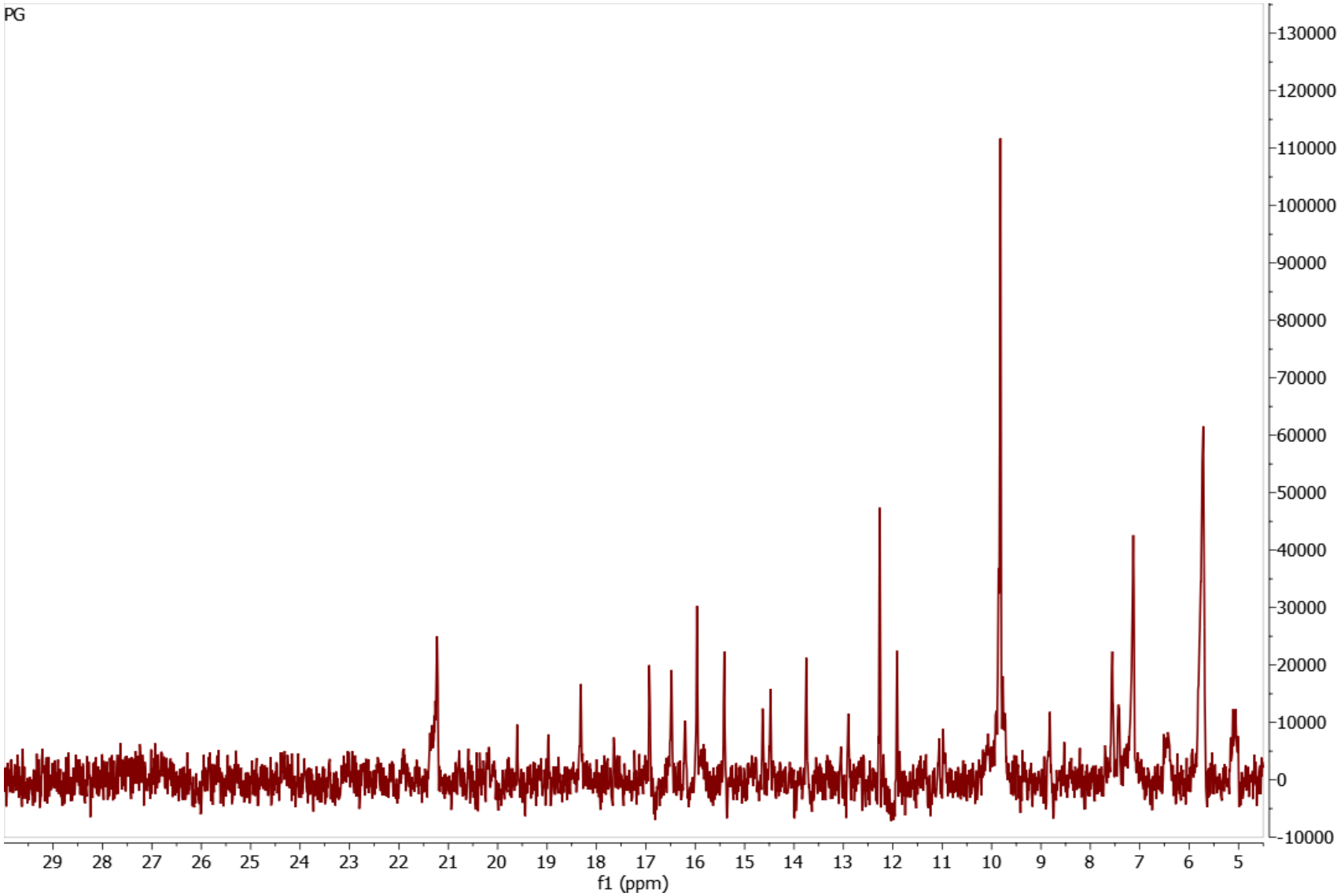

Figure 6.49. GC-MS spectrum of X.

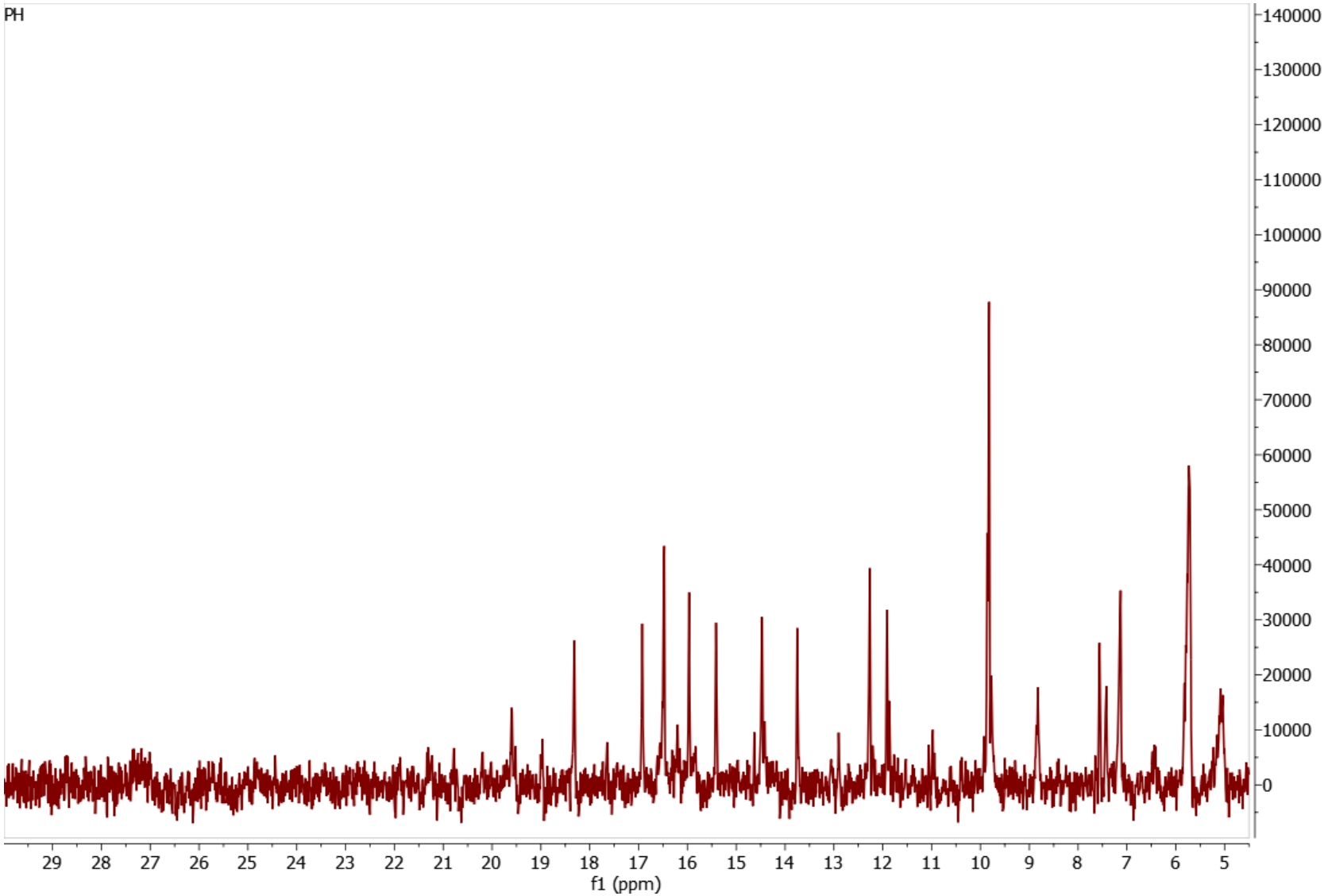

Figure 6.50. GC-MS spectrum of Y.